STUDIES

ON

THE REACTIONS OF THE FIRST-ROW TRANSITION METAL SCHIFF BASE COMPLEXES WITH MOLECULAR OXYGEN AND RELATED SPECIES

(第一遷移金属シッフ塩基錯体と酸素および関連化学種との反応に関する研究)

TAKAYUKI MATSUSHITA

MAY, 1983

Preface

The works in this thesis have been carried out under the guidances of Professor Toshiyuki Shono and Emeritus Professor Koichiro Shinra at Faculty of Engineering, Osaka University, since 1964.

The object of this thesis is to clarify the reactions of the first-row transition metal Schiff base complexes with molecular oxygen and related species. The author expects that the findings obtained from these studies would serve for understanding the functions of metalloenzymes in the biological oxygen cycle.

May, 1983 Takayuki Matsushita

List of Publications

The contents of this thesis are composed of the following papers.

1) Oxygenation and Oxidation of Manganese(II) Complexes of N,N'-Ethylenebis(salicylideneimine) and Analogues
T. Yarino, T. Matsushita, I. Masuda, K. Shinra, *J. Chem. Soc. Chem. Commun.*, 1970, 1317.

2) Peroxo-, Oxo-, and catena-Oxo-Manganese Complexes with N,N'-Ethylenebis(salicylideneimine) Analogues
T. Matsushita, T. Yarino, I. Masuda, T. Shono, and K. Shinra, *Bull. Chem. Soc. Jpn.*, 46, 1712 (1973).

3) Adducts of Bis(β-diketonato)manganese(II) with N,N-Dimethylformamide, Dimethyl Sulfoxide, and Pyridine
T. Matsushita, I. Masuda, and T. Shono, *Technol. Repts. Osaka Univ.*, 24, 345 (1974).

4) Reactions of Dichloromanganese(IV) Schiff Base Complexes with Water as Model for Water Oxidation in Photosystem II
T. Matsushita, M. Fujiwara, and T. Shono, *Chem. Lett.*, 1981, 631.

5) The Preparation and Characterization of Dichloromanganese(IV) Schiff Base Complexes
T. Matsushita, H. Kono, and T. Shono, *Bull. Chem. Soc. Jpn.*, 54, 2646 (1981).

6) Reactions of Manganese(III) Schiff Base Complexes with Superoxide Ion in Dimethyl Sulfoxide
T. Matsushita and T. Shono, *Bull. Chem. Soc. Jpn.*, 54, 3743 (1981).

7) Preparation and Characterization of Dichlorobis(N-alkyl-salicylideneaminato)manganese(IV) Complexes
T. Matsushita, Y. Hirata, and T. Shono, *Bull. Chem. Soc. Jpn.*, 55, 108 (1982).

8) Reactions of Chloroiron(III) Schiff Base Complexes with Superoxide Ion in Dimethyl Sulfoxide
T. Matsushita, H. Kono, M. Nishino, and T. Shono, *Bull. Chem. Soc. Jpn.*, 55, 2581 (1982).

9) Reactions of Polymeric Chloromanganese(III) Schiff Base Complexes with Superoxide Ion in Dimethyl Sulfoxide
T. Matsushita, M. Nishino, and T. Shono, *Bull. Chem. Soc. Jpn.*, 55, 2663 (1982).

10) Oxidative Dehydrogenation of Bis(salicylideneaminato)copper(II) Complex in Pyridine and Formation of 2-Cyanophenolato Complex
T. Matsushita and T. Shono, *Bull. Chem. Soc. Jpn.*, 56, 727 (1983).

11) Preparation and Characterization of Dichlorobis(N-alkyl-substituted salicylideneaminato)manganese(IV) Complexes
T. Matsushita and T. Shono, *Polyhedron*, in press.

12) Preparation of Iron(II) Schiff Base Complexes Supported on Polystyrene and Their Oxygenation in Solution
T. Matsushita, M. Fukuda, and T. Shono, in contribution.

13) Preparation of Binuclear Manganese(III) and Iron(III) Schiff Base Complexes and Their Reactions with Superoxide Ion in Dimethyl Sulfoxide
T. Matsushita, M. Nishino, and T. Shono, to be published.

14) Preparation and Reaction of Monomeric and Polymeric Iron(III) Schiff Base Complexes with Superoxide Ion in Dimethyl Sulfoxide
T. Matsushita, M. Nishino, and T. Shono, to be published.

Contents

INTRODUCTION

The earth was environed with reducing atmosphere such as hydrogen, ammonia, and methane at least 10^9 years ago. Since green-algae and green plants generated and evolved molecular oxygen (O_2) by the photosynthetic water oxidation, substantial amounts of free O_2 have accumulated gradually in our atmosphere. Anaerobic organisms have evolved to aerobic organisms which utilize O_2 for their survival. At the present stage, O_2 is essential for life of aerobic organisms: O_2 is uptaken by respiration, stored, transported, and consumed for oxidation of substrates at appropriate sites. On the other hand, it has been found that O_2 with high concentration and its reduction products are toxic to the organisms: O_2 is toxic not because of its own reactivity but rather because its reactive reduction intermediates such as superoxide radical (O_2^-), hydrogen peroxide (H_2O_2), and hydroxyl radical (HO·), which are generated naturally by a series of single electron transfers from O_2 to water. It has been found two decades ago that organisms which utilize O_2 have the defence mechanisms for the oxygen toxicity, such as superoxide dismutases and catalase.

Such a biological oxygen metabolism is represented according to Hill as follows.[1)]

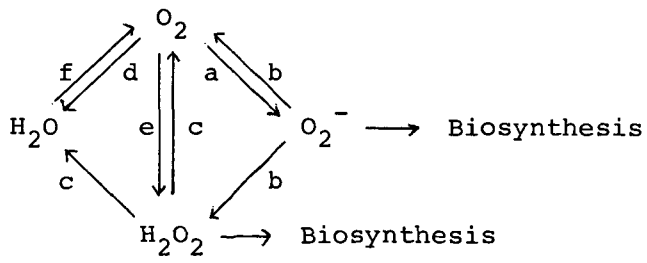

A schematic representation of the biological oxygen cycle.[1)]

In these systems, the following many metalloenzymes play a significant role and function specifically.

(a) various enzymes; Xanthine oxidase, Indoleamine-2,3-dioxygenase, Enzymes in chloroplast.

(b) Superoxide dismutases (SOD).

(c) Catalase.

(d) Cytochrome oxidase.

(e) various enzymes; Aminoacid oxidases.

(f) Enzymes in chloroplast.

Recently, the structures of the metalloenzymes and their functions have been elucidated considerably by the development of the physicochemical methods (X-ray analysis, NMR, ESR, and so on). They are, however, so complex that many unresolved problems have remained; the bonding type of O_2 to iron(II) atom in hemoglobin and myoglobin[2], structures of Fe-SOD and Mn-SOD[3], and manganese-containing enzymes in chloroplasts which play an important role for O_2 generation by the photosynthetic water oxidation in green plants.[4,5] Thus, many metal complexes with various ligands have been investigated so far in order to elucidate the active sites of metalloenzymes, such as oxygen-carrying cobalt(II) complexes[6,7] and modified iron(II) porphyrin complexes.[8] These studies have served considerably for understanding the specific functions of metalloenzymes.

The author has aimed to clarify the unrevealed functions of the metalloenzymes, hemoglobin and myoglobin, Fe-SOD and Mn-SOD, and Mn-enzymes in chloroplasts, using the metal Schiff base complexes which are considered as models for their active sites.

In this thesis, the preparation and characterization of the first-row transition metal complexes (chiefly manganese complexes)

of the Schiff base ligands and their reactions with O_2, O_2^-, and water will be described.

In Chapter I, the reactions of O_2 with the manganese(II) Schiff base complexes, the iron(II) Schiff base complexes, and the latter supported on polystyrene have been investigated.

In Chapter II, the adducts of the bis(β-diketonato)manganese(II) complexes with N,N-dimethylformamide, dimethyl sulfoxide (DMSO), and pyridine are isolated and characterized.

In Chapter III, the reactions of superoxide ions (O_2^-) with a series of mononuclear, binuclear, and polynuclear manganese(III) Schiff base complexes in DMSO have been investigated in connection with Mn-SOD. In Chapter IV, the reactions of O_2^- and a series of mononuclear, binuclear, and polynuclear iron(III) Schiff base complexes in DMSO have been investigated.

In Chapter V, a series of novel dichloromanganese(IV) Schiff base complexes has been prepared and fully characterized.

In Chapter VI, the reactions of the dichloromanganese(IV) Schiff base complexes with water have been investigated in connection with the photosynthetic water oxidation in green plants.

In Chapter VII, the oxidative dehydrogenation of copper(II) complexes with salicylideneamine and its analogs by O_2 in pyridine has been investigated.

The results obtained in this study should provide good information concerning the functions of metalloenzymes, especially the biological redox processes involving O_2 and related species, which have not yet been elucidated so far.

References

1) H. A. O. Hill, "New Trends in Bio-inorganic Chemistry," ed by R. J. P. Williams and J. J. R. F. Da Silva, Acad. Press, New York (1978), p. 173.

2) C. A. Reed, "Metal Ions in Biological Systems," ed by H. Sigel, Marcel Dekker Inc., New York (1978), Vol. 7, p. 277.

3) D. O. Hall, *Adv. Chem. Ser.*, 162, 227 (1977).

4) G. M. Cheniae, *Ann. Rev. Plant Physiol.*, 21, 467 (1970).

5) K. Sauer, *Acc. Chem. Res.*, 13, 249 (1980).

6) R. P. Michel and A. Daniel, *Bull. Soc. Chim. Fr.*, 1976, 1431.

7) R. D. Jones, D. A. Summerville, and F. Basolo, *Chem. Rev.*, 79, 139 (1979).

8) J. P. Collman, *Acc. Chem. Res.*, 10, 265 (1977).

Chapter I

I - 1 Peroxo-, Oxo-, and catena-Oxo-Manganese Complexes with N,N'-Disalicylideneethylenediamine Analogs

Introduction

The Mn^{II}(salen)[1] was first reported by Tsumaki[2] to react with oxygen to yield Mn^{III}(salen)OH, for which Lewis *et al.*[3] later proposed a polymeric structure including unitary Mn^{III}(salen)-O-Mn^{III}(salen)·H_2O on the basis of the magnetic property. Recently, Johnson *et al.*[4] have reported that Mn^{II}(salpn)[1] takes up molecular oxygen in a benzene solution.

In this Chapter, three types of complexes involving Mn^{III}-O_2-Mn^{III}, -(-Mn^{IV}-O-)$_n$-, and Mn^{IV}=O bonds respectively are shown to be obtainable upon reacting the Mn^{II}(salen) and its analogs with molecular oxygen in organic solvents.

Experimental

Manganese(II) Complexes. The preparation of Mn^{II}(salen) and Mn^{II}(3-MeOsalen)·H_2O[1] was carried out in a nitrogen atmosphere according to a modification of the procedure of the literature.[3] Mn^{II}(5-NO_2salen)[1] was obtained by allowing the pyridine adduct, Mn^{II}(5-NO_2salen)·2py, which had been prepared by the reaction of 5-NO_2salenH_2 with $MnCl_2$·$4H_2O$ in a *ca.* 50% aqueous pyridine solution, to stand *in vacuo* at 90 – 100 °C for 12 h. The compounds were confirmed by elemental analyses.

Peroxo-, Oxo-, and catena-Oxo-Manganese Complexes. *μ-Peroxo-bis[N,N'-disalicylideneethylenediaminatomanganese(III)], [Mn^{III}(salen)]$_2O_2$:* Mn^{II}(salen) (2.0 g) was dissolved in DMSO (150 cm^3) in a nitrogen atmosphere and then the solution was kept in oxygen (1 atm) at room temperature for about 12 h.

Two grams of precipitates were thus separated. The precipitates were extracted with CH_2Cl_2 (1 L), and then the solvent was evaporated to *ca.* 50 cm^3 to leave reddish brown crystals. They were separated by filtration and then dried *in vacuo* at 50 °C for 6 h. Yield: 0.2 g. When the solution of Mn^{II}(salen) was kept in a nitrogen atmosphere which contained about 2.0 vol% of oxygen, the crystals of the μ-peroxo complex could be obtained in a *ca.* 90% yield. The μ-peroxo complex is soluble in CH_2Cl_2 (*ca.* 0.4 g/L) and is slightly soluble in DMSO and DMF.

Oxo[N,N'-di(3-methoxysalicylidene)ethylenediaminato]-manganese(IV) Methanol Adduct, O=Mn^{IV}(3-MeOsalen)·2MeOH: Mn^{II}(3-MeO-salen)·H_2O (2.0 g) was suspended in absolute MeOH (200 cm^3), and then oxygen gas was bubbled through the mixture while it was being stirred for *ca.* 20 h. The solution turned greenish brown, and dark green, crystalline needles were separated. The crystals were filtered and dried *in vacuo*. Further crystals were obtained by concentrating the filtrate. Yield: 1.4 g. The complex was recrystallized from methanol.

Poly, catena-oxo(N,N'-disalicylideneethylenediaminato)-manganese(IV), -[-Mn^{IV}(salen)-O-]$_n$: Mn^{II}(salen) (1.0 g) was dissolved in pyridine (100 cm^3) under a nitrogen atmosphere, and then the solution was allowed to stand for about 20 h in dry oxygen (1 atm). The brown precipitates thus separated were centrifuged, washed with MeOH, and then dried *in vacuo*. Yield: 0.95 g.

Poly, catena-oxo[N,N'-di(3-methoxysalicylidene)ethylenediaminato]manganese(IV), -[-Mn^{IV}(3-MeOsalen)-O-]$_n$: The complex was obtained from Mn^{II}(3-MeOsalen)·H_2O in the way described above. Yield: 93%.

Poly, catena-oxo[N,N'-di(5-nitrosalicylidene)ethylenediaminato]-

manganese(IV) Dimethylformamide Adduct, $-[-Mn^{IV}(5\text{-}NO_2salen)\text{-}O-]_n \cdot (DMF)_n$: The complex was prepared by a similar reaction of $Mn^{II}(5\text{-}NO_2salen)$ in a DMF solution. Yield: 90%.

These catena-oxo complexes are amorphous, and they are insoluble in water and in common organic solvents.

Measurements. The oxygen uptake was measured by using a Warburg manometer. The infrared spectra were obtained in Nujol mulls using a JASCO IR-L spectrophotometer in the 400 – 4000 cm^{-1} region, and a Hitachi EPI-L spectrophotometer in the 200 – 700 cm^{-1} region. The electronic spectra were recorded on a Hitachi EPS-3 spectrophotometer. The magnetic susceptibility was measured for a powder sample by the Faraday method, using a torsion balance[5] over the temperature range from 77 to 293 K, and by the Gouy method at room temperature. The equipment was calibrated using a standard nickel chloride solution. Thermogravimetric and differential thermal analyses were carried out using a Rigaku Denki DG-CIH Thermoflex, at a heating rate of 5 °C/min or 2.5 °C/min, and under a nitrogen stream.

Results and Discussion

As is shown in Table 1, the analytical data of the aerial

Table 1. Analytical data

	Complex	Found (%)				Calcd (%)			
		C	H	N	Mn	C	H	N	Mn
I	$[Mn^{III}(salen)]_2O_2$	56.00	4.04	8.13	16.60	57.00	4.19	8.31	16.29
II	$-[-Mn^{IV}(salen)\text{-}O-]_n$	56.12	4.04	8.26	16.47	57.00	4.19	8.31	16.29
III	$-[-Mn^{IV}(3\text{-}MeOsalen)\text{-}O-]_n$	53.50	4.65	6.84	13.63	54.41	4.57	7.05	13.76
IV	$-[-Mn^{IV}(5\text{-}NO_2salen)\text{-}O-]_n \cdot (DMF)_n$	45.39	3.77	13.77	10.89	45.60	3.84	14.00	10.98
V	$O{=}Mn^{IV}(3\text{-}MeOsalen)\cdot 2MeOH$	51.75	5.93	5.76	12.13	51.85	5.63	6.04	11.85

oxidation products of Mn^{II}-(Xsalen) are in fair agreement with the Mn(Xsalen)O formula. The data of the manometric measurements shown in Table 2 indicate that the Mn^{II}(Xsalen) uptake oxygen in a Mn : O_2 molar ratio of 1 : 0.5 is consistent with the above results. However, as will be discussed below, these products can be classified into three types of complexes, including Mn^{III}-O_2-Mn^{III}, $-(-Mn^{IV}-O-)_n-$, and Mn^{IV}=O bonds respectively, on the basis of their physicochemical data.

Table 2. Oxygen uptake of Mn^{II}(Xsalen)[a]

Complex	Solvent	Molar ratio: O_2/complex	Time[b] / min
Mn^{II}(salen)	DMSO	0.53	30
	DMF	0.46	5
	MeOH	0.30	1440
Mn^{II}(3-MeOsalen)·H_2O	DMSO	0.48	40
	MeOH	0.40	1200
Mn^{II}(5-NO_2salen)·2py	DMF	0.40	2160

a) Measurements were carried out at 20 °C.

b) The time needed for attaining equilibrium.

Solubility. Complex I (*cf.* Table 1) is slightly soluble in such organic solvents as CH_2Cl_2, DMF, and DMSO, while Complexes II and III are insoluble in these solvents. Complex IV is soluble in DMSO, but sparingly so. It should be noted that Complex V is soluble in MeOH without decomposition, whereas in a py, DMF, DMSO, or CH_2Cl_2 solution it is converted to an insoluble Complex III, in an almost quantitative yield.

Thermogravimetric Analyses. Complexes II, III, and IV show a similar pattern in the TGA curves (Fig. 1), decreasing in weight in the 200 – 225 °C range and with subsequent decomposition. These weight losses correspond to that caused by the release of 0.5 mole of oxygen per manganese atom.

Though Complex I shows a similar weight loss at 198 °C which is thought to be caused by the liberation of 0.5 mole of oxygen per manganese atom (observed, 4.6%; calcd, 5.3%), no other

remarkable decomposition is, in this case, observed to occur until *ca.* 250 °C. It should be noticed that, upon heating at about 200 °C for 1 h *in vacuo*, the complex was converted to the Mn^{II}(salen) in an 85% yield.

Complex V decreases in weight corresponding to the release of two moles of MeOH per manganese atom between 70 and 140 °C, and then it decomposes.

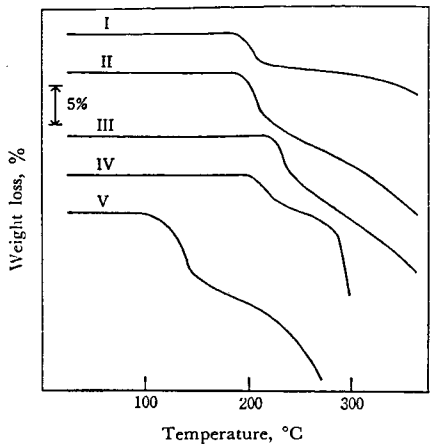

Fig. 1. TGA curves.
I: $[Mn^{III}(salen)]_2O_2$, II: $-[-Mn^{IV}(salen)-O-]_{\overline{n}}$, III: $-[-Mn^{IV}(3\text{-MeOsalen})-O-]_{\overline{n}}$, IV: $-[-Mn^{IV}(5\text{-}NO_2\text{salen})-O-]_{\overline{n}}$, V: $O{=}Mn^{IV}(3\text{-MeOsalen})\cdot 2MeOH$.

Magnetic Properties. Lewis *et al.*[3] have reported that polymeric $[Mn(salen)\text{-}O\text{-}Mn(salen)]\cdot H_2O$ shows a room-temperature magnetic moment of 2.03 – 1.92 BM, and that there exists a large antiferromagnetic interaction with J=-90 cm^{-1} for a binuclear cluster (S=2, g=2.00, and $N\alpha$=0 or S=1, g=2.05, and $N\alpha$=0). Complex I in the present study shows 1.96 BM (Table 3) at room temperature, a value which is considerably lower than those (4.96 – 4.98 BM) found for the Mn^{III}(salen)X-type complexes where X is Br^- or I^-.[6] Moreover, a significant deviation from the Curie-Weiss law is observed over the temperature range from 77 to 296 K (Fig. 2).

Table 3. Magnetic mometns and characteristic IR bands

Complex		μ_{eff} [a] / BM	IR band / cm^{-1}
	Mn^{II}(salen)	5.28 (5.27)[b]	
	Mn^{II}(3-MeOsalen)·H_2O	5.92	
I	$[Mn^{III}(salen)]_2O_2$	1.96	645, 631
II	$-[-Mn^{IV}(salen)-O-]_{\overline{n}}$	1.99	662, 602
III	$-[-Mn^{IV}(3\text{-MeOsalen})-O-]_{\overline{n}}$	1.58	655, 609
V	$O{=}Mn^{IV}(3\text{-MeOsalen})\cdot 2MeOH$	3.81	840

a) Measured at 296 K. b) Taken from ref. 3.

Below *ca.* 130 K, the data fit fairly well a curve calculated by assuming a binuclear cluster $Mn\text{-}O_2\text{-}Mn$, with J=-85 cm^{-1}, S=1, g=2.00, and $N\alpha$=0. However, at higher temperatures they deviate from the curve and fit, rather, one calculated for J=-90 cm^{-1}, S=2, g=2.00, and $N\alpha$=0. These magnetic data can be understood by taking into consideration the thermal equilibrium between spin-free and spin-paired configurations in the complex. As for Complexes II and III, their room-temperature magnetic moments are lower than that (3.75 BM) of the spin-only value expected for the octahedral Mn(IV) complexes. Moreover, the magnetic susceptibilities deviate from the Curie-Weiss law (Fig. 2); this deviation is probably caused by antiferromagnetic interaction between manganese atoms bridged by the oxygen atom. Kubo *et al.*[7] have reported that the magnetic susceptibilities of ammonium pentafluoromanganate(III), which has a linear chain structure, fit the curve calculated for a one-dimensional array of Ising spins S=2 above 80 K, assuming a "reduced" spin magnetic moment. The data for Complexes II and III do not fit the curve calculated assuming Ising spins S=3/2. As is shown in Fig. 2, the data fit, rather, the curve calculated by assuming a binuclear cluster including Mn-O-Mn bonding with S=3/2. Moreover,

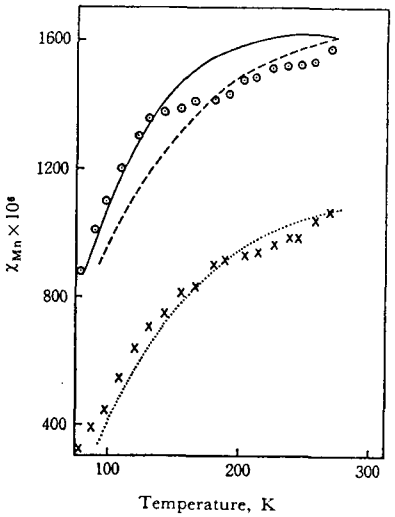

Fig. 2. Magnetic susceptibilities. ⊙: Experimental results for $[Mn^{III}(salen)]_2O_2$. ——: calculated for a binuclear cluster S=1, J=-85cm^{-1}, g=2.00, $N\alpha$=0. ---: calculated for a binuclear cluster S=2, J=-90 cm^{-1}, g=2.00, $N\alpha$=0. x: Experimental results for $-[-Mn^{IV}$(3-MeOsalen)-O-$]_n$. ···: calculated for a binuclear cluster S=3/2, J=-125 cm^{-1}, g=2.00, $N\alpha$=0.

J=-95 cm^{-1} and -125 cm^{-1} are proposed Complexes II and III respectively. As for Complex V, the room-temperature magnetic moment, 3.81 BM, is consistent with that expected for a high-spin Mn(IV). In this case, the magnetic susceptibilities fit the Curie-Weiss law well.

Infrared Spectra. Complexes I-IV show IR spectral frequencies which are comparable with those of the corresponding Mn^{II}(Xsalen) in the 700 – 4000 cm^{-1} region. On the other hand, as is shown in Fig. 3 and Table 3, the spectra of the complexes in the 600 – 700 cm^{-1} region are characterized by two intense absorption bands. The μ-oxo, $[Fe(salen)]_2O$,[3] and μ-peroxo, $[[Co(NH_3)_5]_2O_2](NO_3)_4$, including a metal-oxygen bond, show similar bands at 820 and 560 cm^{-1} respectively. In the case of Complex V, a new band is observed at 840 cm^{-1}. In view of the fact that the $[O=Mn(salen)]_2O_2$ complex, which is considered to involve both Mn=O and $Mn-O_2-Mn$ bonds, shows

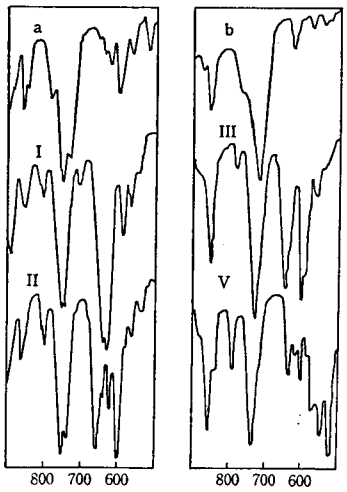

Fig. 3. IR spectra (in Nujol mulls). a: Mn^{II}(salen), I: $[Mn^{III}(salen)]_2O_2$, II: $-[-Mn^{IV}(salen)-O-]_n$, b: Mn^{II}(3-MeOsalen)·H_2O, III: $-[-Mn^{IV}(3\text{-MeOsalen})-O-]_n$, V: $O=Mn^{IV}$(3-MeOsalen)·2MeOH.

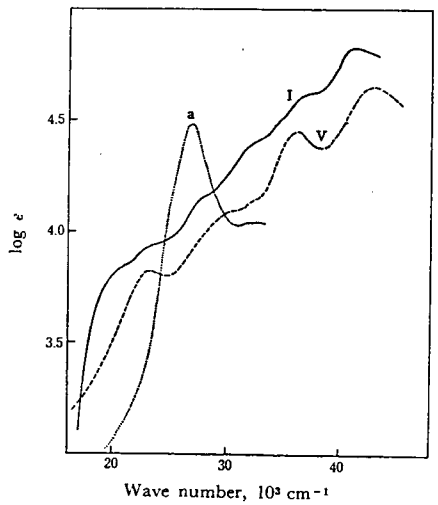

Fig. 4. Electronic spectra. a: Mn^{II}(salen) in pyridine, I: $[Mn^{III}(salen)]_2O_2$ in dichloromethane, V: $O=Mn^{IV}$(3-MeOsalen)·2MeOH in methanol.

the characteristic band at 884 cm^{-1} referred to the Mn=O, and those at 640 and 623 cm^{-1} referred to Mn-O bonds,[8] it is likely to ascribe the above bands in the 600 – 700 cm^{-1} to the Mn-O bond, and the band at 840 cm^{-1}, to the Mn=O bond.

Electronic Spectra. The electronic absorption spectra of the Mn^{II}(salen) and Complexes I and V in solution are represented in Fig. 4. The absorption bands appearing in the wave-number region higher than 25000 cm^{-1} are thought to be associated mainly with the ligand transitions. As may be seen in Fig. 4, the Mn^{II}(salen) shows no intense absorption band in the visible region. Information concerning the structure of the oxygenated complexes may be obtained by inspecting the visible spectral features. It has been reported that the spin-free manganese(III) complexes with an octahedral configuration give rise to a d-d transition band ($^5E_g \rightarrow {}^5T_{2g}$) with log ε=2.5 around 20000 cm^{-1}.[9] On the other hand, the spin-free penta-coordinate Mn^{III}(salen)X, where X is Br^- or I^-, shows two absorption bands, around 20000 cm^{-1} with log ε= 3.0 and around 25000 cm^{-1} with log ε=3.5; these have been described by Prabhakaran *et al.*[6] as a d-d transition and a charge-transfer band respectively. As can be seen in Fig. 4, the spectral pattern of Complex I with two absorption bands at *ca.* 20000 and *ca.* 23200 cm^{-1} resembles that of the penta-coordinate manganese(III) complexes. Thus, as for Complex I, the visible and the IR spectral properties, as well as the thermal property, which indicates a reversible release of oxygen, led the author to conclude that Complex I includes a μ-peroxo bond and that the structure can be depicted as is shown in Fig. 5-(a). As has been mentioned, the magnetic moment, 1.96 BM, of Complex I (*cf.* Table 3), lower than that expected for the penta-coordinate manganese(III) complexes with a square-pyramidal

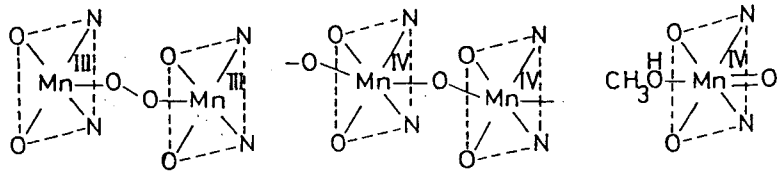

(a) (b) (c)

Fig. 5. Schematic structures for the complexes.

structure, can be explained in terms of an antiferromagnetic exchange which may be caused by the formation of a binuclear structure through the μ-peroxo bond. The magnetic moment, 3.81 BM, of Complex V (*cf.* Table 3) agrees with the assumption that the complex includes a spin-free Mn(IV). The visible electronic spectrum of Complex V, unlike that of Complex I, shows only one peak, at 23200 cm^{-1}. This spectral feature is not inconsistent with those of such spin-free, octahedral manganese(IV) complexes as $[MnF_6]^{2-}$ and $[MnCl_6]^{2-}$, which show absorption maxima at 21800 and 17900 cm^{-1} respectively.[10] On the basis of these facts, a proposed structure for Complex V is shown in Fig. 5-(c). The insolubility of Complexes II, III, and IV did not allow measurements of the electronic spectra in solution. However, the magnetic properties and the IR spectral data, as well as the fact they are obtained from the oxo complexes, led the author to propose the structure for the complexes shown in Fig. 5-(b).

Effects of Oxygen Partial Pressure, Solvent, and Substituent on the Oxidation Reaction. As has been discussed above, three types of complexes containing a μ-peroxo, catena-oxo-, or oxo-bond were isolated in the reactions of the Mn^{II}(Xsalen) with oxygen in organic solvents. The effects of the oxygen partial pressure and of the nature of the solvents and substituents, X, on the complex formation will be considered.

As has been described in Experimental, the Mn^{II}(salen) yielded, upon reaction with oxygen in a DMSO solution, the μ-peroxo complex as a precipitate plus precipitates of the catena-oxo complex. As can be seen in Table 4, the amount of the μ-peroxo complex of the above precipitates increases with a decrease in the partial pressure of oxygen applied in the reaction system; it increases up to 86% when oxygen diluted to 1.7 vol% by mixing with nitrogen is used. It can be noticed that, in py and DMF solutions, the reaction using dilute oxygen gave the μ-peroxo complex, although the reaction using pure oxygen only afforded the catena-oxo complex.

The results (*cf.* Table 4) suggest that the formation of the μ-peroxo complex is favored in the solvents in the following order; py < DMF < DMSO, and that it is also favored when oxygen with a lower partial pressure is allowed to react.

Table 4. The effects of oxygen partial pressure and solvents on the formation of $[Mn^{III}(salen)]_2O_2$ and $-[-Mn^{IV}(salen)-O-]_n$ [a]

P_{O_2} (vol%) [b]	Yield [c]		
	DMSO	DMF	Py
1.7	86	82	21
10	—	50	—
20	—	16	0
100	10	0	0

a) The reactions were carried out using Mn^{II}(salen) (1 g) and solvent (50 ml), at room temperature for 15 hr.. $[Mn^{III}(salen)]_2O_2$ was separated as soluble part by extraction with CH_2Cl_2.

b) Represented in volume % of O_2 in mixed $O_2 + N_2$ at atmospheric pressure and room temperature.

c) Corresponds to $\frac{[Mn^{III}(salen)]_2O_2}{[Mn^{III}(salen)]_2O_2 + -[-Mn^{IV}(salen)-O-]_n} \times 100$ in gram.

As for the Mn^{II}(3-MeO-salen)·H_2O and Mn^{II}(5-NO_2salen)·2py complexes, the corresponding μ-peroxo complex could not be obtained even if the reaction was carried out in a DMSO solution using dilute oxygen of 1.7 vol%. The oxo complex, $O=Mn^{IV}$(3-MeOsalen)·2MeOH, was successfully isolated only for the 3-methoxy substituted complex in a MeOH solution. Further, it is of importance that, in a DMF, DMSO, or py solution, the oxo complex is transformed to the insoluble catena-oxo complex, $-[-Mn^{IV}(3\text{-MeOsalen})-O-]_n$, almost quantitatively, indicating that the reaction forming the catena-oxo complex proceeds

via the oxo complex. The low solubility of the catena-oxo and μ-peroxo complexes did not allow kinetical measurements. However, in view of the results obtained in the present study, it can be interpreted by assuming that the reactions proceed as follows:

$$S\text{-}(Mn^{II})\text{-}S + O_2 \xrightarrow{k_1} S\text{-}(Mn^{III})\text{-}O_2 + S \quad (1)$$

$$S\text{-}(Mn^{III})\text{-}O_2 + O_2\text{-}(Mn^{III})\text{-}S \xrightarrow{k_2} 2S\text{-}(Mn^{III})\text{-}O\cdot + O_2 \quad (2)$$

$$S\text{-}(Mn^{III})\text{-}O\cdot \longrightarrow S\text{-}(Mn^{IV})=O \quad (2\text{-}1)$$

$$n[S\text{-}(Mn^{IV})=O] \longrightarrow -[-(Mn^{IV})\text{-}O\text{-}]_n^- + n\cdot S \quad (2\text{-}2)$$

$$S\text{-}(Mn^{III})\text{-}O_2 + S\text{-}(Mn^{II})\text{-}S \xrightarrow{k_3} S\text{-}(Mn^{III})\text{-}O_2\text{-}(Mn^{III})\text{-}S \quad (3)$$

((Mn) represents a parent complex, Mn^{II}(Xsalen).)

As is illustrated in Fig. 4, the Mn^{II}(salen) shows an electronic absorption maximum at 27000 cm^{-1} (log ε=4.5); this maximum is shifted to a lower frequency with the solvents in the order of MeOH (28700 cm^{-1}) > DMF (27700 cm^{-1}) > DMSO (27600 cm^{-1}) > py (27000 cm^{-1}). Similar spectral behavior is observed for the substituted Mn^{II}(Xsalen). These results seem to indicate that the complexes are coordinated with the solvent in solutions. In fact, an adduct with a solvent, *e.g.*, Mn^{II}(5-NO_2salen).2py, is isolated. Hence, the reaction of the manganese(II) complexes with oxygen could be initiated by replacing a coordinated solvent molecule with oxygen, thus forming an intermediate superoxo complex, as is represented in Eq. 1. When assuming that the unstable superoxo complex thus formed undergoes reactions to yield both oxo- and μ-peroxo complexes, following Eqs. 2 and 3, respectively, the reaction rate in respect to the superoxo complex can be given as:

$$d[S\text{-}(Mn^{III})\text{-}O_2]/dt = k_1[O_2][S\text{-}(Mn^{II})\text{-}S] - k_2[S\text{-}(Mn^{III})\text{-}O_2]^2 - k_3[S\text{-}(Mn^{II})\text{-}S][S\text{-}(Mn^{III})\text{-}O_2] \quad (4)$$

where k_1, k_2, and k_3 are the rate constants in Reactions 1, 2, and 3 respectively.[11] Reactions 2-1 and 2-2 are thought to follow Reaction 2 very rapidly in DMF, DMSO, and py solutions. In view of the fact that the catena-oxo, and μ-peroxo complexes were separated out of the reaction system as precipitates, the concentration of the superoxo complex involved in solution must remain approximately constant during the reaction; that is,

$$d[S\text{-}(Mn^{III})\text{-}O_2]/dt = 0 \quad (5)$$

Thus, the ratio of the yield of the catena-oxo complex to the μ-peroxo complex can qualitatively be described as:[11]

$$\frac{\text{catena-oxo complex}}{\text{μ-peroxo complex}} \propto \frac{k_1 k_2}{k_3^2} \cdot \frac{[O_2]}{[S\text{-}(Mn^{II})\text{-}S]} \quad (6)$$

proportinal to the ratio of $[O_2]$ to $[S\text{-}(Mn^{II})\text{-}S]$. This relation can explain the experimental finding (*cf.* Table 4) that the yield of the catena-oxo complex decreases with a decrease in the oxygen concentration.

In a solvent such as pyridine, which tends to coordinate with a stronger affinity toward the central manganese ion, it is not unreasonable to expect a smaller k_1 than in another solvent. Hence, the higher yield of the catena-oxo complex by the reaction in the pyridine solution implies smaller k_3 and k_1 values. The failure to obtain the μ-peroxo compound of the Mn^{II}(3-MeOsalen)·H_2O may be attributed mainly to a larger k_1 caused by the electron-donating methoxy group, which weakens the bonding of the central manganese

ion with the solvent. The fact that the $Mn^{II}(5\text{-}NO_2salen)\cdot 2py$ yielded the catena-oxo complex, even in the DMSO solution, can be explained in terms of a stronger bonding with the solvent due to the electron-withdrawing nitro group.

The author wishes to thank Associate Professor C. Miyake for the use of equipment for magnetic susceptibility measurements by means of the Faraday method.

Summary

By the reaction of Mn^{II}(salen) and its analogs with molecular oxygen in organic solvents, three types of complexes including as structural units the $Mn^{III}\text{-}O_2\text{-}Mn^{III}$, $-(-Mn^{IV}\text{-}O\text{-})_{\overline{n}}$, and $Mn^{IV}{=}O$ bonds respectively, have been obtained, and characterized by means of their electronic and infrared spectra, by thermogravimetric analysis, and in terms of their magnetic properties. The lower magnetic moments for $[Mn^{III}(salen)]_2O_2$ and $-[-Mn^{IV}(salen)\text{-}O\text{-}]_{\overline{n}}$ than those expected have been interpreted in terms of antiferromagnetic interactions. The oxo complex was found to give the catena-oxo complex quantitatively in a DMF, DMSO, or py solution. The effects of the oxygen partial pressure and the nature of the substituent in the organic part on the complex formation were investigated. A lower partial pressure of oxygen has the advantage of yielding the μ-peroxo complex in a higher yield. The reaction mechanism is discussed.

References and notes

1) The following abbreviations are used; $salenH_2$; N,N'-disalicylideneethylenediamine, $3\text{-}MeOsalenH_2$; N,N'-di(3-methoxysalicylidene)-

ethylenediamine, 5-NO_2salenH_2; N,N'-di(5-nitrosalicylidene)-ehtylenediamine, salpnH_2; N,N'-disalicylidene-1,3-propanediamine, DMF; N,N-dimethylformamide, DMSO; dimethyl sulfoxide, py; pyridine, MeOH; methanol.

2) T. Tsumaki, *Nippon Kagaku Zasshi*, 55, 1245 (1934).

3) J. Lewis, F. E. Mabbs, and H. Weigold, *J. Chem. Soc., A*, 1968, 1969.

4) G. L. Johnson and W. D. Beveridge, *Inorg. Nucl. Chem. Lett.*, 3, 323 (1967).

5) T. Mori, C. Miyake, and T. Sano, *Trans. JIM*, 4, 158 (1963).

6) C. P. Probhakaran and C. C. Patel, *J. Inorg. Nucl. Chem.*, 31, 3319 (1969).

7) S. Emori, M. Inoue, M. Kishita, and M. Kubo, *Inorg. Chem.*, 8, 1385 (1969).

8) T. Tamaki, I. Masuda, and K. Shinra, *Chem. Lett.*, 1972, 165.

9) R. Dingle, *Acta Chem. Scand.*, 20, 33 (1966).

10) A. B. P. Lever, "Inorganic Electronic Spectroscopy," Elsevier Publishing Co., (1963), p. 283.

11) From Eqs. 4 and 5, concentration of superoxo complex is given as follows:

$$[S\text{-}(Mn^{III})\text{-}O_2] = \frac{[S\text{-}(Mn^{II})\text{-}S]}{2k_2} \times \left(-k_3+\sqrt{k_3^2+4k_1k_2[O_2]/[S\text{-}(Mn^{II})\text{-}S]}\right) \quad \text{(i)}$$

And, the rate equation respect to catena-oxo, and μ-peroxo complexes are given by Eqs. (ii) and (iii), respectively:

$$d[-(-(Mn^{IV})\text{-}O\text{-})_{\overline{n}}]/dt = (1/n)\cdot d[S\text{-}(Mn^{III})\text{-}O\cdot]/dt = (k_2/n)[S\text{-}(Mn^{III})\text{-}O_2]^2 \quad \text{(ii)}$$

$$d[S\text{-}(Mn^{III})\text{-}O_2\text{-}(Mn^{III})\text{-}S]/dt = k_3[S\text{-}(Mn^{III})\text{-}O_2][S\text{-}(Mn^{II})\text{-}S] \quad \text{(iii)}$$

Then, from the Eqs. (i), (ii), and (iii) the ratio of reaction

rate for catena-oxo complex to that for μ-peroxo complex is derived as,

$$\frac{d[-(-(Mn^{IV})-O-)_n-]/dt}{d[S-(Mn^{III})-O_2-(Mn^{III})-S]/dt} = \frac{k_2[S-(Mn^{III})-O_2]}{nk_3[S-(Mn^{II})-S]}$$

$$= (1/2n)\left(-1 + \sqrt{1 + (4k_1k_2/k_3^2)\frac{[O_2]}{[S-(Mn^{II})-S]}} \right) \quad \text{(iv)}$$

Eq. (iv) can be qualitatively transformed as shown by Eq. 6.

I - 2 Preparation of Iron(II) Schiff Base Complexes Supported on Polystyrene and Their Oxygenation in Solution

Introduction

It is well known that reversible oxygenation of hemoglobin and myoglobin can be accompolished by the steric and hydrophobic effects of globin proteins.[1] Wang has reported a synthetic model which was made by embeding molecules of the diethyl ester of hemes in a hydrophobic matrix of polystyrene and 1-(2-phenylethyl)-imidazol.[2] These embeded heme groups have been found to combine with O_2 reversibly even in the presence of water. Recently, iron(II) complexes with modified porphyrins such as "picket-fence"[3] and "capped"[4] porphyrins have been synthesized as models for myoglobin and found to combine with O_2 reversibly to form 1 : 1 superoxo complexes at or near room temperature.

In this section, the preparation and oxygenation of iron(II) Schiff base complexes which are bonded covalently to polystyrene (shown below) will be described.

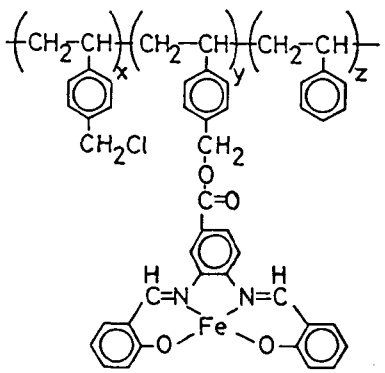

Fe(Pst-salphen)

Experimental

Measurements. IR spectra were recorded on a Hitachi 215 grating spectrophotometer. UV and VIS spectra were recorded on a Hitachi 340 recording spectrophotometer. Polarograms were measured with a Yanagimoto P-8 polarograph. Magnetic susceptibilities were determined by the Gouy method. Oxygen uptakes were measured by use of a Warburg manometer.

Materials. All the reagents were of reagent grade. Solvents were purified by a usual manner. Polystyrenes having molecular weights 2500 (highmer-ST_{120}) and 1400 (highmer-ST_{95}) which were obtained from Sanyo Chemical Ind. Co. were used without further purification.

Preparation of Chloromethylated Polystyrene. Chloromethylated polystyrenes were prepared by the following modified method described in the literature.[5] Zinc chloride (4.5 g) was added to a chloromethyl ethyl ether (200 cm^3) solution of polystyrene with MW=1400 (28.5 g). The mixture was warmed in a water-bath kept at 49 - 50 ^{o}C for 70 min. After a dioxane solution (75% wt/wt) of water equimolar to the $ZnCl_2$ had been added, an equivolume amount of water to the dioxane solution was added to separate two phases. The upper phase solution was separated, followed by evaporation to remove the chloromethyl ethyl ether under reduced pressures yielding a gel product. This was dissolved in dioxane (20 cm^3). The solution was filtered, and the filtrate was poured into a large volume of methanol (300 cm^3) to produce a white precipitate. It was reprecipitated from a mixture of tetrahydrofuran (THF) and methanol. The yield was 13.6 g. The extent of chloromethylation was calculated to be *ca.* 26% from the content of chlorine (7.98%).

The chloromethylated polystyrene using polystyrene with MW=2500 was obtained in a similar manner. The extent of chloromethylation was calculated to be *ca.* 32.7% from the content of chlorine (9.67%).

Preparation of a Schiff Base Ligand; N,N'-disalicylidene-4-carboxy-1,2-phenylenediamine, 4'-COOH-salphenH_2. To a THF (150 cm^3) solution of 3,4-diaminobenzoic acid (4.56 g, 0.03 mol) was added salicylaldehyde (14.4 g, 0.12 mol). The mixture was refluxed for 1 h and filtered. The filtrate was evaporated to dryness under reduced pressures. Ether (100 cm^3) was added to this to give an orange-yellow precipitate. It was collected on a glass filter, washed with ether, and dried *in vacuo*. Yield : 8.7 g. mp, 199.5–201.5 ^{o}C. Found: C, 69.54; H, 4.38; N, 7.71%. Calcd for $C_{21}H_{16}N_2O_4$: C, 69.99; H, 4.48; N, 7.77%.

Preparation of Schiff Base Ligands Supported on Polystyrene; Pst-salphenH_2-(I). To a dioxane solution (150 cm^3) of the chloromethylated polystyrene (4.0 g) which was obtained from polystyrene with MW=1400 were added 4'-COOH-salphenH_2 (3.0 g) and triethylamine (2.0 g). The mixture was refluxed for 3 h and then evaporated under reduced pressures to give a yellow solid. It was dissolved in N,N-dimethylformamide (DMF, 20 cm^3), and the solution was poured onto a large volume of water (500 cm^3). The resulting yellow product was collected on a glass filter, washed with methanol several times, and dried *in vacuo*. The yield was 4.0 g. The content of the Schiff base was calculated to be 0.47 mmol/g from the elemental analysis. Another Pst-salphenH_2-(II) was obtained in a similar manner by use of the chloromethylated polystyrene which was prepared from polystyrene with MW=2500.

This contained the Schiff base ligand of 0.41 mmol/g. The analytical values obtained for the two polymers indicate the inclusion of one molecular unit of the Schiff base per a polymer chain.

Preparation of the Iron(II) Complex; [Fe(4'-COOH-salphen)·H_2O]. To a THF (30 cm^3) solution of 4'-COOH-salphenH_2 (1.0 g) were added Mohr's salt, $Fe(SO_4)(NH_4)_2SO_4 \cdot 6H_2O$, (1.07 g) and a mixture of pyridine (2 cm^3) and water (11 cm^3). The resulting solution was kept at 50 °C for 20 min, followed by the addition of water (100 cm^3) to give an olive precipitate. It was filtered, washed with water and then ether, and dried *in vacuo*. All the procedures were carried out under nitrogen atmosphere. The yield was 1.1 g. Found: C, 57.28; H, 3.31; N, 6.65; Fe, 11.97%. Calcd for $Fe(C_{21}H_{14}N_2O_4)(H_2O)$: C, 58.36; H,3.73; N, 6.48; Fe, 12.92%. This complex was stored in an evacuated tube to avoid aerial oxidation.

Preparation of Polymeric Iron(II) Complexes; [Fe(Pst-salphen)]-(I). To a DMF (20 cm^3) solution of Pst-salphenH_2-(I)(1.0 g) was added dropwise a methanol solution (20 cm^3) of triethylamine (0.3 g) with stirring. An aqueous solution (5 cm^3) of Mohr's salt (0.12 g) was added to the solution with stirring. After allowing to stand for 20 min, the resulting pale brown solid was filtered, washed with water, a mixture of water and methanol (1 : 1), and then methanol, and dried *in vacuo*. All the procedures were carried out under nitrogen atmosphere. The yield was 0.8 g. The content of iron atom in this polymeric complex was determined to be 1.9%.

[Fe(Pst-salphen)]-(II). This complex was prepared in a manner similar to that described above, using the Pst-salphenH_2-(II)

which was obtained from polystyrene with MW=2500. The content of iron atom in this polymeric complex was determined to be 1.2%.

Results and Discussion

The purpose of this work is the preparation of iron(II) Schiff base complexes supported on polystyrene which are soluble in organic solvents. Thus, polystyrenes having relatively low molecular weights (1400 and 2500) were chosen as starting materials. The degree of chloromethylation of these polystyrenes was controlled to be *ca.* 30%, avoiding formation of cross-linked polymers. By controlling the reaction conditions the contents of Schiff base ligand bonded to the polystyrene were regulated to be 0.5 mmol ligand/g or less than that. In these polymers the Schiff base group is involved its one molecular unit per a polymer chain. The polymeric iron(II) complexes, [Fe(Pst-salphen)]-(I) and (II), are soluble in DMF and in pyridine.

Table 1 summarizes the magnetic moments of the monomeric and polymeric iron(II) complexes at room temperature and their oxygen uptakes. The values of magnetic moments are not contradict with that expected for complexes with d^6 high-spin electron configuration. The oxygen uptake of [Fe(4'-COOH-salphen)·H_2O] shows the ratio of O_2 to Fe nearly equal to 0.25, indicating the formation of μ-oxo dimers. On the other hand, the polymeric iron(II) complexes show the oxygen uptake beyond 0.5 (O_2/Fe). This is suggestive of the formation of 1 : 1 adducts with dioxygen.

Figures 1 A and 1 B show the changes in the polarograms of [Fe(4'-COOH-salphen)·H_2O] and [Fe(Pst-salphen)]-(I), respectively, in the course of the reaction with O_2 in DMF. The monomeric

Table 1. Magnetic moments and oxygen uptake of iron(II) Schiff base complexes

Complex	μ_{eff} [a] / BM	Oxygen uptake / O_2/Fe
[Fe(4'-COOH-salphen)·H_2O]	5.31	0.27[b]
[Fe(Pst-salphen)]-(I)	5.19	0.77[c]
[Fe(Pst-salphen)]-(II)	5.46	0.62[c]

a) Measured at room temperature. b) Measured in DMF at 25 °C. c) Measured in DMF at 0 °C.

iron(II) complex shows the cathodic wave at -1.50 V due to the reduction of Fe(II) to Fe(0) under nitrogen (N_2) atmosphere as shown in curve 1. The cathodic waves are observed at -0.32 and -0.80 V by introducing O_2 to the solution. When N_2 was bubbled to the solution again, the former remains without change but the latter wave disappears. Thus, the cathodic waves at -0.32 and -0.80 V can be assigned to the reductions of Fe(III) to Fe(II) and of free O_2 in solution, respectively, on the basis of the reduction potentials. This indicates that the monomeric iron(II) complex is oxidized to iron(III) complex irreversibly by O_2. On the other hand, the polarograms of [Fe(Pst-salphen)]-(I) show a behavior different from those for the monomeric iron(II) complex. The cathodic wave at -0.28 V observed by introducing O_2 disappears by passing N_2 through the solution showing curve 2 in Fig. 1 B. Such a cycle can be repeated at least three times without change in the polarograms. The polarogram observed after allowed to stand for 24 h under dry air shows the cathodic wave at -0.08 V as shown in curve 3. This wave can be assigned to the reduction of Fe(III)

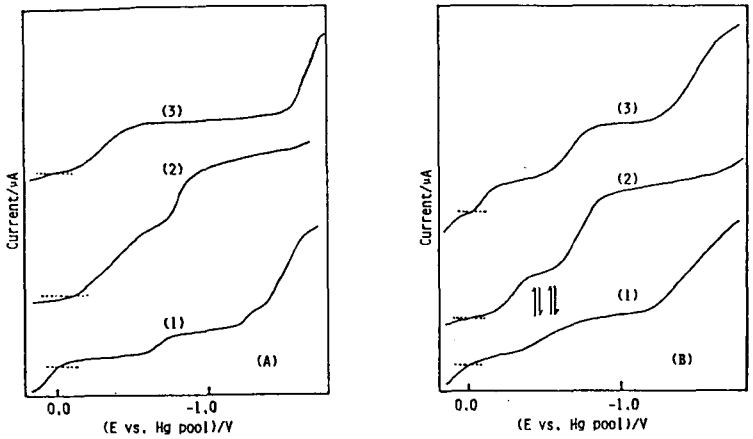

Fig. 1. Polarograms of [Fe(4'-COOH-salphen)·H_2O] (A) and [Fe(Pst-salphen)]-(I) (B) in the course of the reaction with O_2 in DMF at 25 °C.
(A): (1), under N_2; (2), under O_2; (3), after bubbled N_2 into the solution shown in curve 2. (B): (1), under N_2; (2), under O_2; (3), after allowed to stand for 24 h under dry air.

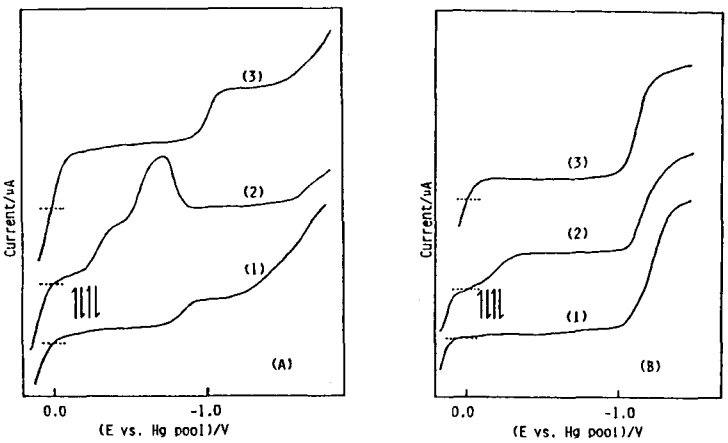

Fig. 2. Polarograms of [Fe(Pst-salphen)]-(I) in the course of the reaction with O_2 in pyridine (A) and in a mixture of pyridine and water (99/1 in v/v) (B) at 25 °C.
(A) and (B): (1), under N_2; (2), under O_2; (3), after allowed to stand for 24 h under dry air.

to Fe(II), indicating that the polymeric iron(II) complex was oxidized to iron(III) complex gradually by O_2. Therefore, the cathodic wave at -0.28 V can be assigned to the reduction of the oxygenated complex, probably the 1 : 1 adduct with dioxygen.

Such reversible oxygenations have been found to occur in a pyridine solution and even in a mixed solution of pyridine and water (99/1 in v/v) of [Fe(Pst-salphen)]-(I), as shown in Figs. 2 A and 2 B, respectively. The same behavior was observed in polarograms of [Fe(Pst-salphen)]-(II) in the course of the reaction with O_2. These results indicate that the reversible oxygenation may take place in the iron(II) complexes supported on polystyrene. This may be caused by the polystyrene matrix which protects the iron(II) complexes from the irreversible oxidation *via* dimerization and *via* nucleophilic attack of water molecules by the steric hindrance and hydrophobic effects.

Unfortunately, the UV and VIS absorption spectra accompanied by the oxygenation of the polymeric iron(II) complexes have not been observed clearly owing to disturbance of intense absorption bands of the Schiff base ligand bonded to the polymers. Furthermore, oxygenated products of the polymeric iron(II) complexes have not been characterized by other physicochemical methods in this work, because of the instability of oxygenated iron complexes which formed in solution.

Summary

The iron(II) Schiff base complexes supported on polystyrene combine with O_2 reversibly in solution, although the corresponding monomeric complex is oxidized to the iron(III) complex irreversibly.

References

1) C. L. Nobbs, H. C. Watson, and L. C. Kendrew, *Nature*, 209, 339 (1966).

2) J. H. Wang, *Acc. Chem. Res.*, 3, 90 (1970).

3) J. P. Collman, R. R. Gagne, T. R. Halbert, J. C. Marchon, and C. A. Reed, *J. Am. Chem. Soc.*, 95, 7868 (1973).

4) J. Almog, J. Baldwin, R. L. Dyer, and M. Peters, *J. Am. Chem. Soc.*, 97, 226 (1975).

5) D. J. Giffin, *Ind. Eng. Chem.*, 44, 2686 (1952).

Chapter II

Adducts of Bis(β-diketonato)manganese(II) with N,N-Dimethylformamide, Dimethyl Sulfoxide, and Pyridine

Introduction

The manganese(II) complex of acetylacetone $Mn(acac)_2$, first prepared by Emmert,[2] has been reported to form the adducts with formulas $Mn(acac)_2B_2$ where B is H_2O, NH_3, pyridine derivatives, quinoline, isoquinoline, or primary amines; and $Mn(acac)_2B$ where B is pyridine derivatives, pyrazine, or allylamine.[2 - 7] Recently, Koda *et al.*[8] have revealed by X-ray study that crystalline $Mn(acac)_2(NH_2\text{-}CH_2\text{-}CH{=}CH_2)$ has a dimer structure containing six-coordinate manganese ions and two moles of acetylacetonate groups as bridging ligand. Graddon *et al.*[4] have shown on the basis of the molecular weight measurements that $Mn(acac)_2B_2$ and $Mn(acac)_2B$, where B is pyridine and its analogs, tend to dissociate the axial bases and form a dimer and/or a trimer complexes in the non-coordinating solvents such as benzene and triphenylmethane. Hudson *et al.* pointed out by inspection of the ESR spectra that anhydrous $Mn(acac)_2$ is monomeric in a DMF solution, dimeric in a mixed ether-pentane-ethanol solution, and trimeric in an *ortho*-terphenyl solution.[9]

In the course of the study on the reaction of the transition metal complexes with molecular oxygen in organic solvents such as DMF, DMSO, or pyridine, it was found that the reaction of the manganese(II) complexes depends remarkably upon the nature of the solvents, as described in section I-1. This prompted the author to investigate the adduct formation of $Mn^{II}(\beta\text{-diketonato})_2$ with these solvents.

Experimental

Measurements. The IR spectral measurements, thermogravimetric analyses, and magnetic susceptibility measurements were carried by using instruments described in section I-1.

Materials. All reagents were of reagent grade. Solvents were purified in a usual manner. $Mn(acac)_2 2H_2O$ and $Na[Mn(acac)_3]$ were prepared by the method in the literature.[4] $Mn(bzac)_2 2H_2O$, $Mn(dbm)_2 2H_2O$, and $Mn(tfac)_2 2H_2O$ were obtained by a similar way to the above.

Preparation of the Adducts. $Mn(acac)_2 py$ and $Mn(acac)_2 2py$ were prepared by the literature.[4]

$[Mn(acac)_2]_2 DMF$: $Mn(acac)_2 2H_2O$ (2.0 g) was dissolved in an oxygen free, anhydrous DMF (30 cm^3). The solution was evaporated very slowly in a desiccator under reduced pressure at room temperature until crystals began to separate. Ivory colored crystals separated were collected on a filter, and washed with a small amount of anhydrous ether, and then dried *in vacuo*. Yield: 1.7 g.

$Mn(acac)_2 DMSO$: The complex was obtained similarly from a DMSO solution of $Mn(acac)_2 2H_2O$ by evaporating the solution to dryness. The adduct was kept on a filter paper in a desiccator. Yield: 1.4 g. Washing with ether caused a decomposition of the adduct.

The adducts with DMF, DMSO, and py obtained in a similar way are listed in Table 1.

Results and Discussion

Table 1 includes the analytical data of the adducts. These data indicate a $Mn(acac)_2$ to DMF molar ratio of 2 : 1, and a

Table 1. Melting points, color, and analytical data of the adducts

Compounds	M.P. °C	Color	Analysis (%) Found (Calcd) C	H	N	Mn
$[Mn(acac)_2]_2DMF$	decomp.	ivory	47.57 (47.68)	6.04 (6.09)	2.37 (2.42)	19.22 (18.97)
$Mn(acac)_2DMSO$	decomp.	ivory	43.22 (43.51)	5.93 (6.08)		16.45 (16.58)
$Mn(bzac)_2 2DMF$	70-71	yellow	59.81 (59.66)	6.39 (6.16)	5.59 (5.35)	10.91 (10.49)
$Mn(bzac)_2 2DMSO$	109-110	orange	53.93 (54.03)	5.66 (5.67)		10.49 (10.30)
$Mn(bzac)_2 2py$	98.5-99.5	wine red	67.06 (67.54)	5.29 (4.91)	5.03 (5.25)	10.80 (10.30)
$Mn(dbm)_2 2DMF$	222-223	wine red	66.94 (66.77)	5.47 (5.60)	4.32 (4.33)	8.70 (8.48)
$Mn(dbm)_2 2DMSO$	251-252	wine red	62.16 (62.09)	5.18 (5.21)		8.82 (8.35)
$Mn(dbm)_2 2py$	234-235	wine red	72.51 (72.83)	4.99 (4.89)	4.18 (4.25)	8.60 (8.33)
$Mn(tfac)_2 2DMSO$	109	yellow				10.66 (10.62)
$Mn(tfac)_2 2py$ [a]	98-98.5	yellow				10.85 (10.60)

a) py; Found: 30.2%, Calcd: 30.4%. Pyridine content was analyzed by a modification[10] of Kieldahl method.

$Mn(acac)_2$ to DMSO molar ratio of 1 : 1. Whereas, in the cases of the other β-diketonate complexes, only bis-adducts with DMF, DMSO, or py could be obtained.

As shown in Fig. 1, the TGA curves of DMF, DMSO, and py adducts of acetylacetonate clearly show a weight loss in the 90 - 160 °C range corresponding to the release of the bases. The bis-adducts of the other β-diketonates do not show a clear thermal dissociation of the additional bases.

DMF Adducts: It is well established that the coordination of DMF to the transition metal ions through the oxygen results in a shift of the C=O stretching band to a lower frequency than that of free DMF.[11 - 13] The spectrum of $[Mn(acac)_2]_2DMF$ in Nujol mulls shows a new band comparing with that of $Mn(acac)_2$ at 1656 cm^{-1} which can be ascribed to the oxygen-coordinated DMF (*cf.* Table 2). While in the cases of $Mn(bzac)_2 2DMF$ and $Mn(dbm)_2$-2DMF, it is noticed that newly two bands are observed in the above region, *i.e.*, at 1669 and 1641 cm^{-1} in the former; at 1664 and 1642 cm^{-1} in the latter (*cf.* Table 2 and Figs. 2 and 3). These facts suggest different two molecules of DMF being bonded in the compounds.

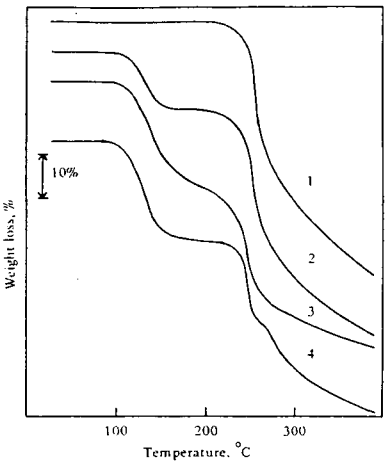

Fig. 1. TGA curves measured at a heating rate of 2.5 °C/min under a nitrogen stream.
1: $Mn(acac)_2$, 2: $[Mn(acac)_2]_2DMF$, 3: $Mn(acac)_2DMSO$, 4: $Mn(acac)_2py$.

As is seen in Fig. 2, in a 1,2-dichloroethane solution, above characteristic two bands disappeared, and an intense band appeared at 1678 cm^{-1} which

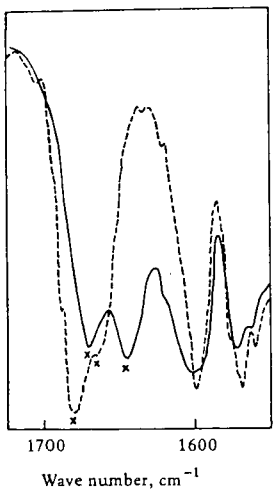

Fig. 2. IR spectra of $Mn(bzac)_2 2DMF$; —— in Nujol, --- in $C_2H_4Cl_2$.

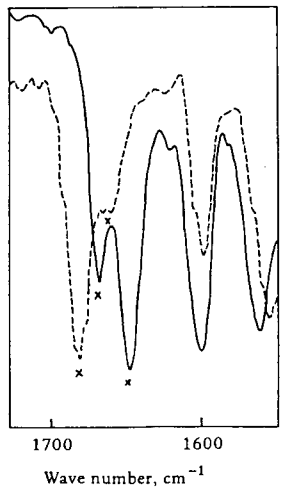

Fig. 3. IR spectra of $Mn(dbm)_2 2DMF$; —— in Nujol, --- in $C_2H_4Cl_2$.

Table 2. Characteristic IR-bands,[a] (cm^{-1})

Compound	ν(C=O)	ν(S=O)	CH_3 rocking
DMF[b]	1678		
$[Mn(acac)_2]_2$DMF	1656		
$Mn(bzac)_2$2DMF	1669, 1641		
$Mn(dbm)_2$2DMF	1664, 1642		
DMSO[b]		1065	950
$Mn(acac)_2$DMSO		1064	960
$Mn(bzac)_2$2DMSO		1020	956
$Mn(dbm)_2$2DMSO		1043	951
$Mn(tfac)_2$2DMSO		1015	960

Measured, a) in Nujol mulls and b) in $C_2H_4Cl_2$.

quite agrees with that of free DMF in a 1,2-dichloroethane solution. A shoulder band at *ca.* 1660 cm^{-1} was not observed in a diluted solution. Similar spectral behavior is also observed as for $Mn(dbm)_2$2DMF (*cf.* Fig. 3). These results are thought to indicate that the DMF adducts dissociate the DMF in the solution. And the apparent degree of the dissociation has been evaluated as shown in Table 3, on the basis of the IR spectral change.

DMSO Adducts: The DMSO molecule coordinated through the oxygen to the first-row transition-metal ions is known to be characterized by the infrared S=O stretching band observed in the 985 - 1025 cm^{-1} region, being shifted to a lower frequency than that of free DMSO.[14] As shown in Figs. 4 and 5, the characteristic S=O band can also be visualized in the spectra of the present DMSO adducts. The numerical data are listed in Table 2. In a 1,2-dichloroethane solution, this band apparently disappeared and an intense band is observed at 1065 cm^{-1} which agrees with that of free DMSO, indicating that the adducts dissociate the DMSO in the solution (*cf.* Figs. 4 and 5). Further, it is noticed that the band observed at around

955 cm^{-1} for DMSO adducts in Nujol mulls, which may be ascribed predominantly due to the CH_3 rocking mode of the DMSO, is realized to appear at 950 cm^{-1} in a 1,2-dichloroethane solution which farely corresponds to the free DMSO. And the degree of the dissociation is evaluated as given in Table 3.

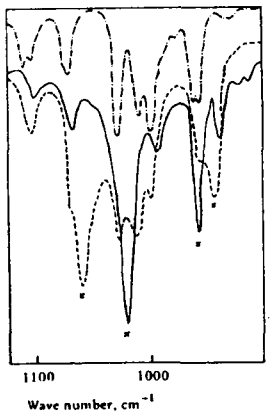

Fig. 4. IR spectra of $Mn(bzac)_2 2DMSO$; —— in Nujol, --- in $C_2H_4Cl_2$, and of $Mn(bzac)_2 2H_2O$; -·- in Nujol.

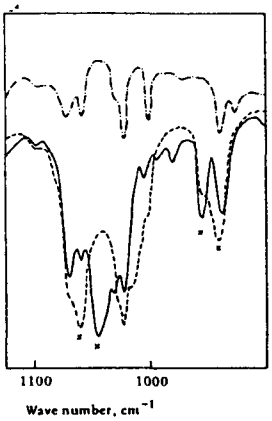

Fig. 5. IR spectra of $Mn(dbm)_2 2DMSO$; —— in Nujol, --- in $C_2H_4Cl_2$, and of $Mn(dbm)_2 2H_2O$; -·- in Nujol.

Table 3. Degree of dissociation of the adducts in 1,2-dichloroethane

Compound	Concentration of adduct/ mol dm^{-3}	Degree of dissociation/ %[a)]
$Mn(bzac)_2 2DMF$	0.031	80.7
$Mn(dbm)_2 2DMF$	0.031	62.3
$Mn(bzac)_2 2DMSO$	0.028	73.5
$Mn(dbm)_2 2DMSO$	0.035	72.3

a) The degree of dissociation was evaluated by using the concetration of free DMF or DMSO in solution determined from the optical density of the band at 1678 cm^{-1} for DMF adduct, or 1065 cm^{-1} for DMSO adduct, on the basis of the calibration curve.

The IR spectra of DMF, DMSO, and py adducts of $Mn(acac)_2$ in the 300 - 700 cm^{-1} region are shown in Fig. 6. The absorption bands observed for $[Mn(acac)_2]_2DMF$ at 356, 375, and 673 cm^{-1}, and for $Mn(acac)_2DMSO$ at 317 and 332 cm^{-1} can be assigned due to the DMF[16] and DMSO[17], respectively. In the region of 400 - 500 cm^{-1} where metal-oxygen vibration are expected to appear,[18, 19] anhydrous $Mn(acac)_2$ shows two intense bands at 399 and 449 cm^{-1}, while $Mn(acac)_2 2H_2O$ shows only one intense band at 412 cm^{-1}. As for the pyridine adducts, the spectral feature around 400 cm^{-1} appears to be complicated comparing with that of $Mn(acac)_2 2H_2O$. However, it is considered to be caused by mixing with the absorption bands of pyridine in this region; and spectral pattern may be interpreted as being in analogy to that of $Mn(acac)_2 2H_2O$ with one intense band. The difference in the spectral pattern described

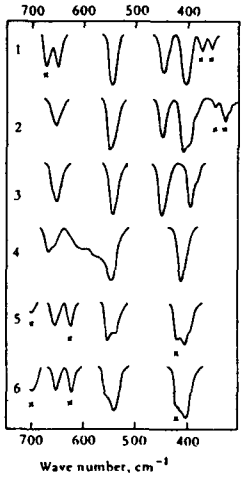

Fig. 6. IR spectra (in Nujol)
1: $[Mn(acac)_2]_2DMF$,
2: $Mn(acac)_2DMSO$, 3: $Mn(acac)_2$
4: $Mn(acac)_2 2H_2O$, 5: $Mn(acac)_2 py$,
6: $Mn(acac)_2 2py$.

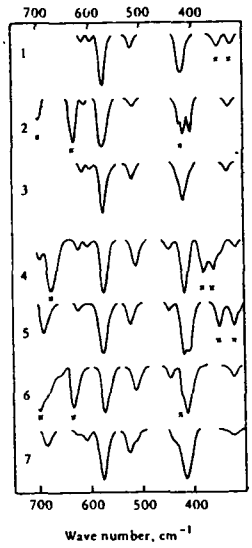

Fig. 7. IR spectra (in Nujol)
1: $Mn(tfac)_2 2DMSO$, 2: $Mn(tfac)_2 2py$,
3: $Mn(tfac)_2 2H_2O$, 4: $Mn(bzac)_2 2DMF$,
5: $Mn(bzac)_2 2DMSO$, 6: $Mn(bzac)_2 2py$,
7: $Mn(bzac)_2 2H_2O$.

above would arise from the following difference in the structures of the compounds. As described before, $Mn(acac)_2$ is considered to have a trimeric structure in a solid state in view of the results of molecular weight determination[4] and ESR spectral investigation.[9] On the other hand, $Mn(acac)_2 2H_2O$ as well as $Mn(acac)_2 2py$ might have a monomeric, six-coordinate structure with two molecules of axial ligands. Thus, the absorption band observed at 449 cm^{-1} for $Mn(acac)_2$ may be ascribed to a structure which includes acetylacetonato ligands arrayed octahedrally around the manganese ion. Different metal-oxygen vibration modes in above two types of the complexes would caused the different features in the spectra. The spectra of $Na[Mn(acac)_3]$ with two intense bands at 400 and 423 cm^{-1}, and of $Mn^{III}(acac)_3$ with three bands at 409, 432, and 460 cm^{-1} [21] are not thought to be inconsistent with above assumption. Further, it is suggested from the following facts that the spectra in 400 - 500 cm^{-1} region of tetrameric $[Co(acac)_2]_4$[22] and of trimeric $[Ni(acac)_2]_3$[20] which include bridged acetylacetonato ligands show three absorption bands at 407, 420, and 443 cm^{-1} and at 412, 420, and 443 cm^{-1}, respectively: on the other hand, dihydrate complexes, $Co(acac)_2 2H_2O$ and $Ni(acac)_2 2H_2O$ have only one intense band at 422 and 427 cm^{-1}, respectively.

As shown in Fig. 6, the spectra of $[Mn(acac)_2]_2 DMF$ and $Mn(acac)_2 DMSO$ in this region are composed of two bands at 404 and 447 cm^{-1} in the former, and at 406 and 448 cm^{-1} in the latter, suggesting an octahedral configuration of acetylacetonato ligands. On the basis of these results, a probable structure of $[Mn(acac)_2]_2 DMF$ can be drawn as depicted in Fig. 8, having a unitary structure of octahedrally arrayed acetylacetonato ligands.

It is of significance to note that the spectrum of $Mn(acac)_2$(allylamine) with dimeric structure including bridged acetylacetonato ligands does not clearly show the band which can be comparable with the characteristic one at 447 cm^{-1} for $[Mn(acac)_2]_2$DMF or at 448 cm^{-1} for $Mn(acac)_2$DMSO. It is conceivable since the dimeric structure of the allylamine adduct does not involve a unitary octahedral arrangement of acetylacetonato ligands around the manganese ion.[6] As for $Mn(acac)_2$DMSO, a similar structure to trimeric $Mn(acac)_2$ would be preferable, since the fixation of the DMSO can not be thought to occur through coordination to the central manganese ion judging from the shift of the S=O band upon the adduct formation (*cf.* Table 2) and from an instability of the adduct, *i.e.*, at easy substitution with H_2O in a wet air or easy release of DMSO in a dry air.

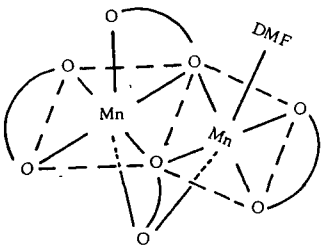

Fig. 8. A proposed structure for $[Mn(acac)_2]_2$DMF.

The spectra of bis-adducts of the other β-diketonates in the 300 - 700 cm^{-1} region were only made of those of the parent Mn^{II}(β-diketonato)$_2 2H_2O$ and of the additional bases, as is exemplified in Fig. 7, suggesting monomeric structure of the adducts with axially coordinated bases.

As represented in Table 4, bis-adducts have magnetic moments in the range of 6.01 - 6.13 BM, which correspond to the spin-only value, 5.92 BM. It has been pointed out by Graddon *et al.*[4] that magnetic moment of $Mn(acac)_2$ (5.68 BM) is lower than that of $Mn(acac)_2 2H_2O$ (6.02 BM). Slightly lower magnetic moments of $[Mn(acac)_2]_2$DMF and $Mn(acac)_2$DMSO than that of $Mn(acac)_2 2H_2O$ is

Table 4. Magnetic moments[a)]

Compound	$\frac{\mu_{eff}}{BM}$	Compound	$\frac{\mu_{eff}}{BM}$
$Mn(acac)_2 2H_2O$	6.17	$Mn(bzac)_2 2DMSO$	6.12
$Mn(acac)_2$	5.93	$Mn(bzac)_2 2py$	6.08
$[Mn(acac)_2]_2 DMF$	5.97	$Mn(dbm)_2 2DMF$	6.13
$Mn(acac)_2 DMSO$	6.03	$Mn(dbm)_2 2DMSO$	6.10
$Mn(bzac)_2 2H_2O$	6.09	$Mn(dbm)_2 2py$	6.01

a) Measured at room temperature by Gouy method: μ_{eff} was calculated by $\mu_{eff} = 2.83\sqrt{X_{corr} \times T}$.

not inconsistent with assumed polymeric structure for these adducts.

Summary

A series of the adducts of $Mn^{II}(\beta\text{-diketonato})_2$ with N,N-dimethylformamide, dimethyl sulfoxide, or pyridine has been prepared. Acetylacetonate complex forms the adducts with formula $[Mn(acac)_2]_2$-DMF and $Mn(acac)_2 DMSO$, while, in the cases of the Mn(II)-complexes with β-diketonato other than acetylacetonato, only bis-adducts, $Mn(\beta\text{-diketonato})_2 B_2$ could be isolated, where B is DMF, DMSO, or py and β-diketonato is benzoylacetonato, dibenzoylmethanato, or trifluoroacetylacetonato ligand. These adducts readily dissociate additional bases in 1,2-dichloroethane. IR spectra of $[Mn(acac)_2]_2$-DMF, $Mn(acac)_2 DMSO$, and $Mn(acac)_2$ in the 300 - 700 cm^{-1} region are characterized by an intense band around 450 cm^{-1} as compared with that of $Mn(acac)_2 2H_2O$. These bands are taken as an indication of the structure where manganese ion is surrounded octahedrally by acetylacetonato ligands. A probable structure of $[Mn(acac)_2]_2 DMF$ is thus drawn to be a dimer with bridged acetylacetonato ligands. The structure of $Mn(acac)_2 DMSO$ is essentially identical with that

of $Mn(acac)_2$, and the DMSO molecule may be included as a crystalline solvent. The bis-adducts can be described as having additional bases at the *trans*-positions.

1) The following abbreviations are used in this Chapter: DMF = N,N-dimethylformamide; DMSO = dimethyl sulfoxide; py = pyridine; acacH = acetylacetone; bzacH = benzoylacetone; dbmH = dibenzoylmethane; tfacH = trifluoroacetylacetone.

References

2) B. Emmert, H. Gsottschneider, and H. Stanger, *Chem. Ber.*, 69, 1319 (1936).

3) E. P. Dwyer and A. M. Sargeson, *J. Proc. Roy. Soc. N. S. W.*, 90, 29 (1956).

4) D. P. Graddon and G. M. Mockler, *Aust. J. Chem.*, 17, 1119 (1964).

5) Das, Asoke K. and Rao, D. V. Raman, *Curr. Sci.*, 39, 60 (1970).

6) Y. Nishikawa, Y. Nakamura, and S. Kawaguchi, *Bull. Chem. Soc. Jpn.*, 45, 155 (1972).

7) F. Cariati, D. Galizzioli, F. Morazzoni, and L. Naldini, *Inorg. Nucl. Chem. Lett.*, 9, 743 (1973).

8) S. Koda, S. Ooi, H. Kuroya, Y. Nishikawa, Y. Nakamura, and S. Kawaguchi, *Inorg. Nucl. Chem. Lett.*, 8, 89 (1972).

9) A. Hudson and M. J. de G. Kennedy, *Inorg. Nucl. Chem. Lett.*, 7, 333 (1971).

10) I. Masuda, *Nippon Kagaku Zasshi*, 82, 125 (1961). (in Japanese)

11) J. Archambault and R. Rivest, *Can. J. Chem.*, 36, 1461 (1958).

12) J. Archambault and R. Rivest, *Can. J. Chem.*, 38, 1331 (1960).

13) G. Matsubayashi, T. Tanaka, and R. Okawara, *J. Inorg. Nucl. Chem.*, 30, 1831 (1968).

14) K. Nakamoto, "Infrared Spectra of Inorganic and Coordination Compounds," 2nd. Wiley-Interscience, a Division of John Wiley & Sons. p. 210 (1970) and the references cited therein.

15) R. S. Drago and D. Meek, *J. Phys. Chem.*, 65, 1446 (1961).

16) J. E. Katon, W. R. Feairheller, Jr., and J. V. Pustinger, Jr., *Anal. Chem.*, 36, 2126 (1964).

17) T. Tanaka, *Inorg. Chim. Acta*, 1, 217 (1967).

18) K. Nakamoto, Y. Morimoto, and A. E. Martell, *J. Phys. Chem.*, 66, 346 (1962).

19) M. Mikami, I. Nakagawa, and T. Shimanouchi, *Spectrochim. Acta*, 23, 1037 (1967).

20) G. J. Bullen, R. Mason, and P. Pauling, *Inorg. Chem.*, 4, 456 (1965).

21) J. P. Dismukes, L. H. Jones, and J. C. Bailar, Jr., *J. Phys. Chem.*, 65, 792 (1961).

22) F. A. Cotton and R. C. Elder, *Inorg. Chem.*, 4, 1145 (1965).

Chapter III

III - 1 Reactions of Manganese(III) Schiff Base Complexes with Superoxide Ion in Dimethyl Sulfoxide

Introduction

Manganese complexes have been of interest in connection with the biological redox processes including catalytic disproportionation of superoxide ion, O_2^-. Examples are the manganese-containing superoxide dismutases (Mn-SOD) and the oxygen evolving photosystem II in green plants.[1] In the Mn-SOD process, a manganese ion may exist in the oxidation state of +III.[2,3] Recently, McAdam *et al.* have reported that the reaction of the Mn-SOD with O_2^- depends on a ratio of O_2^- concentration to the enzyme and that at high ratios (>15) it can not be explained by the simple two-step mechanism proposed for the Cu-SOD. Thus, they have postulated a kinetic model including a form of the enzyme, E_C, as follows:

$$E_A + O_2^- \longrightarrow E_B + O_2$$
$$E_B + O_2^- \xrightarrow{2H^+} E_A + H_2O_2$$
$$E_B + O_2^- \longrightarrow E_C$$
$$E_C \longrightarrow E_A,$$

where E_A represents a native oxidized enzyme, E_B a reduced enzyme, and E_C an enzyme unreactive toward O_2^-.[4]

Howie *et al.* have reported that the reaction of the manganese(II) and -(III) 8-quinolinol complexes with O_2^- in dimethyl sulfoxide (DMSO) can be considered as a redox model for the Mn-SOD.[5] Valentine *et al.* have found that $Mn^{III}(tpp)Cl$ reacts with O_2^- in DMSO to give $Mn^{II}(tpp)$; here tpp denotes tetraphenyl porphyrin dianion.[6] Recently, Stein *et al.* have reported that $Mn^{III}(cydta)^-$ and $Mn^{III}(edta)^-$ react with O_2^- in DMSO to give $Mn^{II}(cydta)^{2-}$ and $Mn^{II}(edta)^{2-}$, respectively, where H_4cydta and H_4edta denote

1,2-cyclohexanediamine-N,N,N',N',-tetraacetic acid and ethylenediaminetetraacetic acid, respectively.[7)]

In this Chapter, the reactions of a series of the chloromanganese(III) Schiff base complexes (Fig. 1) with O_2^- in DMSO will be described.

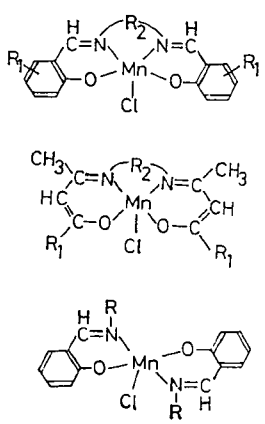

R_1	R_2	L
H	CH_2CH_2	salen
5-CH_3	CH_2CH_2	5-Mesalen
5-Br	CH_2CH_2	5-Brasalen
5-NO_2	CH_2CH_2	5-NO_2salen
5,6-Benzo	CH_2CH_2	5,6-Benzosalen
3-OCH_3	CH_2CH_2	3-MeOsalen
H	C_6H_4	salphen
H	C_6H_{10}	salchxn
H	$CH(CH_3)CH_2$	salpn
CH_3	CH_2CH_2	acacen
C_6H_5	CH_2CH_2	bzacen
CH_3	$CH(CH_3)CH_2$	acacpn
C_6H_5	$CH(CH_3)CH_2$	bzacpn

R	L'
C_3H_7	*N*-Prsai
C_4H_9	*N*-Busai
C_6H_{11}	*N*-c-Hxsai

Fig. 1. Manganese(III) Schiff base complexes studied.

Experimental

Preparation of Chloromanganese(III) Schiff Base Complexes. All the chloromanganese(III) Schiff base complexes were prepared by the following method, adapted from the literature.[8,9)]

Chloro[N,N'-bis(2-benzoyl-1-methylethylidene)ethylenediaminato]-manganese(III), Mn(bzacen)Cl: To a dichloromethane(50 cm^3) - methanol (50 cm^3) solution of N,N'-bis(2-benzoyl-1-methylethylidene)-ethylenediamine (3.47 g) was added manganese(III) acetate dihydrate, $Mn(CH_3COO)_3 \cdot 2H_2O$ (2.68 g). The mixture was allowed to stand at 40 ^oC for 30 min, and then lithium chloride (0.6 g) was added. After having been stirred for 1 h, the solution was concentrated to

ca. 20 cm^3 under reduced pressure. Ether (200 cm^3) was then added to precipitate brown solids. They were collected on a glass filter, washed with small volumes of water, 2-propanol, and then ether, and then dried *in vacuo*. They were recrystallized from dichloromethane. The yield was *ca.* 60%. The analytical data and the magnetic moments of some manganese(III) complexes are given in Table 1.

Isolation of Oxygenated Complexes. *$[Mn(salen)]_2O_2$, Complex 1 and $[Mn(salen)O]_n$, Complex 2*: To a DMSO solution of Mn(salen)Cl-H_2O (0.7 g) and 18-crown-6 (0.5 g) was added potassium superoxide, KO_2 (0.15 g) in a nitrogen atmosphere at room temperature. After having been stirred for 2 h, the solution was evaporated to remove DMSO under reduced pressure. The reddish brown solids which separated were collected on a glass filter, washed with water, methanol, and then ether, and then dried *in vacuo*. They were extracted with dichloromethane (500 cm^3). The dichloromethane solution was evaporated under reduced pressure to give reddish brown needles, complex 1, which was identified to be $[Mn(salen)]_2O_2$ by the infrared spectrum and the magnetic susceptibilities. On the other hand, the insoluble product in dichloromethane was identified to be $[Mn(salen)O]_n$, complex 2. The yields of complexes 1 and 2 were 0.21 and 0.43 g, respectively. When the reaction of Mn(salen)Cl·H_2O with KO_2 in DMSO was carried out in the absence of 18-crown-6, the yields of complexes 1 and 2 were 0.03 and 0.50 g, respectively.

TABLE 1. ELEMENTAL ANALYSES AND MAGNETIC MOMENTS OF MANGANESE(III) COMPLEXES

Complex	Found (%)				Calcd (%)				μ_{eff}[a] / BM
	C	H	N	Mn	C	H	N	Mn	
Mn(acacen)Cl·$(H_2O)_{0.5}$	44.81	5.95	8.71	16.92	45.02	5.72	8.97	17.08	4.96
Mn(acacpln)Cl·$(H_2O)_{0.3}$	46.98	6.22	8.51	16.40	46.93	6.21	8.42	16.51	4.77
Mn(bzacen)Cl	60.20	4.91	6.23	12.35	60.49	5.08	6.41	12.58	4.91
Mn(bzacpln)Cl	61.75	5.60	6.08	12.02	61.27	5.37	6.21	12.19	4.81
Mn(5,6-Benzosalen)Cl	62.84	3.96	5.93	11.89	63.10	3.97	6.13	12.03	4.97

a) Measured at room temperature.

The oxygenated manganese complexes, Mn(salchxn)O·H_2O and Mn(5,6-Benzosalen)O·H_2O were obtained by the reactions of the corresponding chloromanganese(III) complexes with KO_2 in DMSO and benzene, respectively. These complexes were reddish brown powders and were insoluble in common organic solvents. Therefore, further purification could not be performed. Mn(salchxn)O·H_2O: Found: C, 58.70; H, 4.98; N, 6.98; Mn, 13.23%. Calcd for Mn($C_{20}H_{22}N_2O_4$): C, 58.69; H, 5.42; N, 6.84; Mn, 13.42%. IR: 650 and 618 cm^{-1} (νMn-O). Magnetic moment at room temperature: 1.89 BM. Mn(5,6-Benzosalen)O·H_2O: Found: C, 63.93; H, 3.99; N, 6.23; Mn, 12.25%. Calcd for Mn($C_{24}H_{20}N_2O_4$): C, 63.31; H, 4.43; N, 6.15; Mn, 12.06%. IR: 653 and 603 cm^{-1} (νMn-O). Magnetic moment at room temperature: 2.90 BM.

[Mn(bzacen)O]·(CH_2Cl_2)$_{0.3}$: To a benzene solution (200 cm^3) of Mn(bzacen)Cl (0.7 g) and 18-crown-6 (0.5 g) was added KO_2 (0.15 g) in a nitrogen atmosphere. The solution turned the color from brown to reddish brown gradually on stirring for 2 h. The mixture was filtered and the filtrate was evaporated under reduced pressure. The precipitated solids were collected on a filter, washed with small volumes of water and methanol and then thoroughly with ether, and then dried *in vacuo*. On recrystallization from dichloromethane, reddish brown needles were obtained. The yield was *ca.* 0.2 g. The complex is soluble in dichloromethane and slightly soluble in DMSO. Found: C, 60.07; H, 5.16; N, 6.10; Mn, 12.39%. Calcd for Mn($C_{22}H_{22}N_2O_3$)(CH_2Cl_2)$_{0.3}$: C, 60.48; H, 5.14; N, 6.33; Mn, 12.40%. IR: 650 cm^{-1} (νMn-O). Magnetic moment at room temperature: 2.55 BM.

The oxygenated complex, Mn(bzacpln)O·(CH_2Cl_2)$_{0.4}$ was obtained in a similar manner. Found: C, 60.45; H, 5.25; N, 6.02; Mn, 11.84%. Calcd for Mn($C_{23}H_{24}N_2O_3$)(CH_2Cl_2)$_{0.4}$: C, 60.40; H, 5.37; N, 6.02;

Mn, 11.81%. IR: 644 cm^{-1} (νMn-O). Magnetic moment at room temperature: 1.87 BM.

Reagents. All reagents were of reagent grade. Potassium superoxide, KO_2, was purchased from Alfa products Inc. (Above 96.5%). Dimethyl sulfoxide was distilled twice under reduced pressure prior to use. Benzene was distilled over sodium. Acetonitrile was refluxed over diphosphorus pentaoxide and distilled twice prior to use. Dichloromethane was distilled over calcium chloride.

Preparation of DMSO Solution of KO_2. A DMSO solution of KO_2 (*ca.* 10^{-2} M, 1 M = 1 mol dm^{-3}) was prepared by dissolving KO_2 (18.7 mg) into DMSO (25 cm^3) in the presence of 18-crown-6 (0.1 g). The O_2^- concentration of the solution was determined by spectrophotometry.[10]

Reaction of Manganese(III) Complexes with KO_2. The reactions of the manganese(III) complexes with O_2^- were carried out under nitrogen atmosphere.

Measurements. The UV, VIS, and NIR spectra were recorded on Hitachi EPS-3 and Hitachi 340 recording spectrophotometers. The IR spectra in the 4000 - 650 and 700 - 250 cm^{-1} regions were recorded on a Hitachi 215 and on a Hitachi EPI-L grating spectrophotometer, respectively. Polarograms were obtained by using a Yanagimoto P-8 polarograph. A dropping mercury electrode and a mercury pool were used as the working and the reference electrode, respectively, this avoided any effect of water on the reaction systems that would occur if a saturated calomel electrode was used. Tetrabutylammonium perchlorate, Bu_4NClO_4, was used as the supporting electrolyte and Triton-X 100 as the maximum suppressor. Magnetic susceptibilities were measured by a Gouy method at room temperature.

Results and Discussion

It is supposed that in the native Mn-SOD the nitrogen and/or oxygen atoms of the amino acid residues of the protein are coordinated with manganese ions, although the details of coordiantion structure have not yet been clarified. Recently, the manganese ion in the native Mn-SOD has been found to be in the oxidation state +III.[2,3] The reactions of the manganese(III) Schiff base complexes with O_2^- investigated here afford information in connection with the catalytic disproportionation of O_2^- by the Mn-SOD.

Visible Absorption Spectra. Figure 2 shows the spectral changes of Mn(salen)Cl·H_2O in the DMSO solution caused by the addition of KO_2 in different molar ratios. The spectra changed remarkably, showing an isosbestic point at 390 nm. And a broad absorption band which appeared for the first time around 480 nm increased in intensity on the addition of KO_2 up to $[KO_2]/[complex] = 4$; further amounts of KO_2 caused a decrease in the intensity

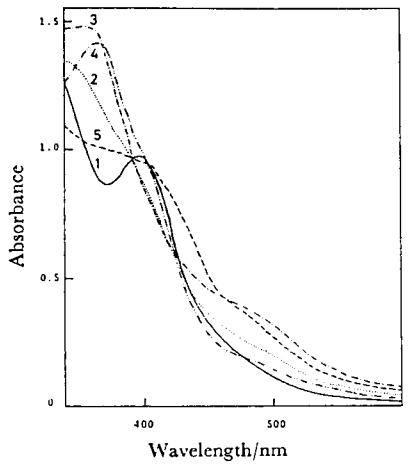

Fig. 2. Spectral changes of a DMSO solution of Mn-(salen)Cl·H_2O, 2×10^{-4} M, caused by the addition of KO_2.
1): No addition, 2): $[KO_2]/[complex]=2$, 3): 4, 4): 6, 5): after passing O_2 through the solution shown by curve 4. Cell length: 1 cm.

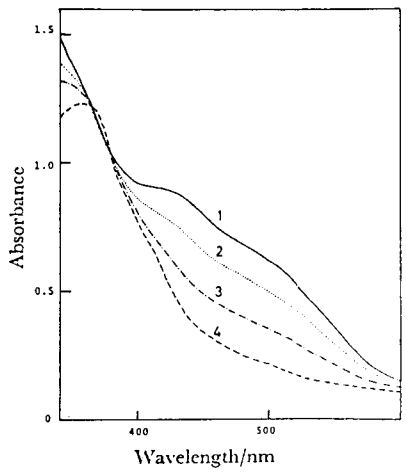

Fig. 3. Spectral changes of a DMSO solution of [Mn-(salen)]$_2O_2$, 8×10^{-5} M, caused by the addition of KO_2.
1): No addition, 2): $[KO_2]/[complex]=3$, 3): 6, 4): 10. Cell length: 1 cm.

and the appearance of an absorption band at 364 nm. These spectral changes can be interpreted as follows. The absorption band around 480 nm may be due to the formation of the oxygenated complex. This is supported by the fact that the oxygenated complex, $[Mn(salen)]_2O_2$, obtained by the reaction of Mn^{II}(salen) with molecular oxygen in DMSO is characterized by an intense absorption band in the same range, as described in Chapter I-1. The spectral changes observed on the further addition of KO_2 are considered to be due to a reaction of the oxygenated complex formed in solution with an excess amount of O_2^- to yield the manganese(II) complex, Mn^{II}(salen). This is confirmed by the facts that the absorption spectrum shown by curve 4 is in agreement with that of Mn^{II}(salen) in DMSO, and that by introducing molecular oxygen (O_2) into this solution it comes to show an absorption curve similar to that of the oxygenated complex, $[Mn(salen)]_2O_2$; this complex again reacts with O_2^-, showing similar spectral changes, as seen in Fig. 3.

Figure 4 shows the spectral changes for the complex Mn(acacpln)-Cl by the addition of KO_2. These are similar to those observed for the complex Mn(salen)Cl·H_2O. This indicates that the oxygenation of Mn(acacpln)Cl occurs because of the reaction with O_2^-.

Figure 5 shows the spectral changes for the complex Mn(5-NO_2-salen)Cl. Unlike the above two complexes, the intensity of the weak absorption band around 500 nm decreases with increasing

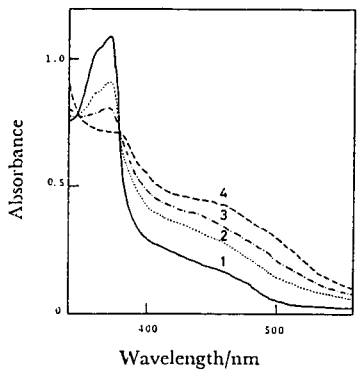

Fig. 4. Spectral changes of a DMSO solution of Mn-(acacpln)Cl·$(H_2O)_{0.3}$, 2×10^{-4} M, caused by the addition of KO_2.
1): No addition, 2): $[KO_2]/[complex]=1.5$, 3): 2, 4): 2.5. Cell length: 1 cm.

intensity of a new absorption band at 402 nm. The final absorption curve shown by curve 4 in Fig. 5 is coincident with that of Mn^{II}(5-NO_2salen) in DMSO. This indicates that Mn(5-NO_2salen)Cl is reduced with O_2^- to form the manganese(II) complex. The spectral changes for the complex Mn^{III}(3-MeOsalen)Cl·H_2O are shown in Fig. 6. The author previously reported that Mn^{II}(3-MeOsalen)·H_2O was readily oxidized by O_2 in common organic solvents to give the oxidized complex. It is clearly evidenced in Fig. 6 that Mn^{III}(3-MeOsalen)Cl·H_2O is reduced with O_2^- to the manganese-(II) complex. Bubbling O_2 into the solution including [KO_2]/[complex] = 3 and showing absorption curve 4 results in the change of the absorption to curve 5, which is quite like that observed in the reaction of Mn^{II}(3-MeOsalen)·H_2O with O_2 in DMSO.

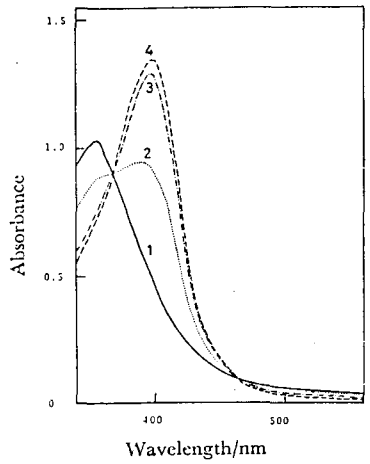

Fig. 5. Spectral changes of a DMSO solution of Mn(5-NO_2salen)Cl, 4×10^{-5} M, caused by the addition of KO_2.
1): No addition, 2): [KO_2]/[complex] = 1, 3): 2, 4): 3. Cell length: 1 cm.

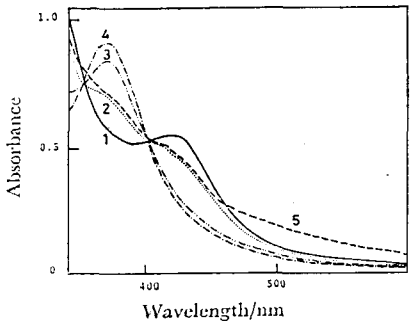

Fig. 6. Spectral changes of a DMSO solution of Mn(3-MeOsalen)Cl·H_2O, 1.0×10^{-4} M, caused by the addition of KO_2.
1): No addition, 2): [KO_2]/[complex] = 1, 3): 2, 4): 3, 5): after passing O_2 through the solution shown by curve 4. Cell length: 1 cm.

Polarograms. The polarograms of the manganese(III) complexes show one cathodic wave around -0.2 V and one- or two-step cathodic waves in the -1.5 - -2.0 V range. The polarogram of Mn(5-NO_2salen)Cl in DMSO is shown by curve 1 in Fig. 7. The first cathodic wave can be assigned to the reduction of Mn(III) to

Mn(II) and the second and third waves may involve the reductions of the coordinated Schiff base ligand.[11, 12] An addition of KO_2 to the solution of the complex ($[KO_2]/[complex] = 2$) caused a decrease in the height of the first cathodic wave and the appearance of a new cathodic wave at a half-wave potential of -0.6 V. With increasing amounts of KO_2, the wave height of the former decreased and that of the latter increased. The above new cathodic wave can be easily assigned to the reduction of free O_2 in the solution, because the half-wave potential is nearly equal to that observed for dissolved O_2 and the wave would disappear readily if nitrogen gas was passed through the solution. The solution obtained after passing nitrogen gas has a polarogram which resembles that of $Mn^{II}(5\text{-}NO_2\text{-salen})$. These results indicate that $Mn(5\text{-}NO_2salen)Cl$ is reduced with O_2^- to yield the manganese(II) complex and O_2, $Mn^{III}L^+ + O_2^- \longrightarrow Mn^{II}L + O_2$, where L denotes $5\text{-}NO_2salen$. This is consistent with the results observed in the absorption spectral changes.

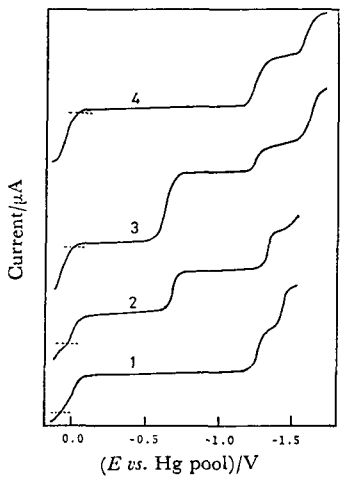

Fig. 7. Changes in polarograms during the reaction of $Mn(5\text{-}NO_2salen)Cl$, 2×10^{-4} M, with KO_2 in DMSO. 1): No addition of KO_2, 2): $[KO_2]/[complex] = 2$, 3): 4, 4): after passing N_2 through the solution shown by curve 3.

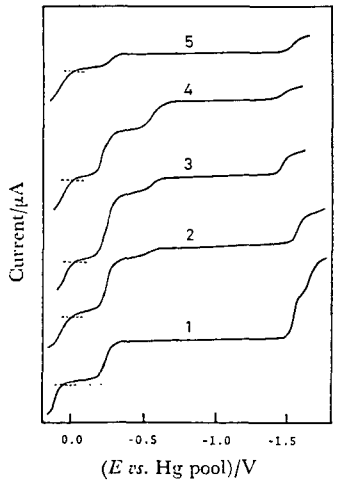

Fig. 8. Changes in polarograms during the reaction of Mn(bzacen)Cl, 2×10^{-4} M, with KO_2 in DMSO. 1): No addition of KO_2, 2): $[KO_2]/[complex] = 1$, 3): 2, 4): 4, 5): after passing N_2 through the solution shown by curve 4.

The polarogram of Mn(bzacen)Cl shown in Fig. 8 exhibits three cathodic waves at the half-wave potentials of -0.3, -1.6, and -1.8 V. The first cathodic wave is due to the reduction of Mn(III) to Mn(II). By the addition of KO_2, the cathodic wave due to free O_2 barely appeared in the solution composed with $[KO_2]/[complex] = 2$, though the wave height around -0.3 V was observed to increase. Further addition of KO_2 ($[KO_2]/[complex] = 4$) caused a decrease in this wave height and an increase in the wave height due to free O_2. The polarogram obtained after passing nitrogen gas through the solution (shown by curve 4 in Fig. 8) exhibits only a small wave height at -0.3 V; this may be due to the residue of the manganese(III) complex. From these polarographic observation, the reaction of Mn(bzacen)Cl with O_2^- can be explained as follows. The increase in the wave height at -0.3 V observed at the molar ratio change from 1 to 2 may be caused by the formation of the oxygenated complex, hence the cathodic wave due to O_2 is slightly observed. At the molar ratio of 4 the oxygenated complex reacts with O_2^- to give the manganese(II) complex and O_2.

Reactivity toward O_2^-. In view of the reactivity toward O_2^- observed in the spectral and polarographic behavior, the chloromanganese(III) Schiff base complexes investigated here can be classified into two types: one involving the complexes which form the oxygenated complex in the solution containing KO_2 in

Table 2. Reduction potentials of manganese(III) complexes and reactivity toward O_2^-

Complex	$-E_{1/2}$ a) *vs.* Hg pool V Mn(III)→Mn(II)	Reactivity toward O_2^-
Mn(acacen)Cl·$(H_2O)_{0.5}$	0.39	Oxygenation
Mn(acacpln)Cl·$(H_2O)_{0.3}$	0.33	Oxygenation
Mn(bzacen)Cl	0.32	Oxygenation
Mn(bzacpln)Cl	0.30	Oxygenation
Mn(salchxn)Cl	0.21	Oxygenation
Mn(5-Mesalen)Cl	0.20	Oxygenation
Mn(5,6-Benzosalen)Cl	0.19	Oxygenation
Mn(salen)Cl·H_2O	0.19	Oxygenation
Mn(salpln)Cl	0.18	Reduction
Mn(3-MeOsalen)Cl·H_2O	0.15	Reduction
Mn(5-Brsalen)Cl	0.15	Reduction
Mn(salphen)Cl	0.08	Reduction
Mn(5-NO_2salen)Cl	0.03	Reduction
Mn(*N*-Busai)$_2$Cl	0.02	Reduction
Mn(*N*-Prsai)$_2$Cl	0.02	Reduction
Mn(*N*-c-Hxsai)$_2$Cl	0.00	Reduction

a) Measured in acetonitrile containing 0.1 mol dm^{-3} $(Bu)_4NClO_4$ at 25 °C.

the molar ratio of $[KO_2]/[complex] < 2 - 3$, and the other involving the complexes which are only reduced to the corresponding manganese-(II) complexes with the evolution of molecular oxygen. These results are summarized in Table 2, along with the half-wave potentials for the reduction of Mn(III) to Mn(II). The reactivity toward O_2^- is clearly correlated with the reduction potentials of the complexes. That is, the complexes having more negative potentials than that of Mn(salen)Cl·H_2O form the oxygenated complexes, whereas the complexes having more positive potentials than that of Mn(salpln)Cl are reduced to the manganese(II) complexes.

Isolation and Characterization of the Oxygenated Complexes. Several oxygenated manganese complexes were isolated by the reactions of chloromanganese(III) Schiff base complexes with KO_2 in DMSO or benzene. In the case of Mn(salen)Cl·H_2O, two types of the oxygenated complexes, $[Mn(salen)]_2O_2$ and $[Mn(salen)O]_n$, were isolated. The former complex shows an intense broad absorption band around 480 nm. In the IR spectrum the former complex shows a strong band assignable to the Mn-O stretching vibration at 645 cm^{-1}, while the latter, which is insoluble in common organic solvents, shows two strong bands due to the Mn-O stretching vibrations at 665 and 605 cm^{-1}. The effective magnetic moments of $[Mn(salen)]_2O_2$ and $[Mn(salen)O]_n$ were 2.16 and 2.04 BM, respectively. These values are lower than the spin-only one which is expected for a complex with the d^4 or d^3 high-spin configuration; they may be caused by the antiferromagnetic interactions observed for the complexes where the manganese atoms are probably linked by the oxygen atoms: $Mn^{III}-O_2-Mn^{III}$ and $\vdash Mn^{IV}-O\dashv_n$, as described in Chapter I-1.

The other oxygenated manganese complexes obtained in this study also show lower magnetic moments. The IR spectra of the

oxygenated complexes, Mn(salchxn)O and Mn(5,6-Benzosalen)O, which are insoluble in common organic solvents, show two strong bands in the 700 to 600 cm^{-1} region. Therefore, these complexes may have a structure similar to that of $[Mn(salen)O]_n$. On the other hand, the IR spectra of the oxygenated complexes, Mn(bzacen)O and Mn(bzacpln)O, which are soluble in dichloromethane, show one strong band in the 700 to 600 cm^{-1} region. Moreover, the electronic spectrum of Mn(bzacen)O in dichloromethane shows an intense absorption band around 500 nm, as shown in Fig. 9. These results suggest that the oxygenated complexes may have a structure similar to that of $[Mn(salen)]_2O_2$. Since the manganese(II) complexes with the Schiff bases derived from β-diketones and diamines have not been isolated due to the instabilities, there has been no attempt to prepare their oxygenated complexes by reacting them with O_2.

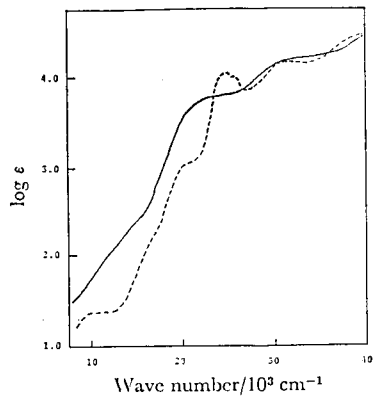

Fig. 9. Electronic spectra.
——: Mn(bzacen)O·$(CH_2Cl_2)_{0.3}$ in dichloromethane,
------: Mn(bzacen)Cl in DMSO.

Among the oxygenated manganese-Schiff base complexes, the compounds with such unitary groups as oxo (Mn=O), μ-oxo (Mn-O-Mn), catena-μ-oxo (-(- Mn-O-)-$_n$), μ-peroxo (Mn-O-O-Mn), and di-μ-oxo (Mn<O>Mn) have so far been reported.[1b] However, these structures have been determined only by the elemental analyses and the conventional physicochemical measurements, with the exception of the oxygenated product of $Mn^{II}(salpn)\cdot H_2O$. This has been revealed by X-ray structural analysis to be a di-μ-hydroxo structure (Mn<OH>Mn), where $salpnH_2$ denotes N,N'-disalicylidene-1,3-propanediamine.[13]

The reactivity of KO_2 with the present manganese(III) complexes

will open a new route for synthesis and will provide a method of characterization for the oxygenated complexes.

Summary

The reactions of the chloromanganese(III) complexes of the Schiff bases derived from salicylaldehydes or β-diketones and diamines or monoamines with superoxide ion, O_2^-, in DMSO were investigated. The complexes are found to react to give either the oxygenated manganese Schiff base complexes or the reduced manganese-(II) Schiff base complexes. The difference in the reactivity toward O_2^- can be correlated with the polarographic half-wave potentials corresponding to the reduction of Mn(III) to Mn(II) of the complexes. Some oxygenated complexes are isolated and characterized.

References

1) a) G. D. Lawrence and D. T. Sawyer, *Coord. Chem. Rev.*, 27, 173 (1978); b) W. M. Coleman and L. T. Taylor, *ibid.*, 32, 1 (1980).

2) J. A. Fee, E. R. Shapiro, and T. H. Moss, *J. Biol. Chem.*, 251, 6157 (1976).

3) J. J. Villafranca, F. J. Yost, Jr., and I. Fridovich, *J. Biol. Chem.*, 249, 3532 (1974).

4) a) M. E. McAdam, R. A. Fox, F. Lavelle, and E. M. Fielden, *Biochem. J.*, 165, 71 (1977); b) M. E. McAdam, F. Lavelle, R. A. Fox, and E. M. Fielden, *ibid.*, 165, 81 (1977).

5) J. K. Howie and D. T. Sawyer, *J. Am. Chem. Soc.*, 98, 6698 (1976).

6) J. S. Valentine and A. E. Quinn, *Inorg. Chem.*, 15, 1997 (1976).

7) J. Stein, J. P. Fackler, Jr., G. J. McClune, J. A. Fee, and L. T. Chan, *Inorg. Chem.*, 18, 3511 (1979).

8) L. J. Boucher and V. W. Day, *Inorg. Chem.*, 16, 1360 (1977).

9) L. J. Boucher, *J. Inorg. Nucl. Chem.*, 36, 531 (1974).

10) S. Kim, R. DiCosimo, and J. S. Filippo, Jr., *Anal. Chem.*, 51, 679 (1979).

11) W. M. Coleman, R. R. Goehring, L. T. Taylor, J. G. Mason, and R. K. Boggess, *J. Am. Chem. Soc.*, 101, 2311 (1979).

12) R. K. Boggess, J. M. Hughes, W. M. Coleman, and L. T. Taylor, *Inorg. Chim. Acta*, 38, 183 (1980).

13) H. S. Maslen and T. N. Waters, *J. Chem. Soc., Chem. Commun.*, 1973, 760.

III - 2 Reactions of Polymeric Chloromanganese(III) Schiff Base Complexes with Superoxide Ion in Dimethyl Sulfoxide

Introduction

In the previous section, the monomeric manganese(III) Schiff base complexes are classified into two types according to their reactivity toward O_2^-: one gives the oxygenated complexes and the other is reduced to the manganese(II) complexes. This behavior can be correlated with the polarographic half-wave potentials for the reduction of Mn(III) to Mn(II).

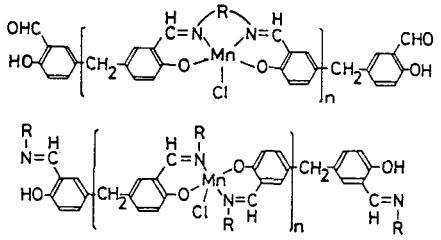

R	Abbreviation
$CH(CH_3)CH_2$	Mn(p-salpln)Cl
C_6H_{10}	Mn(p-salchxn)Cl
$(CH_2)_3NH(CH_2)_3$	Mn(p-saldpt)Cl
$(CH_2)_3N(CH_3)(CH_2)_3$	Mn(p-salMedpt)Cl
n-C_3H_7	Mn(*N*-Prdisai)Cl
n-C_4H_9	Mn(*N*-Budisai)Cl
c-C_6H_{11}	Mn(*N*-*c*-Hxdisai)Cl

Polymeric manganese(III) complexes.

In this section, the reactions of the polymeric manganese(III) Schiff base complexes (shown above) with O_2^- in DMSO will be described.

Experimental

The monomeric manganese(III) complexes, Mn(saldpt)Cl and Mn(salMedpt)Cl, were prepared by a modification of the method described in section III-1, where saldptH_2 and salMedptH_2 denote bis[3-(salicylideneamino)propyl]amine and bis[3-(salicylideneamino)propyl]methylamine, respectively.

Preparation of Polymeric Schiff Bases. The polymeric Schiff base, p-salplnH_2, was obtained by the polycondensation of 5,5'-methylenedisalicylaldehyde (disalH_2) with propylenediamine in

dichloromethane. This was reprecipitated from dichloromethane and ether. The other polymeric Schiff bases, p-salchxnH_2, p-saldptH_2, and p-salMedptH_2, were obtained in a similar manner. The analytical data, specific viscosities (Table 1), and ^1H NMR data (Table 2)

Table 1. Elemental analyses and specific viscosities of Schiff bases

Ligand	Found (%)			Calcd (%)			η_{sp} c)
	C	H	N	C	H	N	
p-salplnH_2	72.40	6.22	7.95	72.89	5.91	7.82 a)	0.049
p-salchxnH_2	74.44	6.75	8.25	74.60	6.32	7.03 a)	0.057
p-saldptH_2	71.76	7.28	9.44	71.54	6.79	10.11 a)	0.028
p-salMedptH_2	71.91	7.04	9.35	71.92	6.93	9.32 b)	0.035
N-PrdisaiH_2	74.59	7.70	8.18	74.53	7.74	8.28	
N-BudisaiH_2	75.19	8.26	7.67	75.38	8.25	7.64	
N-*c*-HxdisaiH_2	77.28	8.17	6.40	77.48	8.19	6.69	

a) Calculated as a tetramer. b) Calculated as a trimer. c) Measured in chloroform (0.40 g/100 cm^3) at 25±0.1 °C.

Table 2. ^1H NMR data of the polymeric Schiff bases ligands

Proton	δ in $CDCl_3$ p-salplnH_2	p-salchxnH_2	p-saldptH_2	p-salMedptH_2
OH	12.8(br)	13.0(br)	13.0(br)	13.3(br)
CHO	9.75(s)	9.78(s)	9.82(s)	9.78(s)
CH=N	8.24(d)	8.24(s)	8.24(s)	8.21(s)
φ	*ca.* 7(m)	*ca.* 7(m)	*ca.* 7(m)	*ca.* 7(m)
φ-CH_2-φ	3.78(s)	3.76(br)	3.84(d)	3.79(s)
$CH_{(2)}N=$	3.70(d)	3.52(br) 3.28	3.58(t)	3.56(t)
CH_2-N			2.65(t)	2.37(t)
-CH_2-		1.60(m)	1.82(m)	1.80(m)
CH_3	1.36(m)			2.17(s)
Peak intensity ratio				
$\frac{\phi\text{-}CH_2\text{-}\phi}{CH=N}$	1.24	1.20	1.20	1.32

indicate that these polymeric Schiff bases are oligomers whose degrees of condensation (n) are within a range of three to five.

N,N'-Dibutyl-5,5'-methylenedisalicylideneamine, N-BudisaiH$_2$: This was obtained by the condensation of disalH$_2$ with n-butylamine in tetrahydrofuran. This was recrystallized from a mixture of of ether - petroleum ether. The other Schiff base ligands, N-PrdisaiH$_2$ and N-c-HxdisaiH$_2$ were obtained in a similar manner. Their analytical data are given in Table 1.

Preparation of Polymeric Manganese(III) Complexes. The polymeric manganese(III) complex, Mn(p-salpln)Cl was obtained by reacting p-salplnH$_2$ with Mn(CH$_3$COO)$_3$·2H$_2$O and LiCl in a mixed solvent of dichloromethane and methanol. It was reprecipitated from methanol and ether. The polymeric complexes, Mn(p-salchxn)Cl, Mn(p-saldpt)Cl, and Mn(p-salMedpt)Cl were obtained in a similar manner. The other polymeric complexes, Mn(N-Rdisai)Cl (R=Pr, Bu, and c-Hx) were obtained in a manner similar to that used for Mn(p-salpln)Cl, and were reprecipitated from dichloromethane and ether. These polymeric complexes are soluble in methanol and in DMSO. The analytical data and specific viscosities (Table 3) indicate that they are oligomers whose degrees of condensation are within a range of three to five.

Measurements. ^{1}H NMR spectra were taken on a JEOL JNM-PS 100 spectrometer using TMS as the internal standard. The specific viscosities were determined using an Ostwald's viscometer at 25±0.1 ^{o}C (0.40 g/solvent 100 cm^3). Other physical measurements were carried out by the method described in section III-1.

The reactions of the manganese(III) complexes with KO$_2$ in DMSO were made by the procedure described in section III-1.

Table 3. Elemental analyses and specific viscosities of the polymeric manganese(III) Schiff base complexes

Complex	Found (%)				Calcd (%)				η_{sp} d)
	C	H	N	Mn	C	H	N	Mn	
Mn(p-salpln)Cl	58.05	3.90	5.78	12.78	58.47	4.29	6.27	12.30[a]	0.051
Mn(p-salchxn)Cl·H_2O	58.60	4.40	5.52	10.77	58.88	3.99	5.55	10.88[a]	0.058
Mn(p-saldpt)Cl·H_2O	58.23	4.94	7.62	10.09	58.26	5.58	8.31	10.86[a]	0.033
Mn(p-salMedpt)Cl·H_2O	57.65	5.46	7.28	8.85	58.19	5.61	7.54	9.86[b]	0.044[e]
Mn(N-Prdisai)Cl·$(H_2O)_{0.5}$	57.96	5.59	6.21	11.84	57.87	5.78	6.45	12.61[c]	0.028[e]
Mn(N-Budisai)Cl	61.73	6.30	5.73	12.00	60.73	6.20	6.16	12.08[c]	0.028[f]
Mn(N-*c*-Hxdisai)Cl·$(H_2O)_2$	60.33	6.24	4.98	10.01	59.73	6.68	5.16	10.12[c]	0.020[f]

a) Calculated as a tetramer. b) Calculated as a trimer. c) Calculated as these complexes comprised of a Schiff base ligand per manganese atom. d) Measured in DMSO (0.40 g/100 cm^3) at 25±0.1 °C. e) Measured in methanol. f) Measured in chloroform.

Results and Discussion

As described in the preceding section, the absorption spectral and polarographic measurements can be used to distinguish clearly either the formation of oxygenated complexes or the reduction of Mn(III) to Mn(II) in the course of the reactions of the manganese-(III) Schiff base complexes with O_2^- in DMSO. Figure 1 shows the spectral changes of a DMSO solution of Mn(p-salpln)Cl caused by the addition of KO_2. A broad absorption band appears around 500 nm at the $[KO_2]/[Mn] = 3$, indicating the formation of the oxygenated complex. The other polymeric manganese(III) complexes investigated here show spectral changes similar to the above.

Figures 2-A and -B show the changes in polarograms during the reactions of O_2^- with the monomeric Mn(N-Prsai)$_2$Cl and polymeric Mn(N-Prdisai)Cl in DMSO, respectively. In the former case, as the ratio $[KO_2]/[Mn]$ increases, the wave height at -0.03 V, which

is due to the reduction of Mn(III) to Mn(II), decreases and a new cathodic wave appears at -0.55 V; this can be assigned to the reduction of free molecular oxygen. The results indicate that $Mn(N\text{-}Prsai)_2Cl$ is reduced to the manganese(II) complex and O_2^- is oxidized to O_2. In the latter case, a new cathodic wave is observed at *ca.* -0.25 V by the addition of KO_2 ($[KO_2]/[Mn] = 1 - 3$), indicating the formation of the oxygenated complex. The other polymeric manganese(III) complexes show polarograms similar to the above. These results indicate that all the polymeric manganese(III) complexes react with O_2^- to give the oxygenated complexes, although the corresponding monomeric

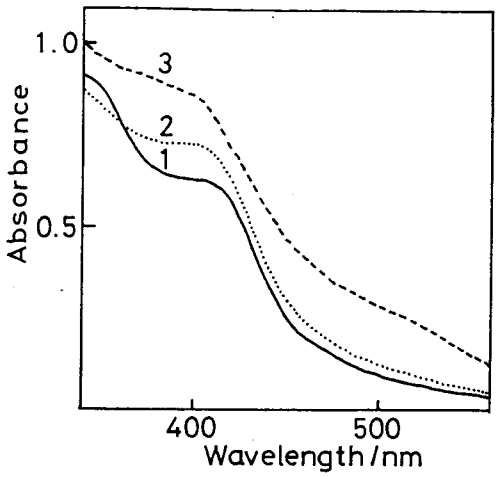

Fig. 1. Spectral changes of a DMSO solution of Mn(p-salpln)Cl ($1x10^{-4}$ unit mol dm^{-3}) caused by the addition of KO_2, cell length 1 cm. 1): No addition, 2): $[KO_2]/[Mn] = 1$, 3): 3.

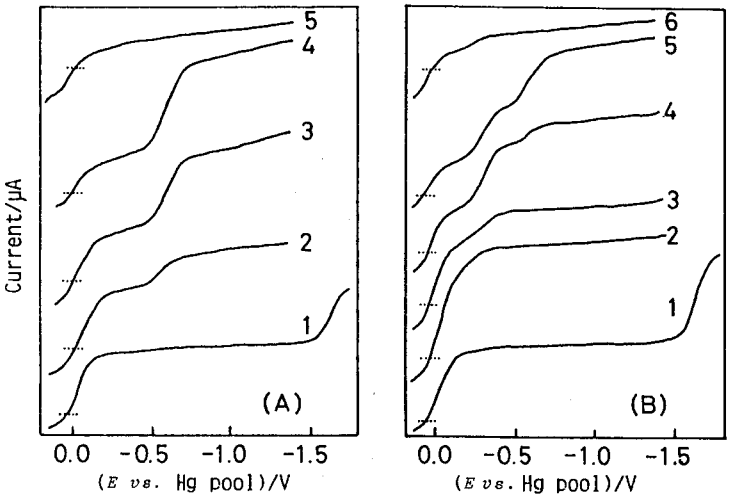

Fig. 2. Polarograms in the course of the reactions (A) $Mn(N\text{-}Prsai)_2Cl$ ($2x10^{-4}$ mol dm^{-3}) and (B) Mn(N-Prdisai)Cl ($2x10^{-4}$ unit mol dm^{-3}) with KO_2 in DMSO containing 0.1 mol dm^{-3} Bu_4NClO_4 at 25 °C. (A); 1): no addition, 2): $[KO_2]/[Mn] = 1$, 3): 3, 4): 6, 5): after passing N_2 through the solution shown by curve 4. (B); 1): no addition, 2): $[KO_2]/[Mn] = 1$, 3): 2, 4): 3, 5): 4, 6): after passing N_2 through the solution shown by curve 5.

Table 4. Magnetic moments, absorption maxima, and reduction potentials of the polymeric manganese(III) complexes, Mn(p-L)Cl and Mn(N-Rdisai)Cl, and of the corresponding monomeric complexes, Mn(L)Cl and $Mn(N\text{-}Rsai)_2Cl$

Complex L or R	μ_{eff} [a] / BM	λ_{max} / nm DMSO	λ_{max} / nm Solid	$-E_{1/2}$ *vs.* Hg pool [b] / V Mn(III) → Mn(II)
salpln	4.92 (5.03)	620 sh (605)	630 sh (618 sh)	0.07 (0.18)
salchxn	4.97 (4.96)	605 (588)	628 sh (612 sh)	0.00[c] (0.21)
saldpt	4.96 (5.14)	595 (584)	618 (610)	0.01 (0.05)
salMedpt	5.10 (4.77)	592 (570)	616 (608)	-0.01 (0.16)
Pr	5.04 (4.86)	596 (580)	670 (666)	0.02[c] (0.05)
Bu	4.94 (5.03)	596 (580)	670 (658)	0.02 (0.02)
c-Hx	5.06 (4.89)	566 (572)	636 sh (679)	0.02 (0.00)

a) Measured at room temperature and calculated from manganese content for the polymeric complexes. b) Measured in acetonitrile containing 0.1 mol dm^{-3} Bu_4NClO_4 at 25 °C. c) Measured in DMSO. Values in parentheses correspond to the monomeric complexes.

manganese(III) complexes are reduced by O_2^- to the manganese(II) complexes, with the exception of Mn(salchxn)Cl which gives the oxygenated complex as described in section III-1.

The polymeric complexes showed slightly positive reduction potentials compared with those for the monomeric complexes (Table 4). Nevertheless, the oxygenated complexes are found to be formed in the polymeric complexes. This may be caused by a polymeric structure in which the central manganese atom is not isolated from the surroundings, unlike the monomeric complexes. In such an environment, interaction between DMSO molecules and the central manganese atom may be weakened by steric repulsion and thus the oxygenated complex may be protected from dissociation into the manganese(II) complex and O_2, because the dissociation should

proceed *via* displacement of coordinated dioxygen with DMSO molecules. This consideration is not contradict with the spectral data (Table 4): The ligand field bands assignable to the $d_{xy} \rightarrow d_{x^2-y^2}$ transition[1] are observed at longer wavelengths in the polymeric complexes than those in the monomeric complexes.

Summary

The polymeric manganese(III) Schiff base complexes react with O_2^- in DMSO to give the oxygenated complexes, while the corresponding monomeric manganese(III) complexes are reduced by O_2^- to the manganese(II) complexes. This may be ascribed to the polymeric structure.

References

1) L. J. Boucher and V. W. Day, *Inorg. Chem.*, 16, 1360 (1977).

III - 3 Preparation of Binuclear Manganese(III) Schiff Base Complexes and Their Reactions with Superoxide Ion in Dimethyl Sulfoxide

Introduction

In the previous sections III-1 and -2, the reactions of monomeric and polymeric manganese(III) Schiff base complexes with O_2^- in DMSO have been studied in connection with the disproportionation of O_2^- by Mn-containing superoxide dismutases (Mn-SOD).[1,2] In the monomeric complexes, two types of the reaction pathways have been found to occur; the oxygenation of the complex and the reduction of Mn(III) to Mn(II) of the complex. The reactivity of the monomeric complexes toward O_2^- can be correlated with their polarographic reduction potentials from Mn(III) to Mn(II). In the polymeric complexes, their oxygenation has been found to occur. These reactions can be distinguished by measuring the visible absorption spectral and polarographic changes in the course of the reactions.

In this section the preparation of binuclear manganese(III) Schiff base complexes shown below and their reactions with O_2^- in DMSO will be described.

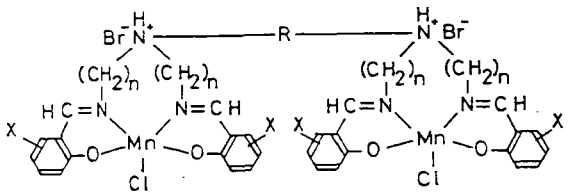

R = 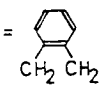

n = 2 Mn_2(B-o-x-X saldien·2HBr)Cl_2
X = H, 5-Br, 3-MeO

n = 3 Mn_2(B-o-x-X saldpt·2HBr)Cl_2
X = H, 5-Br, 3-MeO, 5,6-Benzo

Binuclear manganese(III) Schiff base complexes.

Experimental

Preparation of Schiff Base Ligands with Bifunctional Chelating Groups, α,α'-bis[bis[3-(salicylideneamino)propyl]ammonio]-o-xylene dibromide, (B-o-x-saldptH$_2$·2HBr). To a tetrahydrofuran (THF) solution (100 cm^3) of α,α'-dibromo-*o*-xylene (1.32 g, 5 mmol) was added a THF solution (30 cm^3) of bis[3-(salicylideneamino)propyl]-amine (saldptH$_2$, 3.39 g, 10 mmol). The mixed solution was refluxed for 2 h with stirring. The resulting yellow precipitate was collected on a glass filter, washed with a small amount of THF and then ether, and dried *in vacuo*. It was recrystallized from acetonitrile. Other Schiff base ligands were prepared in a similar manner. Their analytical data are given in Table 1, along with their melting points.

Preparation of Binuclear Manganese(III) Schiff Base Complexes, Mn$_2$(B-o-x-saldpt·2HBr)Cl$_2$. To a mixed solution of methanol (50 cm^3) and dichloromethane (50 cm^3) containing B-o-x-saldptH$_2$·2HBr (4.71 g, 5 mmol) were added manganese(III) acetate dihydrate (2.68 g, 10 mmol) amd lithium chloride (0.84 g, 20 mmol). The mixture was allowed to stand at 45 °C for 1 h with stirring, and then evaporated to dryness under reduced pressure. The resulting olive-green solid was collected on a glass filter, washed with a small amount of methanol and then ether, and dried *in vacuo*. It was reprecipitated twice from methanol and ether. Other binuclear manganese(III) complexes were prepared in a similar manner. Their analytical data are given in Table 2. These complexes are soluble in methanol, DMSO, and pyridine, but are insoluble in benzene and ether.

All the mononuclear manganese(III) complexes investigated here were prepared by the modified method described in section III-1. They were abbreviated as follows. Mn(Xsaldpt)Cl: Chlorobis[[3-(substituted salicylideneamino)propyl]aminato]manganese(III), where

X can be 5-Br, 3-MeO, and 5,6-Benzo groups. Mn(Xsaldien)Cl: Chloro-bis[[3-(substituted salicylideneamino)ethyl]aminato]manganese(III), where X can be 5-Br and 3-MeO groups.

Reaction with O_2^-. The reactions of the manganese(III) complexes with KO_2 in DMSO were made by the procedure described in section III-1.

Measurements. All physical measurements were carried out by the methods described in section III-1.

Materials. All reagents were of reagent grade. Solvents were purified by a usual manner.

Results and Discussion

Table 3 summarizes the properties of binuclear and mononuclear manganese(III) complexes and their reactivities toward O_2^- in DMSO. The magnetic moments of the binuclear complexes fall within the range of 4.80 to 5.10 BM, which is consistent with the value expected for the complex with d^4 high-spin electron configurations. The mononuclear complexes Mn(3-MeOsaldien)Cl and Mn(5,6-Benzosaldpt)Cl exhibit slightly lower magnetic moments which suggest that there may be magnetic interactions in these complexes. No further study on magnetic properties has been made. All the complexes in methanol and DMSO exhibit an absorption maximum due to ligand field transitions in the 500 to 700 nm range. The absorption band is shifted to high energy in the spectra of methanol and DMSO solutions compared with that in the solid reflectance spectra (Table 3). This indicates that these complexes may assume a six-coordinate configuration in solution where the solvent molecules are coordinated to the central manganese atom.[3,4] The polarograms of the complexes show the cathodic wave due to the one-electron reduction from Mn(III) to

Table 1. Melting points and analytical data for B-o-x-$LH_2 \cdot 2HBr$

Ligand	M.P.	Found (%)			Calcd (%)		
LH_2	°C	C	H	N	C	H	N
$saldptH_2$	133-135	60.92	6.10	8.87	61.51	6.20	8.91
$saldienH_2$	145-151	59.54	5.59	9.40	59.51	5.70	9.50
$5\text{-}BrsaldptH_2$	153-155	45.63	4.21	6.83	45.81	4.33	6.68
$5\text{-}BrsaldienH_2$	128-135	43.90	3.87	7.08	43.95	3.86	6.99
$3\text{-}MeOsaldptH_2$	79- 80	58.58	6.26	8.08	58.76	6.26	7.91
$3\text{-}MeOsaldienH_2$	93- 94	56.63	6.00	8.81	57.26	5.81	8.35
$5,6\text{-}BenzosaldptH_2$	199-201	66.34	5.59	7.29	67.25	5.82	7.35

Table 2. Analytical data for $Mn_2(B\text{-}o\text{-}x\text{-}L \cdot 2HBr)Cl_2$

Complex	Found (%)				Calcd (%)			
L	C	H	N	Mn	C	H	N	Mn
saldpt	51.88	4.92	7.49	9.68	52.24	4.93	7.62	9.96
saldien	50.41	4.63	8.06	9.75	49.69	4.36	7.90	10.33
5-Brsaldpt	40.26	3.74	6.13	7.26	40.17	3.51	5.86	7.66
5-Brsaldien	38.82	3.47	6.29	7.37	38.32	3.07	6.09	7.97
3-MeOsaldpt[a)]	49.50	5.00	6.65	8.22	48.96	5.20	6.59	8.61
3-MeOsaldien[a)]	47.40	4.70	7.46	9.14	47.27	4.79	6.89	9.00
5,6-Benzosaldpt	58.93	4.79	6.14	8.22	58.24	4.73	6.37	8.32

a) These complexes include two molecules of H_2O.

Mn(II) around -0.05 V. There is little difference between the potentials of the mononuclear and binuclear complexes.

Figure 1 shows the absorption spectral changes of the DMSO solutions of $Mn_2(B\text{-}o\text{-}x\text{-}5\text{-}Brsaldien \cdot 2HBr)Cl_2$ (A) and $Mn_2(B\text{-}o\text{-}x\text{-}5,6\text{-}Benzosaldpt \cdot 2HBr)Cl_2$ (B) caused by the addition of KO_2.

Table 3. Properties of Mn_2(B-o-x-L·2HBr)Cl_2 and Mn(L)Cl and their reactivities toward O_2^-

Complex L	μ_{eff} a) / BM	λ_{max} / nm MeOH	DMSO	Solid	$-E_{1/2}$ vs. Hg. pool b) / V Mn(III) → Mn(II)	Reactivity toward O_2^- c)
saldien	4.80	534 sh	590 sh	620 sh	0.02	Redn
	(4.83)	(552 sh)	(592 sh)	(630 sh)	(0.15)	(Oxygn)
5-Brsaldien	4.91	520 sh	620 sh	626 sh	0.03	Redn
	(4.98)	(560 sh)	(590 sh)	(640 sh)	(0.03)	(Redn)
3-MeOsaldien	4.87	518 sh	620	680 sh	0.01	Redn
	(4.56)	(508)	(632 sh)	(680 sh)	(0.00)	(Redn)
saldpt	4.83	592	572	602	0.02	Redn + Oxygn
	(5.14)	(587)	(564)	(572)	(0.06)	(Redn)
5-Brsaldpt	4.99	591	556	608	0.01	Redn
	(4.76)	(592)	(580)	(608)	(0.05)	(Redn)
3-MeOsaldpt	5.10	636	588 sh	636	0.01	Redn + Oxygn
	(4.72)	(604)	(594)	(608)	(0.09)	(Redn + Oxygn)
5,6-Benzosaldpt	4.98	592 sh	592 sh	616 sh	0.10	Oxygn
	(4.50)	(590 sh)	(598 sh)	(600)	(0.13)	(Oxygn)

Values and reactivity in the parentheses are those for the mononuclear complexes.

a) Measured at room temperature. b) Measured in DMSO containing 0.1 M Bu_4NClO_4 at 25 °C.

c) Redn and Oxygn represent the reduction and oxygenation of the complexes, respectively.

In the former complex, as the ratio $[KO_2]/[Mn]$ increases, the intensity of a newly appeared absorption band at 380 nm increases remarkably and the intensity around 480 nm decreases (Fig. 1 A). Such spectral changes indicate that the manganese(III) complex is reduced by O_2^- to give the manganese(II) complexes as discussed in the previous sections III-1 and -2. On the contrary, in the latter complex, the intensity around 450 nm increases slightly with increasing the ratio $[KO_2]/[Mn]$ (Fig. 1 B). This indicates that the oxygenation of the complex occurs.

Figure 2 shows the changes of the polarograms of Mn_2(B-o-x-5-Brsaldien·2HBr)Cl_2 (A) and Mn_2(B-o-x-5,6-Benzosaldpt·2HBr)Cl_2 (B) in the course of the reactions with O_2^- in DMSO. In the former

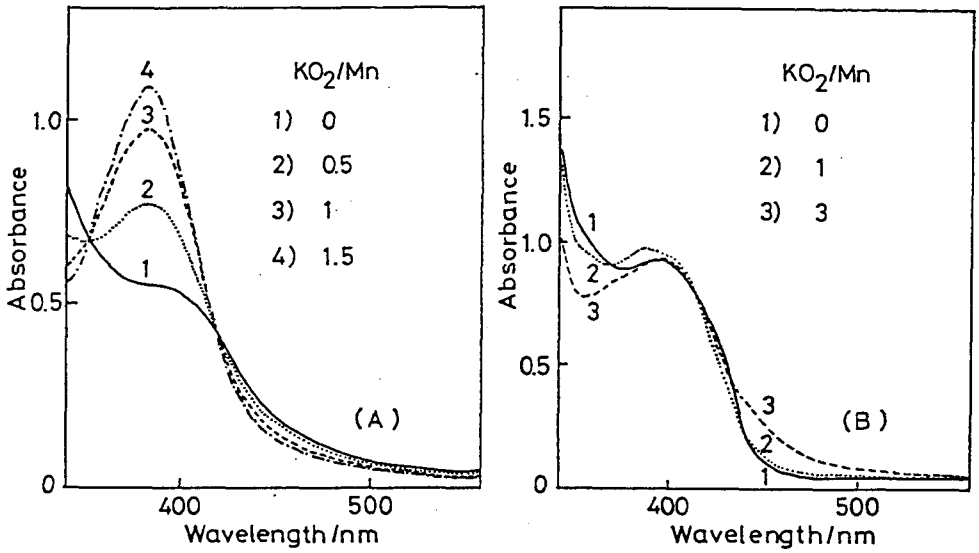

Fig. 1. Spectral changes of (A) Mn_2(B-o-x-5-Brsaldien·2HBr)Cl_2 (5×10^{-5} mol dm^{-3}) and (B) Mn_2(B-o-x-5,6-Benzosaldpt·2HBr)Cl_2 (4×10^{-5} mol dm^{-3}) caused by the addition of KO_2 in DMSO, cell length 1 cm.

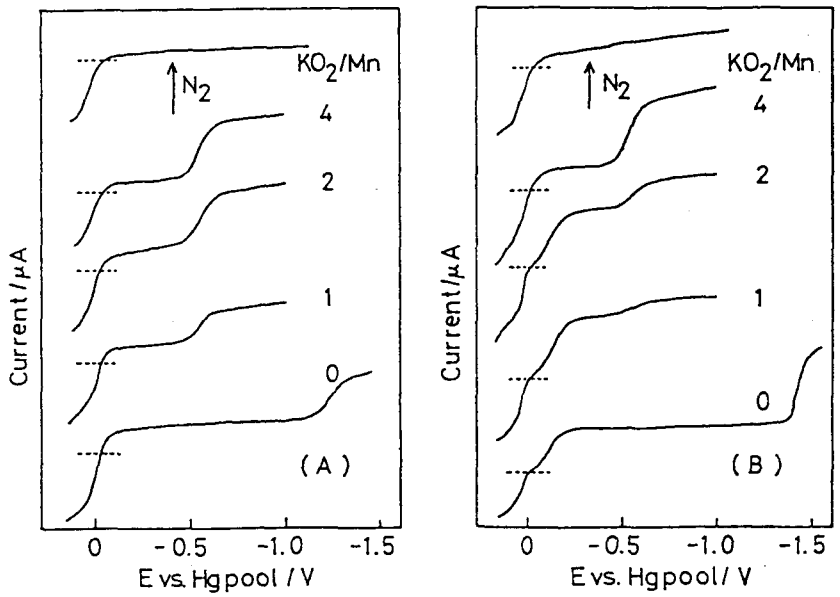

Fig. 2. Polarograms in the course of the reactions of (A) Mn_2(B-o-x-5-Brsaldien·2HBr)Cl_2 (5×10^{-4} mol dm^{-3}) and (B) Mn_2(B-o-x-5,6-Benzosaldpt·2HBr)Cl_2 (5×10^{-4} mol dm^{-3}) with KO_2 in DMSO containing Bu_4NClO_4 (0.1 mol dm^{-3}) at 25 °C.

case, as the ratio $[KO_2]/[Mn]$ increases, the wave height at -0.3 V due to the reduction from Mn(III) to Mn(II) decreases and a new cathodic wave appears at -0.55 V, which can be assigned to the reduction of free molecular oxygen. This indicates that the manganese(III) complex is reduced by O_2^-. In the latter case, the wave height at -0.20 V increases by the addition of KO_2 ($[KO_2]/[Mn]$ = 1 - 2), indicating the formation of the oxygenated complex. These results are consistent with those obtained from the absorption spectra.

The reactivities of the mononuclear and binuclear manganese(III) complexes toward O_2^- (Table 3) are found to be correlated with their polarographic reduction potentials as described in section III-1. The complexes Mn(5,6-Benzosaldpt)Cl, Mn(saldien)Cl, and Mn_2(B-o-x-5,6-Benzosaldpt·2HBr)Cl_2, which are reduced at more negative potentials than other complexes, react with O_2^- to give their oxygenated complexes. On the other hand, the other complexes are found to be reduced by O_2^- to the manganese(II) complexes except three complexes, Mn(3-MeOsaldpt)Cl, Mn_2(B-o-x-saldpt·2HBr)Cl_2, and Mn_2(B-o-x-5,6-Benzosaldpt·2HBr)Cl_2. These complexes exhibit that the both reduction and oxygenation may occur simultaneously in the reaction with O_2^- ($[KO_2]/[Mn]$ = 1 - 7), judging from the changes in the absorption spectra and polarograms (not shown in Figure). Thus, they are considered as a possible model for Mn-SOD.

Summary

The binuclear chloromanganese(III) Schiff base complexes have been synthesized and their reactions with O_2^- in DMSO have been compared with those for the corresponding mononuclear complexes.

In both mononuclear and binuclear complexes, three different types of the reactions are found to occur; the reduction from Mn(III) to Mn(II), simultaneous reduction and oxygenation, and oxygenation. These reactivities toward O_2^- are found to be correlated with their polarographic half-wave potentials corresponding to the reduction from Mn(III) to Mn(II).

References

1) G. D. Lawrence and D. T. Sawyer, *Coord. Chem. Rev.*, 27, 173 (1978).

2) W. M. Coleman and L. T. Taylor, *Coord. Chem. Rev.*, 32, 1 (1980).

3) L. J. Boucher, *J. Inorg. Nucl. Chem.*, 36, 531 (1974).

4) W. M. Coleman, R. K. Boggess, J. W. Hughes, and L. T. Taylor, *Inorg. Chem.*, 20, 1253 (1981).

Chapter IV

IV - 1 Reactions of Chloroiron(III) Schiff Base Complexes with Superoxide Ion in Dimethyl Sulfoxide

Introduction

The reactions of iron complexes with superoxide ions, O_2^-, are of interest in connection with the biological processes: the disproportionation of O_2^- by the iron-containing superoxide dismutases (Fe-SOD) and the catalytic utilization of molecular oxygen by the hemoproteins.

Hill *et al.* reported that $Fe^{III}(ppde)ClO_4$[1] reacts with O_2^- in N,N-dimethylformamide (DMF) to give $Fe(ppde)-O_2$ at low temperature (-50 °C).[2] McClune *et al.* proposed the formation of the peroxo complex, $[Fe^{III}(edta)-O_2]^{2-}$, by the reaction of $[Fe^{III}(edta)]^-$ with O_2^- in water on the basis of a stopped-flow spectrophotometry.[3] Recently, McCandlish *et al.* have reported that four different reaction pathways occurred in the reactions of O_2^- with iron porphyrins, as follows:

$$Fe^{III}(por)^+ + O_2^- \longrightarrow Fe^{II}(por) + O_2$$

$$2Fe^{III}(por)^+ + O_2^- \longrightarrow [Fe^{III}(por)]_2O$$

$$Fe^{III}(por)^+ + O_2^- \longrightarrow Fe(por)(O_2)$$

$$Fe^{II}(por) + O_2^- \longrightarrow Fe^{III}(por)(O_2^{2-}).$$

These reactions depend on conditions such as the solvent, the concentration, the presence or absence of water, and the temperature.[4]

In Chapter III, the reactions of the monomeric and polymeric chloromanganese(III) Schiff base complexes with O_2^- in dimethyl sulfoxide (DMSO) have been described. With the monomeric complexes, they can be classified into two types in the reactivity toward O_2^-: one gives the oxygenated complexes and the other is reduced to the corresponding manganese(II) complexes. The reactivities toward O_2^-

are found to be correlated with the polarographic half-wave potential corresponding to the reduction from Mn(III) to Mn(II). In the reactions of the polymeric complexes, the formation of their oxygenate complexes has been found.

In this Chapter, the reactions between O_2^- and the monomeric and polymeric chloroiron(III) Schiff base complexes shown below in DMSO will be described. Some of the polymeric complexes show a clearly different behavior in the changes of the absorption spectra and polarograms during the reactions with O_2^-, as compared with those observed for the monomeric complexes which react with O_2^- to give μ-oxo dimers.

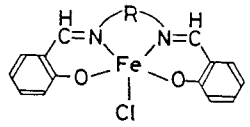

R	Abbreviation of ligands
CH_2CH_2	salen
C_6H_4	salphen
$CH(CH_3)CH_2$	salpln
C_6H_{10}	salchxn
$(CH_2)_2NH(CH_2)_2$	saldien
$(CH_2)_3NH(CH_2)_3$	saldpt
$(CH_2)_3N(CH_3)(CH_2)_3$	salMedpt

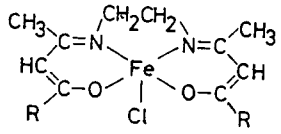

R	Abbreviation of ligands
CH_3	acacen
C_6H_5	bzacen

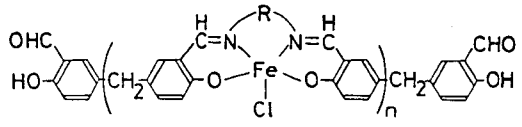

R	Abbreviation of ligands	R	Abbreviation of ligands
CH_2CH_2	p-salen	$(CH_2)_2NH(CH_2)_2$	p-saldien
C_6H_4	p-salphen	$(CH_2)_3NH(CH_2)_3$	p-saldpt
$CH(CH_3)CH_2$	p-salpln	$(CH_2)_3N(CH_3)(CH_2)_3$	p-salMedpt
C_6H_{10}	p-salchxn		

Monomeric and polymeric iron(III) Schiff base complexes.

Experimental

Preparation of Monomeric Chloroiron(III) Schiff Base Complexes. Chloro(N,N'-disalicylideneethylenediaminato)iron(III), Fe(salen)Cl: This complex was obtained by a modified method described in the literature[5] as follows. Anhydrous iron(III) chloride (0.81 g) was added to an absolute ethanol solution (100 cm^3) containing $salenH_2$ (1.34 g) and triethylamine (1.01 g). The mixture was stirred at 70 °C for 1 h, and then allowed to stand overnight in a refrigerator. The resulting precipitate was collected on a glass filter, washed with ethanol and ether, and then dried *in vacuo*. It was recrystallized from dichloromethane. The yield was 1.1 g.

The other monomeric chloroiron(III) Schiff base complexes were prepared in a similar manner. The analytical data for some of the complexes are given in Table 1.

Preparation of Polymeric (Oligomeric) Schiff Base Ligands. The oligomers of the Schiff bases were prepared by the polycondensation of $disalH_2$ with diamines or triamines under the controlled conditions: the molar ratio of $disalH_2$ to amines was maintained at 1.25; the temperature was kept below 20 °C; the reaction was stopped within 5 min; a dichloromethane was used as a reaction solvent.

Polymeric Schiff Base, p-saldienH_2: A dichloromethane solution (20 cm^3) of bis(2-aminoethyl)amine (1.4 g, 0.016 mol) was added to a dichloromethane solution (50 cm^3) of $disalH_2$ (5.2 g, 0.02 mol) with stirring below 20 °C. After the solution had been stirred for 5 min, it was poured into a large volume of ether (300 cm^3) with vigorous stirring. The resulting yellow precipitate was collected on a glass filter, washed with ether, and dried *in vacuo*. It was reprecipitated twice from dichloromethane and ether. Yield: 3.1 g.

Found: C, 69.95; H, 6.40; N, 11.63%. Calcd for a hexamer: C, 70.54; H, 6.33; N, 11.45%. ^{1}H NMR ($CDCl_3$) δ = 12.2 (br, OH), 9.70 (s, CHO), 8.27 (s, CH=N), *ca.* 7 (m, ϕ), 3.80 (s, ϕ-CH_2-ϕ), 3.65 (t, CH_2N=), 2.95 (t, CH_2N-). The specific viscosity (η_{sp}) measured in chloroform (0.4 g/100 cm^3) at 25±0.1 °C was 0.037. The degree of condensation (n) was estimated to be six from the analytical data, the ratios of the peak intensities in the ^{1}H NMR spectra, and the specific viscosity.

The polymeric Schiff bases, p-salplnH_2, p-salchxnH_2, p-saldptH_2, and p-salMedptH_2, described in the previous Chapter III-2, were used. They are found to be oligomers (n = 3 to 5) on the basis of the above measurements. The other polymeric Schiff bases, p-salenH_2 and p-salphenH_2, were prepared in a similar manner. However, their NMR spectra and viscositites could not be measured owing to their poor solubility in organic solvents.

Preparation of Polymeric Chloroiron(III) Schiff Base Complexes. Fe(p-saldien)Cl: To a dichloromethane (50 cm^3)-methanol (20 cm^3) solution containing p-saldienH_2 (1.1 g) and triethylamine (0.6 g) was added anhydrous iron(III) chloride (0.5 g) with stirring at room temperature. The precipitated wine-red solid was collected on a glass filter, washed with water, ethanol, and then ether, and then dried *in vacuo*. It was partly soluble in DMSO or DMF and was insoluble in dichloromethane or methanol. It was extracted with DMF (300 cm^3). The DMF solution was concentrated to *ca.* 30 cm^3 under reduced pressure, and poured into methanol (200 cm^3). The precipitate was collected on a glass filter, washed with ether, and dried *in vacuo*. The yield was 0.2 g.

The other polymeric iron(III) complexes were prepared in a similar manner. They are slightly soluble in DMSO or DMF

(*ca.* 0.1 g/100 cm^3) and are insoluble in methanol or dichloromethane. Therefore, the viscosity for them could not be measured. The infrared spectra of the polymeric complexes indicate that the Schiff base ligands coordinate to iron ions in the same features as the corresponding monomeric complexes. The magnetic moments of the polymeric complexes were determined on the basis of their iron contents.

Isolation of the Reaction Products of Monomeric Complexes with KO_2. *[Fe(acacen)]*$_2O$: To a dichloromethane solution (50 cm^3) containing Fe(acacen)Cl (0.63 g, 0.002 mol) and 18-crown-6 (0.56 g, 0.002 mol) was added potassium superoxide, KO_2 (0.22 g, 0.003 mol). The mixture was stirred for 1 h at room temperature. The wine-colored solution turned gradually orange. The mixture was filtered, and the filtrate was evaporated under reduced pressure to yield an orange solid. It was collected on a glass filter, washed with a small volume of water and methanol, and then ether, and dried *in vacuo*. It was recrystallized from dichloromethane to give orange crystals. The yield was 0.3 g. Found: C, 50.20; H, 6.37; N, 9.84; Fe, 19.23%. Calcd for $Fe_2C_{24}H_{36}N_4O_5$: C, 50.37; H, 6.34; N, 9.79; Fe, 19.52%.

The reaction product of Fe(bzacen)Cl with KO_2 was obtained in a similar manner. The reaction products of the other monomeric complexes with KO_2 were obtained similarly, using DMSO in place of dichloromethane as a reaction solvent.

Preparation of a KO_2 *DMSO Solution.* A DMSO solution of KO_2 (*ca.* 10^{-2} M, 1 M = 1 mol dm^{-3}) was prepared by dissolving KO_2 (0.018 g) into dry DMSO (25 cm^3) in the presence of 18-crown-6 (0.10 g). The O_2^- concentration of the KO_2 DMSO solution was determined by spectrophotometry.[6] The reactions of the iron(III)

complexes with KO_2 in DMSO were carried out in a nitrogen atmosphere.

Materials. Iron(III) chloride was of reagent grade. Potassium superoxide, KO_2, was purchased from Alfa products Inc. (above 96.5%). Dimethyl sulfoxide was distilled twice under reduced pressure prior to use. Other solvents were purified by a usual method.

Measurements. All the physical measurements were made by the methods described in Chapter III.

Results and Discussion

The monomeric and polymeric chloroiron(III) Schiff base complexes were synthesized and their reactions with O_2^- in DMSO were investigated. The degree of the condensation (n) of the polymeric iron(III) complexes could not be determined by the molecular weight and the viscosity measurements owing to their poor solubility. However, they are considered to be oligomers (n = 3 to 6) from the degree of the condensation of the polymeric Schiff base ligands.

Table 2 includes the magnetic moments, the absorption maxima in the visible region, and the polarographic half-wave potentials corresponding to the reduction from Fe(III) to Fe(II). The magnetic moments of the monomeric complexes fall within the range of 5.29 to 6.05 BM, indicating that these complexes have a d^5 high-spin

Table 1. Elemental analyses of iron(III) Schiff base complexes

Complex	Found (%)				Calcd (%)			
	C	H	N	Fe	C	H	N	Fe
Fe(salchxn)Cl	57.84	5.07	6.94	13.35	58.35	4.90	6.80	13.57
Fe(bzacen)Cl	59.77	5.13	6.49	12.62	60.37	5.07	6.40	12.76
Fe(acacen)Cl	45.65	5.89	8.81	18.34	45.96	5.79	8.93	17.81
Fe(saldien)Cl·H_2O	51.68	4.80	10.23	14.43	51.64	5.06	10.05	14.44
Fe(saldpt)Cl·$(H_2O)_{0.5}$	54.88	5.30	9.73	13.03	54.88	5.53	9.60	13.06
Fe(salMedpt)Cl·$(CH_2Cl_2)_{0.9}$	50.73	5.26	8.11	10.97	50.67	5.20	8.09	10.76

TABLE 2. PHYSICAL PROPERTIES OF IRON(III) SCHIFF BASE COMPLEXES

Ligand	μ_{eff}[a] / BM		λ_{max}[b] / nm		$-E_{1/2}$[c] vs. Hg pool / V	
	Monomer	Polymer	Monomer	Polymer	Monomer	Polymer
salen	5.29	5.25	482	506	0.20	0.22
salphen	5.64	5.72	560	572	0.11	−0.01
salpln	5.49	5.73	486	510	0.24	−0.03
salchxn	5.41	5.38	482	510	0.21	−0.04
saldien	5.99	5.82	502	524	0.25	−0.03
saldpt	6.05	5.17	496	512	0.06	−0.02
salMedpt	5.57	5.56	516	528	0.03	−0.01
acacen	5.92		510		0.28	
bzacen	5.99		512		0.21	

a) Measured at room temperature. b) Measured in DMSO. c) Measured in DMSO containing 0.1 M Bu_4NClO_4 at 25 °C.

electron configuration.[5,7] The magnetic moments of the polymeric complexes also fall within the range of 5.17 to 5.85 BM. The low value (5.17 BM) observed for the Fe(p-saldpt)Cl complex may be caused by antiferromagnetic interactions between iron atoms in the complex. No further investigation on the magnetic properties was made in the present study.

The absorption spectra of the monomeric and polymeric complexes in DMSO show an intense absorption band (ε = 4000) around 500 nm, which can be assigned to a charge-transfer transition.[8] The absorption maxima of the polymeric complexes are observed at lower energies than those of the corresponding monomeric complexes. Similar behavior was observed for the monomeric and polymeric chloromanganese(III) Schiff base complexes, as described in section III-2. The monomeric chloroiron(III) complexes with the quadridentate ligands (N_2O_2) in DMSO may have a weak six-coordinate structure by coordination of a DMSO molecule to the central iron atom. It was reported that the Fe(salen)Cl complex is nonelectrolyte in pyridine (py) and has a six-coordinate structure of Fe(salen)Cl-py.[7] The monomeric chloroiron(III) complexes with the quinquedentate

ligands (N_3O_2) may have a six-coordinate structure of a donor set of N_3O_2Cl in DMSO. Wilson *et al.* have reported that the Fe(saltrien)$^+$ cation has a six-coordinate structure (N_4O_2) and that the solvent effect on its spin-equilibrium in solution can be attributed to the hydrogen-bonding interactions between the NH groups of the saltrien and solvents, where saltrien denotes the dianion of N,N'-disalicylidenetriethylenetetramine.[8,9] On the other hand, the coordination featuers of the polymeric chloroiron(III) complexes are considered to be similar to those of the monomeric complexes. However, the coordination or interaction of DMSO with the polymeric complexes may be weaker than that of the monomeric complexes, because the iron atoms in the former complexes are not so isolated from the surroundings as are the latter complexes. This may be one reason why the lower energy shifts are observed in the polymeric complexes.

The polarograms of the chloroiron(III) Schiff base complexes in DMSO show the cathodic wave at the half-wave potential around -0.1 V (*vs.* Hg pool) in Table 2, which can be assigned to the one-electron reduction of Fe(III) to Fe(II).[10] The reduction of the polymeric complexes occurred at more positive potentials than those for the corresponding monomeric complexes. These results are consistent with the absorption spectral data mentioned above on the basis of the electron density in the central iron atoms of the complexes.

Visible Absorption Spectra. Figure 1 shows the absorption spectral changes of a DMSO solution of Fe(salen)Cl caused by the addition of a KO_2 DMSO solution in different molar ratios. As the molar ratio of KO_2 to the complex increases, the intensity of the absorption band at 490 nm decreases, showing an isosbestic point

at 458 nm. The absorption spectrum at the $[KO_2]/[complex] = 3$ is almost the same as that of the μ-oxo dimer, $[Fe(salen)]_2O$. This indicates that Fe(salen)Cl reacts with O_2^- in DMSO at room temperature to give a μ-oxo dimer. All the monomeric chloroiron(III) complexes investigated here showed similar spectral changes to those observed for the above Fe(salen)Cl complex.

Figures 2 and 3 show the comparison of the spectral changes caused by the addition of the KO_2 DMSO solution to the DMSO solutions of Fe(saldien)Cl and Fe(p-saldien)Cl, respectively. The spectral changes for Fe(saldien)Cl are similar to those for Fe(salen)Cl, indicating the formation of the μ-oxo dimer. On the other hand, the spectral

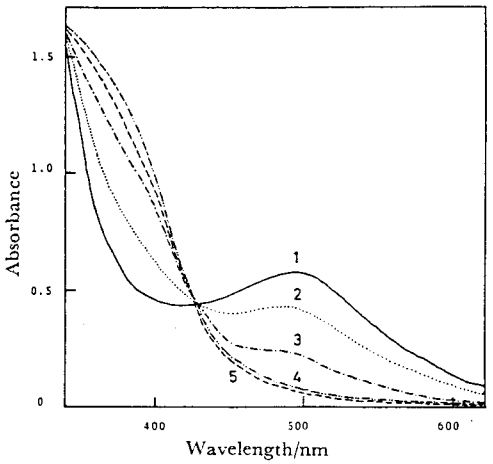

Fig. 1. Spectral changes on the addition of KO_2 to a DMSO solution of 6×10^{-5} M Fe(salen)Cl in different molar ratios.
1): No addition, 2): $[KO_2]/[complex] = 1$, 3): 2, 4): 3, 5): spectrum of 3×10^{-5} M $[Fe(salen)]_2O$ in DMSO. Cell length: 1.0 cm.

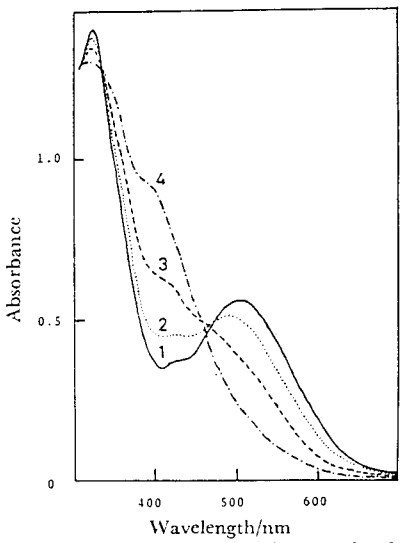

Fig. 2. Spectral changes on the addition of KO_2 to a DMSO solution of 1×10^{-4} M Fe(saldien)Cl in different molar ratios.
1): No addition. 2): $[KO_2]/[complex] = 1$, 3): 2, 4): 4. Cell length: 1.0 cm.

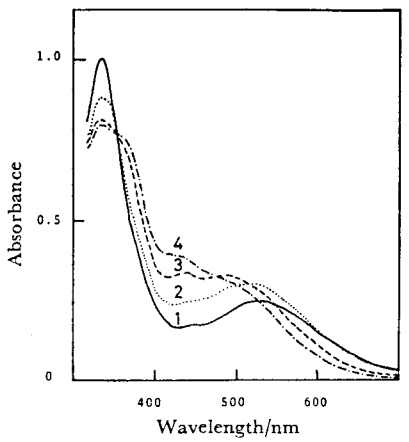

Fig. 3. Spectral changes on the addition of KO_2 to a DMSO solution of 1×10^{-4} unit M Fe(p-saldien)Cl in different molar ratios.
1): No addition, 2): $[KO_2]/[Fe] = 2$, 3): 3, 4): 5. Cell length: 1.0 cm.

changes for the polymeric complex, Fe(p-saldien)Cl, are clearly different from those for the monomeric complex, Fe(saldien)Cl. At the $[KO_2]/[Fe] = 2$, the absorption maximum is shifted to higher energy from 524 to 516 nm and the intensity increases slightly. At the $[KO_2]/[Fe] = 3$, the absorption maximum is shifted to 492 nm and its intensity increases even more. By the further addition of KO_2 ($[KO_2]/[Fe] = 5$), the intensity of the absorption band at 492 nm decreases and a new absorption band appears around 420 nm. This new absorption band at 420 nm can be assigned to the anion of the Schiff base ligand. This is confirmed by the absorption spectrum of p-saldienH_2 in a KOH-DMSO solution. These spectral changes can be explained as follows. The Fe(p-saldien)Cl reacts with O_2^- in the DMSO solutions ($[KO_2]/[Fe] < 3$) to give the oxygenated complex, probably a dioxygen adduct, and it reacts with O_2^- added in excess over the complex ($[KO_2]/[Fe] > 3$) to decompose with some dissociation of the Schiff base ligand.

The polymeric iron(III) complexes of Fe(p-saldpt)Cl and Fe(p-salMedpt)Cl showed similar spectral changes to the above Fe(p-saldien)Cl complex. However, the other polymeric complexes, Fe(p-salen)Cl, Fe(p-salphen)Cl, Fe(p-salpln)Cl, and Fe(p-salchxn)Cl showed the spectral changes similar to those observed for the corresponding monomeric complexes. These results may be attributed to the configurations of the reaction sites in the complexes. As discussed above, the former complexes may have a six-coordinate configuration, while the latter complexes may be taken to have essentially a five-coordinate configuration by neglecting the weak interaction between DMSO molecules and central iron atoms in these polymeric complexes.

Polarographic Measurements. Figure 4 shows the changes in

the polarograms during the reaction of Fe(salen)Cl with KO_2 in DMSO at 25 °C. At the molar ratio of $[KO_2]/[complex] = 1$, the wave height at -0.20 V due to the reduction of Fe(III) to Fe(II) decreases and a new cathodic wave appears around -0.8 V. By the further addition of KO_2 ($[KO_2]/[complex] = 2$), the first cathodic wave disappears and the wave height at -0.8 V increases. The half-wave potential of this cathodic wave is nearly equal to that (-0.89 V) of the μ-oxo dimer, $[Fe(salen)]_2O$. These results indicate that the reaction of Fe(salen)Cl with KO_2 in DMSO at 25 °C produces the μ-oxo dimer. The polarographic observations are consistent with those obtained in the absorption spectra mentioned above. Similar polarographic behavior was observed for all the monomeric iron(III) complexes investigated here.

It was reported that the dioxygen adduct of iron(II) porphyrin complexes can be stabilized at low temperature.[11] Thus, the reaction of Fe(salen)Cl with KO_2 was made in DMF at -25 °C.

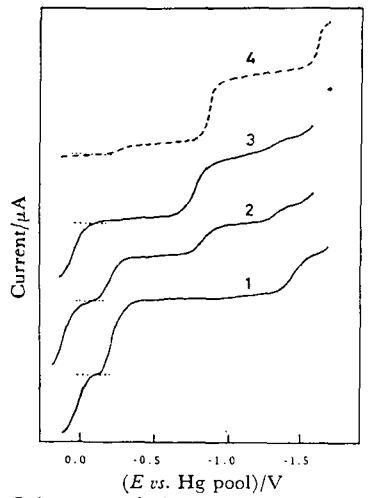

Fig. 4. Polarograms during the reactions of Fe(salen)Cl (5×10^{-4} M) with KO_2 in DMSO at 25 °C.
1): No addition, 2): $[KO_2]/[complex] = 1$, 3): 2, 4): polarogram of $[Fe(salen)]_2O$ (2.5×10^{-4} M) in DMSO.

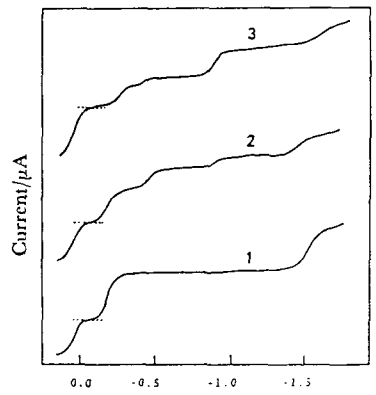

Fig. 5. Polarograms during the reactions of Fe(salen)Cl (5×10^{-4} M) with KO_2 in DMF at −25 °C.
1): No addition, 2): $[KO_2]/[complex] = 0.5$, 3): 1.

Figure 5 shows the changes in the polarograms of Fe(salen)Cl in DMF at -25 °C caused by the addition of a KO_2 DMSO solution. The half-wave potential (-0.19 V) of the first cathodic wave due to the reduction of Fe(III) to Fe(II) is nearly equal to that (-0.20 V) observed in DMSO at 25 °C. At the molar ratio of $[KO_2]/[complex]$ = 0.5, two new cathodic waves appear at the half-wave potentials of -0.48 and -0.88 V and the height of the first cathodic wave decreases. By the further addition of KO_2 ($[KO_2]/[complex]$ = 1), the wave heights of both the first and the second waves decrease and the third cathodic wave height increases. The second cathodic wave observed at -0.48 V may be attributed to the reduction of the oxygenated complex, Fe(salen)-O_2 or Fe(salen)-$O_2^{\cdot}$-Fe(salen), formed in the solution. This may further react with O_2^- to give the μ-oxo dimer. Similar polarographic behavior was observed in the reaction of Fe(salphen)Cl with KO_2 in DMF at -25 °C. From the available data the following scheme is proposed for the reaction of Fe(salen)Cl with O_2^-:

$$\mathrm{FeLCl} + \mathrm{O_2^-} \longrightarrow \mathrm{FeL\text{-}O_2} + \mathrm{Cl^-}$$

$$\mathrm{FeL\text{-}O_2} + \mathrm{FeLCl} \longrightarrow \mathrm{FeL\text{-}O_2^{\cdot}\text{-}FeL} + \mathrm{Cl^-}$$

$$\mathrm{FeL\text{-}O_2^{\cdot}\text{-}FeL} + \mathrm{O_2^-} \longrightarrow \mathrm{FeL\text{-}O_2\text{-}FeL} + \mathrm{O_2}$$

$$\mathrm{FeL\text{-}O_2\text{-}FeL} \longrightarrow \mathrm{FeL\text{-}O\text{-}FeL},$$

where L denotes the dianion of N,N'-disalicylideneethylenediamine. Recently, Chin *et al.* have reported on the mechanism of autoxidation of Fe^{II}(por) and proposed that the intermediate (por)Fe-O_2-Fe(por) can be stabilized at low temperature (-50 °C). This oxygenated complex reacts with Fe^{II}(por) to give (por)Fe-O-Fe(por) or decomposes thermally to (por)Fe-O-Fe(por) *via* iron(IV) complex, (por)Fe^{IV}=O, in the absence of Fe^{II}(por).[12)]

Figures 6 and 7 show the changes in the polarograms during the reactions of Fe(p-saldien)Cl with KO_2 in DMSO. In the former case, the KO_2-DMSO solution was added successively to the DMSO solution of the complex, whereas in the latter case, it was added step by step after passing nitrogen gas through the mixed solutions. The changes in the polarograms (in Fig. 6) are clearly different from those observed for Fe(salen)Cl (in Fig. 4). The cathodic wave at the half-wave potential of +0.01 V is due to the reduction of Fe(III) to Fe(II). The addition of KO_2 ($[KO_2]/[Fe] = 1$) causes the appearance of a new cathodic wave around -0.3 V. At the $[KO_2]/[Fe] = 2$, this wave height decreases slightly and a new cathodic wave appears at the half-wave potential of -0.6 V; this new wave can be assigned to the reduction of free molecular oxygen liberated during the reaction on the basis of its potential. At the $[KO_2]/[Fe] = 3$,

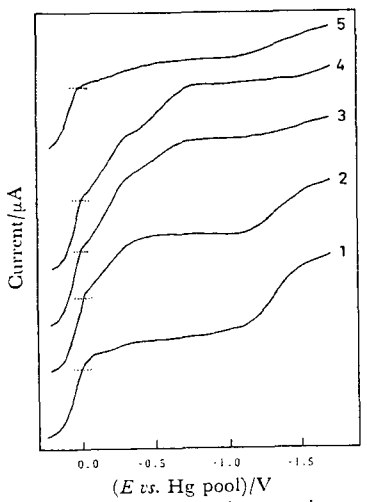

Fig. 6. Polarograms during the reactions of Fe(p-saldien)Cl (5×10^{-4} unit M) with KO_2 in DMSO at 25 °C.
1): No addition, 2): $[KO_2]/[Fe] = 1$, 3): 2, 4): 3, 5): after passing nitrogen gas through the solution shown by the curve 4.

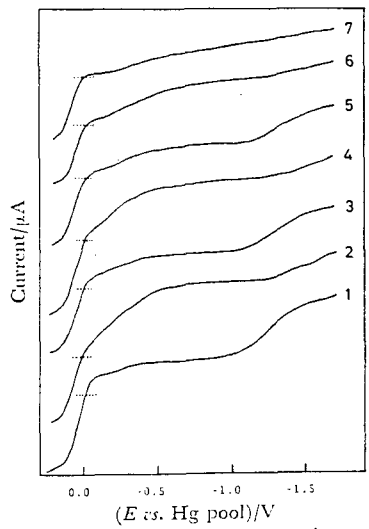

Fig. 7. Polarograms during the reactions of Fe(p-saldien)Cl (5×10^{-4} unit M) with KO_2 in DMSO at 25 °C.
1): No addition, 2): $[KO_2]/[Fe] = 1$, 4): 2, 6): 4, 3), 5), and 7): after passing nitrogen gas through the solutions shown by the curves 2, 4, and 6, respectively.

the wave height around -0.3 V decreases and the wave height around -0.6 V increases. By passing nitrogen gas through the mixed solution, both cathodic waves disappear. The cathodic wave which appeared around -0.3 V may be due to the oxygenated complex, Fe(p-saldien)-O_2. This is confirmed by the observations shown in Fig. 7. The polarogram observed at the $[KO_2]/[Fe] = 1$ is identical to that shown by curve 2 in Fig. 6. By passing nitrogen gas through the solution, the wave height around -0.3 V decreases. Such a cycle (adding KO_2 and passing N_2) was made three times. The polarograms shown by curves 2, 4, and 6 in Fig. 7 did not show cathodic wave at the half-wave potential around -0.6 V. Moreover, the degree of increase in the wave height around -0.3 V lowered gradually by repeating the cycle. These results indicate that the oxygenated complex, Fe(p-saldien)-O_2, may decompose to Fe^{II}(p-saldien) and molecular oxygen by passing nitrogen gas through the mixed solutions. Similar polarographic behavior was observed for the polymeric complexes, Fe(p-saldpt)Cl and Fe(p-salMedpt)Cl.

From the observations in the absorption spectra and the polarographic measurements, the reactions of the polymeric iron(III) complexes with O_2^- may occur as follows:

$$(p\text{-}L)FeCl + O_2^- \longrightarrow (p\text{-}L)Fe\text{-}O_2 + Cl^- \quad ([KO_2]/[Fe] < 2)$$

$$(p\text{-}L)Fe\text{-}O_2 + O_2^- \longrightarrow (p\text{-}L)Fe\text{-}O_2^- + O_2 \quad ([KO_2]/[Fe] > 2)$$

$$(p\text{-}L)Fe\text{-}O_2^- \longrightarrow (p\text{-}L)Fe^- + O_2$$

$$(p\text{-}L)Fe^- \longrightarrow \text{Decomposition},$$

where (p-L) denotes the dianion of the polymeric Schiff base ligands.

The reversible oxygenation of the iron(II) porphyrin complexes can be established by preventing the formation of μ-peroxo diiron complex in one or more of the following ways: (1) steric effects,

(2) immobilization in rigid surfaces, and (3) low-temperature measurements. In addition, it has been proposed that (4) a five-coordinate structure and (5) a nonpolar, hydrophobic environment around iron(II) complex play an important role for the synthesis of iron(II) porphyrin dioxygen adduct.[11] Recently, Niswander *et al.* have reported that Fe^{II}(salen)·py[13] and Fe^{II}(5-NO_2saldpt)[14] react with molecular oxygen to give only the corresponding μ-oxo dimers.

In the present study, the monomeric chloroiron(III) Schiff base complexes react with O_2^- to give only the μ-oxo dimers. On the other hand, the polymeric complexes of Fe(p-saldien)Cl, Fe(p-saldpt)Cl, and Fe(p-salMedpt)Cl form the dioxygen adduct in DMSO solution at room temperature by the reaction with O_2^-. Such behavior suggests that these polymeric complexes may satisfy the above requirements (1), (2), and (4).

Reaction Products of the Iron(III) Complexes with KO_2. The reaction products of the monomeric iron(III) complexes, Fe(acacen)Cl, Fe(bzacen)Cl, Fe(salen)Cl, Fe(salphen)Cl, Fe(salpln)Cl, and Fe(salchxn)Cl, were confirmed to be their μ-oxo dimers from the analytical data and physicochemical properties (in Table 3). However, for the other monomeric complexes, Fe(saldien)Cl, Fe(saldpt)-Cl, and Fe(salMedpt)Cl, their μ-oxo dimers could not be characterized. On the other hand, the reaction products of the polymeric iron-(III) complexes have not been identified with their oxygenated complexes by the analytical data and the physicochemical measurements. This may be caused by the instability of the oxygenated complexes.

Table 3. Physical properties of the reaction products of the monomeric iron(III) complexes with KO_2 in DMSO

Formula	μ_{eff}[a] BM	ν(Fe–O–Fe) cm^{-1}	$-E_{1/2}$[b] *vs.*Hg pool V
$[Fe(salen)]_2O$	1.91	825	0.89
$[Fe(salphen)]_2O$	2.05	820	0.86
$[Fe(salpln)]_2O$	2.02	815	0.97
$[Fe(salchxn)]_2O$	1.87	820	0.98
$[Fe(acacen)]_2O$[c]	1.88	838	1.18
$[Fe(bzacen)]_2O$[c]	2.50	820	1.22

a) Measured at room temperature. b) Measured in DMSO containing 0.1 M Bu_4NClO_4 at 25 °C. c) In dichloromethane.

Summary

A series of monomeric chloroiron(III) complexes with the quadridentate or quinquedentate Schiff bases such as N,N'-disalicylideneethylenediamine or bis[3-(salicylideneamino)propyl]amine reacts with superoxide ions, O_2^-, in dimethyl sulfoxide to give the corresponding μ-oxo dimers. The polymeric chloroiron(III) complexes with the polymeric (oligomeric) Schiff bases derived from 5,5'-methylenedisalicylaldehyde and triamines react with O_2^- in DMSO to give the oxygenated complexes, probably a dioxygen adduct, Fe^{III}-O_2^-. This is suggested by the absorption spectra and the polarographic measurements.

References

1) Abbreviations used in this study: ppde, protoporphyrin IX dimethyl ester dianion; H_4edta, ethylenediaminetetraacetic acid; por, tetraphenyl porphyrin dianion.

2) H. A. O. Hill, D. R. Turner, and G. Pellizer, *Biochem. Biophys. Res. Commun.*, 56, 739 (1974).

3) G. J. McClune, J. A. Fee, G. A. McCluskes, and J. T. Groves, *J. Am. Chem. Soc.*, 99, 5220 (1977).

4) E. McCandlish, A. R. Miksztal, M. Napp, A. Q. Sprenger, J. S. Valentine, J. D. Stong, and T. G. Spiro, *J. Am. Chem. Soc.*, 102, 4268 (1980).

5) M. Gerloch, J. Lewis, F. E. Mabbs, and A. Richards, *J. Chem. Soc., A*, 1968, 112.

6) S. Kim, R. DiCosimo, and J. San Filippo, Jr., *Anal. Chem.*, 51, 679 (1979).

7) M. Gullotti, L. Casella, A. Pasini, and R. Ugo, *J. Chem. Soc., Dalton Trans.*, 1977, 339.

8) M. F. Tweedle and L. J. Wilson, *J. Am. Chem. Soc.*, 98, 4824 (1976).

9) E. Sinn, G. Sim, E. V. Dose, M. F. Tweedle, and L. J. Wilson, *J. Am. Chem. Soc.*, 100, 3375 (1978).

10) K. M. Kadish, K. Das, D. Schaeper, C. L. Merrill, B. R. Welch, and L. J. Wilson, *Inorg. Chem.*, 19, 2816 (1980).

11) R. D. Jones, D. A. Summerville, and F. Basolo, *Chem. Rev.*, 79, 139 (1979).

12) D-H. Chin, G. N. La Mar, and A. L. Balch, *J. Am. Chem. Soc.*, 102, 4344 (1980).

13) R. H. Niswander and A. E. Martell, *Inorg. Chem.*, 17, 2341 (1978).

14) R. H. Niswander and A. E. Martell, *Inorg. Chem.*, 17, 1511 (1978).

IV - 2 Preparation of Binuclear Iron(III) Schiff Base Complexes and Their Reactions with Superoxide Ion in Dimethyl Sulfoxide

Introduction

In section IV-1, the reactions of O_2^- with the monomeric and polymeric chloroiron(III) Schiff base complexes in DMSO have been investigated in connection with the disproportionation of O_2^- by Fe-containing superoxide dismutases (Fe-SOD). The polymeric iron(III) complexes have been found to give their oxygenated complexes by the reaction with O_2^- while the monomeric complexes to give the corresponding μ-oxo dimers.

In this section the preparation of binuclear chloroiron(III) Schiff base complexes shown below and their reactions with O_2^- in DMSO will be described.

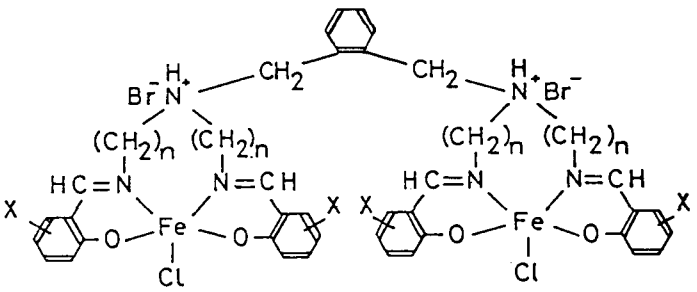

n=2; Fe_2(B-o-x-X saldien·2HBr)Cl_2

n=3; Fe_2(B-o-x-X saldpt·2HBr)Cl_2

X = H, 5-Br, 3-MeO.

Binuclear iron(III) Schiff base complexes.

Experimental

Preparation of Binuclear Iron(III) Schiff Base Complexes.

Fe_2(B-o-x-saldien·2HBr)Cl_2: The Schiff base ligands with bifunctional

chelating groups, which had been described in section III-3, were used. To a methanol solution (50 cm^3) of B-o-x-saldienH_2·2HBr (2.21 g, 2.5 mmol) and triethylamine (1.01 g, 10 mmol) was added anhydrous iron(III) chloride (0.81 g, 5 mmol). The mixture was stirred at room temperature for 3 h, and then concentrated under reduced pressure to yield a brown precipitate. It was filtered, washed with 2-propanol and then ether, and dried *in vacuo*. No further purification has been made. Other binuclear iron(III) complexes were prepared in a similar manner. Their analytical data are given in Table 1. These complexes are soluble in methanol, DMSO, and pyridine.

Preparation of Mononuclear Iron(III) Complexes. All the mononuclear iron(III) complexes were prepared by the modified method described in section IV-1. These complexes were abbreviated as follows: Fe(Xsaldien)Cl, Chlorobis[[2-(substituted salicylideneamino)ethyl]aminato]iron(III); Fe(Xsaldpt)Cl, Chlorobis[[3-(substituted salicylideneamino)propyl]aminato]iron(III).

Reactions with O_2^-. The reactions of the iron(III) complexes with KO_2 in DMSO were made by the procedure described in section IV-1.

Measurements. All physical measurements were carried out by the method described in section IV-1.

Materials. All reagents were of reagent grade. Solvents were purified by a usual manner.

Results and Discussion

Table 2 summarizes the properties of binuclear and mononuclear iron(III) Schiff base complexes and their reactivities toward O_2^- in DMSO. Magnetic moments of the complexes fall within the range from 5.34 to 6.05 BM, indicating that these complexes may adopt

Table 1. Analytical data for Fe_2(B-o-x-L·2HBr)Cl_2

Complex L	Found (%) C	H	N	Fe	Calcd (%) C	H	N	Fe
saldpt[a)]	50.61	5.23	7.32	10.30	50.51	5.12	7.36	9.79
saldien	50.24	4.74	7.74	11.07	49.61	4.35	7.89	10.48
5-Brsaldpt	40.12	3.64	5.64	7.73	40.12	3.51	5.85	7.77
5-Brsaldien	39.12	3.62	6.23	9.22	38.27	3.07	6.09	8.09
3-MeOsaldpt[a)]	47.69	5.09	6.80	9.07	48.89	5.05	6.58	8.74
3-MeOsaldien[a)]	46.18	4.80	7.45	9.64	47.20	4.79	6.88	9.14

a) These complexes include two molecules of H_2O.

Table 2. Properties of Fe_2(B-o-x-L·2HBr)Cl_2 and Fe(L)Cl and their reactivities toward O_2^- in DMSO

Complex L	μ_{eff}[a)] BM	λ_{max} nm DMSO	py	MeOH	$-E_{1/2}$ *vs.* Hg pool[b)] V Fe(III) → Fe(II)	Reactivity[c)] toward O_2^-
saldien	5.64	504	508	528	0.30	Oxygn
	(5.99)	(502)	(508)	(520)	(0.25)	(μ-oxo)
5-Brsaldien	5.65	515	534	542	0.00	Redn
	(5.75)	(506)	(510)	(520)	(0.23)	(μ-oxo)
3-MeOsaldien	5.98	538	536	559	0.30	Oxygn
	(5.86)	(537)	(532)	(554)	(0.27)	(μ-oxo)
saldpt	5.35	512	517	523	0.13	Oxygn
	(6.05)	(496)	(514)	(510)	(0.06)	(μ-oxo)
5-Brsaldpt	5.34	514	520	538	0.00	Redn
	(5.99)	(506)	(516)	(519)	(0.08)	(μ-oxo)
3-MeOsaldpt	5.66	549	560	566	0.16	Oxygn
	(5.95)	(542)	(550)	(550)	(0.15)	(μ-oxo)

Values and reactivity in the parentheses are those for the mononuclear complexes. a) Measured at room temperature. b) Measured in DMSO containing 0.1 M Bu_4NClO_4 at 25 °C. c) Oxygen, Redn, and μ-oxo represent the oxygenation, the reduction, and the formation of μ-oxo dimers, respectively.

d^5 high-spin electron configurations. The visible absorption spectra show an intense absorption band around 500 nm, which can be assigned to a charge-transfer transition.[1] The absorption maximum of the binuclear complexes is observed at slightly lower energy than that of the mononuclear complexes. The absorption maximum is shifted to high energy in the order DMSO > py > MeOH. These results indicate that the complexes may assume six-coordinate configurations in solution where the solvent molecules are coordinated to the central iron atom. The polarograms of the complexes show the cathodic wave due to one-electron reduction from Fe(III) to Fe(II) around -0.1 V.[2] There is little difference between the potentials of the binuclear and mononuclear complexes, with the exception of the 5-bromo substituted complexes; the binuclear 5-bromo substituted complex is reduced at more positive potentials than the corresponding mononuclear complex (Table 2).

Figure 1 shows the absorption spectral changes of DMSO solutions of Fe(3-MeOsaldien)Cl (A) and Fe_2(B-o-x-3-MeOsaldien·2HBr)-Cl_2 (B) caused by the addition of KO_2. In the former case, the intensity of the absorption band at 537 nm decreases remarkably with the isosbestic point at 480 nm as the molar ratio $[KO_2]/[Fe]$ increases (Fig. 1 A). Such spectral changes are similar to those observed for Fe(salen)Cl as shown in Fig. 1 in section IV-1, indicating the formation of the μ-oxo dimer. On the other hand, in the latter binuclear complex, the absorption maximum is shifted from 538 to 530 nm with increasing in intensity at $[KO_2]/[Fe] = 1$. The intensity of the absorption band (530 nm) decreases as the molar ratio $[KO_2]/[Fe]$ increases. These spectral changes are similar to those observed for Fe(p-saldien)Cl (*cf.* Fig. 3 in section IV-1), indicating the formation of the oxygenated complex.

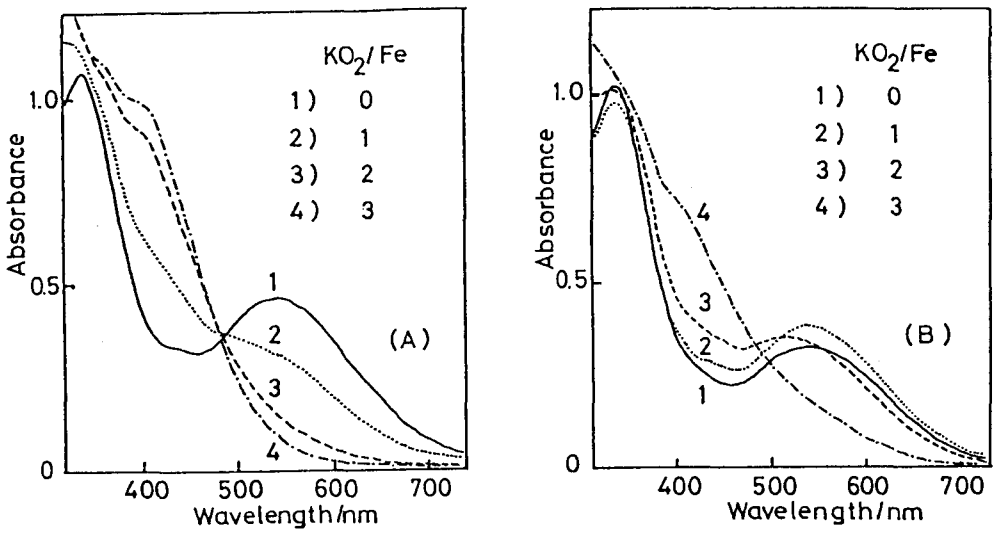

Fig. 1. Spectral changes of (A) Fe(3-MeOsaldien)Cl (5×10^{-4} mol dm^{-3}) and (B) Fe_2(B-o-x-3-MeOsaldien·2HBr)Cl_2 (5×10^{-5} mol dm^{-3}) caused by the addition of KO_2 in DMSO, cell length 1 cm.

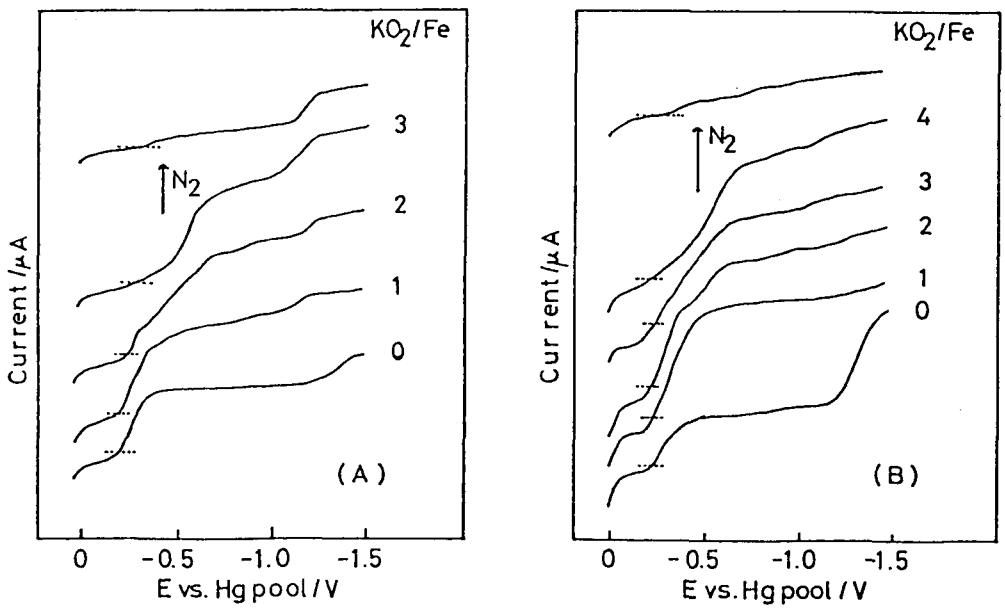

Fig. 2. Polarograms in the course of the reactions of (A) Fe(3-MeOsaldien)Cl (5×10^{-4} mol dm^{-3}) and (B) Fe_2(B-o-x-3-MeOsaldien·2HBr)Cl_2 (5×10^{-4} mol dm^{-3}) with KO_2 in DMSO containing Bu_4NClO_4 (0.1 mol dm^{-3}) at 25 °C.

Figure 2 shows the changes of polarograms of Fe(3-MeOsaldien)Cl (A) and Fe_2(B-o-x-3-MeOsaldien·2HBr)Cl_2 (B) in DMSO caused by the addition of KO_2. In the former complex, as the molar ratio $[KO_2]/[Fe]$ increases, the wave height at -0.27 V due to the reduction from Fe(III) to Fe(II) decreases and two cathodic waves appear at -0.55 and -1.20 V. These waves can be assigned to the reductions of free molecular oxygen (O_2) and of the μ-oxo dimer as described in section IV-1. In the latter complex, the wave height at -0.30 V is the largest at $[KO_2]/[Fe] = 1$, and decreases with increasing the molar ratio $[KO_2]/[Fe]$, accompanying with appearance of the cathodic wave at -0.55 V. Moreover, no cathodic wave is observed around -1.0 V, suggesting that μ-oxo complex is not formed in the solution. These polarographic changes (Fig. 2 B) are similar to those observed for Fe(p-saldien)Cl (*cf.* Fig. 6 in section IV-1)

The observations in the absorption spectra and polarograms lead the author to the conclusion that the mononuclear complex, Fe(3-MeOsaldien)Cl, reacts with O_2^- to give the μ-oxo complex exclusively and the binuclear complex, Fe_2(B-o-x-3-MeOsaldien·-2HBr)Cl_2, to form the oxygenated complex. Other mononuclear complexes exhibited the same behavior in the reactions with O_2^- as the case of Fe(3-MeOsaldien)Cl, indicating the formation of the μ-oxo dimers. On the other hand, the binuclear complexes except the 5-bromo substituted complexes exhibited the same behavior in the reactions with O_2^- as the case of Fe_2(B-o-x-3-MeOsaldien·2HBr)-Cl_2, indicating the formation of the oxygenated complexes. The polarograms of the 5-bromo substituted complexes during the reactions with KO_2 in DMSO suggest that they are reduced by O_2^- to the iron(II) complexes (not shown in Figure). These results are not

contradict with the fact that the complexes have the most positive reduction potentials compared with any others (Table 2).

Summary

The binuclear chloroiron(III) Schiff base complexes have been prepared and their reactions with O_2^- have been investigated in comparison with the corresponding mononuclear complexes. Some of the binuclear complexes react with O_2^- to form their oxygenated complexes, while all the mononuclear complexes react with O_2^- to give the μ-oxo dimers.

References

1) M. F. Tweedle and L. J. Wilson, *J. Am. Chem. Soc.*, 98, 4824 (1976).

2) K. M. Kadish, K. Das, D. Schaeper, C. L. Merrill, B. R. Welch, and L. J. Wilson, *Inorg. Chem.*, 19, 2816 (1980).

IV - 3 Preparation of Monomeric and Polymeric Iron(III) Complexes with Bidentate Schiff Base Ligands and Their Reactions with Superoxide Ion in Dimethyl Sulfoxide

Introduction

In the previous sections IV-1 and -2, the reactions of O_2^- with a series of monomeric, binuclear, and polymeric chloroiron(III) complexes of quadridentate and quinquedentate Schiff bases in DMSO have been described. The monomeric iron(III) complexes have been found to give their μ-oxo dimers exclusively, while some of the binuclear and polymeric iron(III) complexes have been found to give their oxygenated complexes.

In this section the preparation of the monomeric and polymeric chloroiron(III) complexes of the bidentate Schiff bases shown below and their reactions with O_2^- in DMSO will be described.

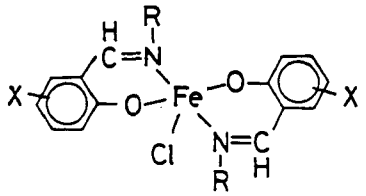

Fe(N-R-X sai)$_2$Cl

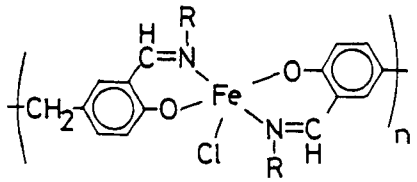

Fe(N-R disai)Cl

R=n-C_4H_9(Bu), n-C_8H_{17}(Oct),
n-$C_{12}H_{25}$(Dod), $CH_2C_6H_5$(Bz).
X= H, 5-NO_2 for R=Bz.

Monomeric and polymeric Fe(III) Schiff base complexes.

Experimental

Preparation of Monomeric Chloroiron(III) Schiff Base Complexes. Bidentate Schiff base ligands used in this section were obtained by the condensation of salicylaldehydes with alkylamines in THF.

Chlorobis(N-octylsalicylideneaminato)iron(III), Fe(N-Octsai)$_2$Cl: To a THF solution (50 cm^3) of N-octylsalicylideneamine (N-OctsaiH, 2.33 g, 10 mmol) and triethylamine (1.01 g, 10 mmol) was added anhydrous iron(III) chloride (0.81 g, 5 mmol). The mixture was stirred for 2 h and then allowed to stand overnight. The resulting precipitate was collected on a glass filter and dried *in vacuo*. It was recrystallized from ether to give the title complex as wine red crystals. Other monomeric iron(III) complexes were obtained in a similar manner. Fe(N-Busai)$_2$Cl and Fe(N-Bzsai)$_2$Cl were recrystallized from acetone. Fe(N-Dodsai)$_2$Cl was recrystallized from petroleum ether. Their analytical data are given in Table 1.

Preparation of Polymeric Chloroiron(III) Schiff Base Complexes. The Schiff base ligands with bifunctional chelating groups were prepared by the condensation of 5,5'-methylenedisalicylaldehyde (disalH$_2$) with alkylamines as follows.

N,N'-Dioctyl-5,5'-methylenedisalicylideneamine, N-OctdisaiH$_2$: To a THF solution (20 cm^3) of disalH$_2$ (2.7 g, 10 mmol) was added a THF solution (20 cm^3) of *n*-octylamine (2.6 g, 20 mmol). The resulting solution was refluxed for 30 min and then evaporated to dryness under reduced pressure. A yellow solid obtained was recrystallized from acetone. The yield was 5.0 g. Other Schiff base ligands (N-BudisaiH$_2$, N-DoddisaiH$_2$, and N-BzdisaiH$_2$) were prepared in a similar manner. Their melting points and analytical data are given in Table 2.

Fe(N-Octdisai)Cl: To a mixed solution of dichloromethane

(100 cm^3) and ethanol (30 cm^3) containing N-OctdisaiH_2 (4.0 g) and triethylamine (1.7 g) was added anhydrous iron(III) chloride (1.4 g). The mixture was stirred for 20 min at 40 ^oC, and then the solution was concentrated to *ca.* 50 cm^3 under reduced pressure and filtered. The filtrate was poured into ethanol (200 cm^3) to give a wine red precipitate. It was collected on a glass filter, washed with ethanol, dried *in vacuo*, and reprecipitated from dichlromethane and ethanol. Other polymeric iron(III) complexes were prepared in a similar manner. The iron contents of the complexes were analyzed. Fe (%): 10.58 for Fe(N-Budisai)Cl, 9.04 for Fe(N-Octdisai)Cl, 7.06 for Fe(N-Doddisai)Cl, and 9.07 for Fe(N-Bzdisai)Cl. The magnetic moments determined at room temperature were calculated from the iron contents (Table 3).

Isolation of Reaction Product of Fe(N-Octdisai)Cl with KO_2. To a DMSO solution (100 cm^3) of Fe(N-Octdisai)Cl (120 mg) was added a DMSO solution of KO_2(17 mg, equimolar amount to the unit mole of the complex) and 18-crown-6 (90 mg) at room temperature. A reddish brown solid immediately precipitated was collected on a glass filter, washed with 2-propanol and then diethyl ether, and dried *in vacuo*. No chlorine was detected in this product by ignition test. Analytical data, Found: C, 64.78; H, 7.74; N, 4.61; Fe, 10.04%. The parent complex, Fe(N-Octdisai)Cl, Found: C, 63.90; H, 7.65; N, 4.49; Fe, 9.04%.

Reactions of Iron(III) Complexes with KO_2. The reactions of the iron(III) complexes with KO_2 were made by the procedure described in section IV-1.

Materials. All reagents were of reagent grade. Solvents used were purified in usual manners. DMSO was distilled twice under reduced pressure prior to use.

Measurements. All physical measurements were carried out by the methods described in section IV-1.

Table 1. Analytical data for the monomeric iron(III) complexes

Complex	Found (%)				Calcd (%)			
	C	H	N	Fe	C	H	N	Fe
$Fe(N\text{-}Busai)_2Cl$	59.17	6.37	6.33	11.96	59.64	6.36	6.31	12.58
$Fe(N\text{-}Octsai)_2Cl$	64.75	7.80	5.00	9.81	64.81	7.98	5.04	10.04
$Fe(N\text{-}Dodsai)_2Cl$	67.81	9.15	4.22	8.70	68.31	9.05	4.19	8.36
$Fe(N\text{-}Bzsai)_2Cl$	65.54	5.03	5.43	10.81	65.71	4.73	5.47	10.91
$Fe(N\text{-}Bz\text{-}5\text{-}NO_2sai)_2(OH)$	57.57	3.80	9.57	8.94	57.65	3.97	9.60	9.57

Table 2. Melting points and elemental analyses of the Schiff base ligands

Schiff base ligand	M.P. °C	Found (%)			Calcd (%)		
		C	H	N	C	H	N
$N\text{-}BudisaiH_2$	38.5 - 39	75.19	8.26	7.67	75.38	8.25	7.64
$N\text{-}OctdisaiH_2$	51 - 52	77.61	9.68	5.67	77.78	9.69	5.85
$N\text{-}DoddisaiH_2$	60.5 - 61	79.31	10.66	4.80	79.27	10.58	4.74
$N\text{-}BzdisaiH_2$	145 -146	80.12	5.94	6.36	80.16	6.03	6.45

Results and Discussion

The polymeric chloroiron(III) complexes with bifunctional chelating Schiff bases were synthesized and their reactivities toward O_2^- in DMSO were compared with those for the corresponding monomeric iron(III) complexes by the use of absorption spectra and polarographic measurements.

Table 3 summarizes magnetic moments, absorption maxima in the

visible region, and half-wave potentials corresponding to the reduction from Fe(III) to Fe(II) for the both monomeric and polymeric iron(III) complexes investigated here. The magnetic moments fall within the range of 5.80 to 6.04 BM, indicating that the complexes may assume d^5 high-spin electron configurations. Those complexes exhibit an intense absorption band (ε = 4000) around 500 nm in the visible region, which can be assigned to a charge-transfer transition on the basis of its intensity. The band for the polymeric complexes is observed at a longer wavelength than that for the corresponding monomeric complexes. This may be caused by a difference in interaction of the solvent molecule (DMSO) with the central iron atom between the monomeric and polymeric complexes. The monomeric complexes may adopt an octahedral configuration by coordination of solvent DMSO to the iron atom.[1)] On the other hand, the interaction of DMSO with the central iron atom in the polymeric complexes is considered to be weaker than that in the monomeric complexes, because the central iron atom in the former is not isolated from the surroundings owing to polymeric structures. Both monomeric and polymeric complexes show a cathodic wave at half-wave potentials around -0.15 V (*vs.* Hg pool). This can be assigned to the one-electron reduction from Fe(III) to Fe(II). The polymeric complexes are found to be reduced at slightly more positive potentials than those for the corresponding monomeric complexes. The results can be explained by the stronger interaction of DMSO molecules with the central iron atom in the monomeric complexes than the polymeric complexes, as described above.

Absorption Spectral Changes. Figure 1 shows the absorption spectral changes of DMSO solutions of $Fe(N\text{-}Octsai)_2Cl$ (A) and Fe(N-Octdisai)Cl (B) caused by the addition of various amounts of

Table 3. Properties of the monomeric and polymeric iron(III) complexes

Complex	μ_{eff} [a] / BM	λ_{max} [b] / nm	$-E_{1/2}$ *vs.* Hg pool [c] / V
Fe(N-Busai)$_2$Cl	5.96	513	0.21
Fe(N-Budisai)Cl	5.82	530	0.18
Fe(N-Octsai)$_2$Cl	5.93	510	0.20
Fe(N-Octdisai)Cl	5.83	529	-0.02
Fe(N-Dodsai)$_2$Cl	5.88	516	0.20
Fe(N-Doddisai)Cl	5.92	522	0.12
Fe(N-Bzsai)$_2$Cl	5.91	517	0.18
Fe(N-Bzdisai)Cl	5.80	528	0.18
Fe(N-Bz-5-NO_2sai)$_2$(OH)	6.04	492	0.11

a) Measured at room temperature. b) Measured in DMSO. c) Measured in DMSO containing Bu_4NClO_4 (0.1 mol dm^{-3}) at 25 °C.

KO_2. In the former complex, the absorption band at 510 nm decreases in intensity with increasing the molar ratio of KO_2 to the complex with an isosbestic point at 438 nm (Fig. 1 A). In the near ultraviolet region, the absorption band at 324 nm is shifted to 332 nm with slightly increasing intensity at the $[KO_2]/[Fe] = 1 - 2$. By further addition of KO_2 ($[KO_2]/[Fe] = 5$), its intensity decreases and a new absorption band appears at 392 nm (curve 4 in Fig. 1 A). By bubbling O_2 through the solution including KO_2 ($[KO_2]/[Fe] = 5$) and showing the absorption curve 4, the absorption band at 392 nm disappears and the absorption band at 332 nm is shifted to 318 nm. These spectral changes can be explained as follows: Fe(N-Octsai)$_2$Cl is reduced by O_2^- to give an iron(II) complex, probably Fe(N-Octsai)$_2$,

which is characterized by the absorption band at 332 nm, and the iron(II) complex further reacts with additional KO_2 to give an oxygen-sensitive complex having the absorption band at 392 nm. This complex is tentatively assigned to $Fe^{II}(N\text{-Octsai})_2\text{-}O_2^-$. All the monomeric complexes exhibit absorption spectral changes similar to those for $Fe(N\text{-Octsai})_2Cl$. On the other hand, the spectral changes of the latter polymeric complex (Fig. 1 B) are clearly different from those of the former, and are similar to those observed for the polymeric complex Fe(p-saldien)Cl, which has been found to give the oxygenated complex, as already described in section IV-1. In the course of the reaction of Fe(N-Doddisai)Cl with KO_2 in DMSO, spectral changes similar to those for Fe(N-Octdisai)-Cl are observed, indicating the formation of the oxygenated complex. However, other polymeric complexes, Fe(N-Budisai)Cl and Fe(N-Bzdisai)Cl, exhibit the spectral changes similar to those for the monomeric complexes, suggesting that these polymeric complexes are reduced by O_2^- to give iron(II) complexes. It is thought that a difference in the reactivities of the polymeric complexes toward O_2^- may result from the effects of alkyl groups attached to the imino nitrogen atoms; the oxygenated complexes can be stabilized by the long-chain alkyl groups such as *n*-octyl and *n*-dodecyl groups.

Polarographic Measurements. Figure 2 shows the changes of polarograms of $Fe(N\text{-Octsai})_2Cl$ (A) and Fe(N-Octdisai)Cl (B) in the course of the reactions with KO_2 in DMSO. In the former complex, the wave height at -0.20 V due to the reduction from Fe(III) to Fe(II) decreases and a new cathodic wave appears at -0.6 V when KO_2 is added successively, $[KO_2]/[Fe] = 1 - 3$,(Fig. 2 A). The cathodic wave at -0.6 V can be assigned to the reduction of molecular oxygen

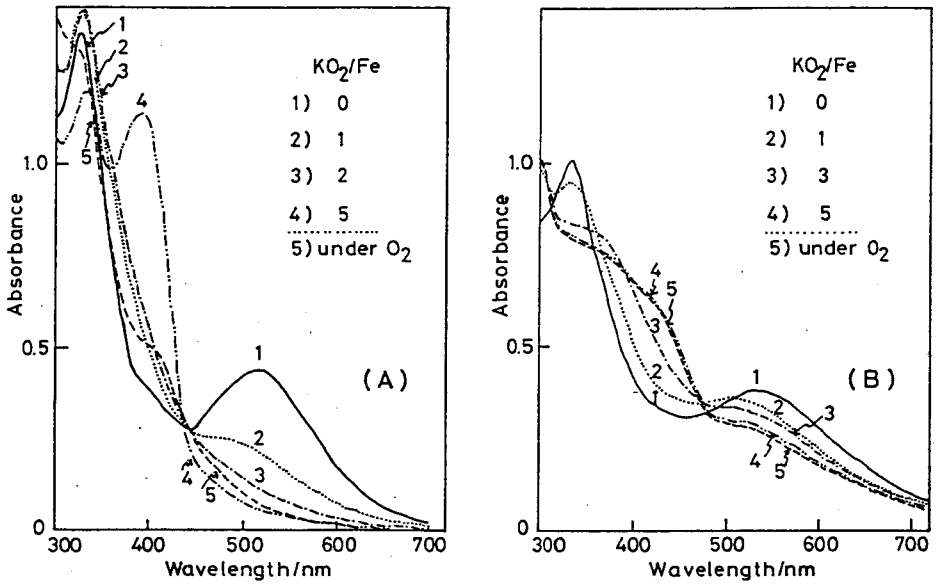

Fig. 1. Spectral changes of (A) $Fe(N\text{-}Octsai)_2Cl$ (1×10^{-4} mol dm^{-3}) and (B) $Fe(N\text{-}Octdisai)Cl$ (1×10^{-4} unit mol dm^{-3}) caused by the addition of KO_2 in DMSO, cell length 1 cm.

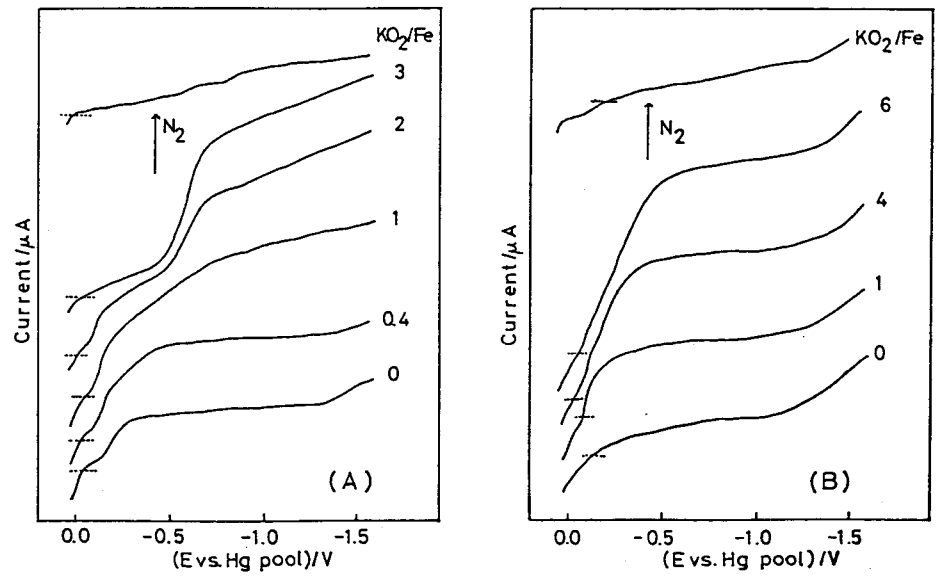

Fig. 2. Polarograms in the course of the reactions of (A) $Fe(N\text{-}Octsai)_2Cl$ (5×10^{-4} mol dm^{-3}) and (B) $Fe(N\text{-}Octdisai)Cl$ (5×10^{-4} unit mol dm^{-3}) with KO_2 in DMSO containing Bu_4NClO_4 (0.1 mol dm^{-3}) at 25 °C.

which was liberated during the reaction. These results indicate that Fe(N-Octsai)$_2$Cl is reduced by O_2^- to give iron(II) complex according to the following equation:

$$Fe^{III}(N\text{-Octsai})_2Cl + O_2^- \longrightarrow Fe^{II}(N\text{-Octsai})_2 + O_2.$$

Other monomeric iron(III) complexes and the polymeric complexes, Fe(N-Budisai)Cl and Fe(N-Bzdisai)Cl, exhibited the polarographic changes similar to those for the above complex, indicating that these complexes are reduced by O_2^- to give iron(II) complexes.

On the other hand, in the latter complex, Fe(N-Octdisai)Cl, the polarographic changes (Fig. 2 B) are clearly different from those for the former monomeric complex. The cathodic wave due to the reduction from Fe(III) to Fe(II) is observed at -0.14 V as an ill-defined wave, which may be caused by its polymeric structure. By the addition of KO_2 ($[KO_2]/[Fe] = 1$) the wave height of the cathodic wave at about -0.2 V is increased. A successive addition of KO_2 ($[KO_2]/[Fe] = 4 - 6$) results in a marked increase in the wave height around -0.3 V. These polarographic changes are similar to those observed for Fe(p-saldien)Cl (*cf.* Figs. 6 and 7 in section IV-1), indicating the formation of the oxygenated complex. Similar polarographic behavior is observed for Fe(N-Doddisai)Cl. These results are consistent with those obtained from the absorption spectral data.

When the polymeric complex, Fe(N-Octdisai)Cl is allowed to react with KO_2 in DMSO at high concentration, a reddish brown precipitate forms immediately, which is insoluble in common organic solvents and does not contain chlorine atom. Its magnetic moment (4.52 BM) is found to be lower than that (5.83 BM) of the parent complex, although a significant difference between them are not observed in the infrared

and diffused reflectance spectra. These results suggest that the product may be a cross-linked polymeric structure where iron atoms of the polymeric complex are bridged through coordination of dioxygen; $-[-Fe(N\text{-}Octdisai)\text{-}O_2\text{-}]_n^-$. The analytical data are consistent with the above formula.

Summary

The monomeric and polymeric chloroiron(III) Schiff base complexes, $Fe(N\text{-}Rsai)_2Cl$ and $Fe(N\text{-}Rdisai)Cl$ respectively, have been synthesized and their reactions with O_2^- in DMSO have been investigated, where R can be n-C_4H_9 (Bu), n-C_8H_{17} (Oct), n-$C_{12}H_{25}$ (Dod), and $CH_2C_6H_5$ (Bz). All the monomeric complexes are found to be reduced by O_2^- to give the iron(II) complexes. The polymeric complexes (R = Oct and Dod) are found to give their oxygenated complexes, whereas the polymeric complexes (R = Bu and Bz) are found to be reduced like the case of the monomeric complexes. The reactivities different between these polymeric complexes toward O_2^- may be ascribed to the effect of the alkyl groups attached to the imino nitrogen atoms; the long-chain alkyl groups (Oct and Dod) are considered to stabilize an oxygenated complex.

References

1) M. Gullotti, L. Cassella, A. Pasini, and R. Ugo, *J. Chem. Soc., Dalton Trans.*, 1977, 339.

Chapter V

V - 1 The Preparation and Characterization of Dichloromanganese(IV) Schiff Base Complexes

Introduction

The manganese ion plays an important role in biological redox systems, which are comprised of the oxygen-evolution process of the photosystem II in green plants and the disproportionation of the superoxide ion, O_2^-, by manganese-containing superoxide dismutases. In these systems, the oxidation states of manganese(II), (III), and/or (IV) are believed to be involved.[1] In relation to its function, manganese complexes with higher oxidation states, such as +III and +IV, have been investigated.[2 - 6] Although manganese(III) complexes with various ligands have thus been synthesized and characterized, few manganese(IV) complexes have been isolated so far, for the manganese (IV) ion is a strong oxidant and its complexes are very unstable.[7,8]

The author has been found that some chloromanganese(III) Schiff base complexes react with hydrogen chloride to give the corresponding manganese(IV) complexes as deep green crystals. In this Chapter, the preparation and characterization of a series of novel dichloromanganese(IV) Schiff base complexes will be described.

Experimantal

Preparation of Manganese(III) Complexes. The quadridentate Schiff base ligands were prepared by the condensation of salicylaldehydes with diamines. They were recrystallized from ethanol or appropriate organic solvents. The bidentate Schiff base ligands were prepared by the condensation of the salicylaldehydes with butylamine. The 5-nitro, 5-bromo, and 5,6-benzo derivatives were

recrystallized from ethanol. All the manganese(III) Schiff base complexes (shown in Fig. 1) were prepared by a modification of the method described in the literature.[9 - 12] To a methanol solution of a quadridentate Schiff base ligand was added an equimolar amount of manganese(III) acetate dihydrate, $Mn(CH_3COO)_3 \cdot 2H_2O$ (a half molar of it when the Schiff bases were bidentate ligands). The solution was warmed at 60 °C for 1 h, and then a 1.5-molar-fold quantity of lithium chloride over the manganese acetate was added to this solution, which was subsequently further warmed at 60 °C for 1 h. The solution was then concetrated under reduced pressure and cooled. The resulting precipitates were collected on a glass filter, washed with a small volume of water and methanol, and then with ether, and dried *in vacuo*. They were recrystallized from methanol or dichloromethane. The yields were 60 – 80%. The elemental analyses of the manganese(III) complexes are given in Table 1, along with their magnetic moments measured at room temperature. The magnetic moment of $Mn(N\text{-}Bu\text{-}5\text{-}NO_2sai)_2Cl$ was found to be lower than those of the other manganese(III) complexes. This may be caused by the magnetic-exchange interaction in this complex.

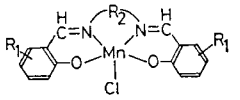

R_1	R_2	L
H	CH_2CH_2	salen
H	C_6H_{10}	salchxn
5-NO_2	CH_2CH_2	5-NO_2salen
5-CH_3	CH_2CH_2	5-Mesalen
5-Br	CH_2CH_2	5-Brsalen
5-Br	$CH(CH_3)CH_2$	5-Brsalpln
5-Br	$CH_2CH_2CH_2$	5-Brsalpn

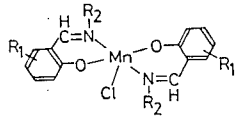

R_1	R_2	L′
H	C_4H_9	*N*-Busai
5-NO_2	C_4H_9	*N*-Bu-5-NO_2sai
5-Br	C_4H_9	*N*-Bu-5-Brsai
5,6-Benzo	C_4H_9	*N*-Bu-5,6-Benzosai

Fig. 1. Manganese(III) Schiff base complexes.

Preparation of Dichloromanganese(IV) Schiff Base Complexes. Dichloro(N,N'-disalicylideneethylenediaminato)manganese(IV) Dichloromethane Adduct, $Mn(salen)Cl_2 \cdot (CH_2Cl_2)_{0.5}$: Into an acetone

solution (200 cm^3) of Mn(salen)Cl.H_2O (0.5 g) was added, drop by drop, a two-molar-fold portion of a methanol solution of HCl over the complex at room temperature. The solution turned brown to deep green. After the solution had been filtered, the filtrate was concentrated to about 20 cm^3 under reduced pressure. Anhydrous ether (200 cm^3) was then added to this solution. The resulting green precipitates were collected on a glass filter, washed with ether, and dried *in vacuo*. They were recrystallized from dichloromethane to give the above complex as deep green crystals. The yield was *ca.* 30%.

The other dichloromanganese(IV) Schiff base complexes were obtained in a similar manner. The elemental analyses of the manganese(IV) complexes obtained are given in Table 2, together with their magnetic moments measured at room temperature. These deep green complexes are soluble in dichloromethane, acetone, and acetonitrile. The solutions were stable in these solvents if kept without contact with moisture. They were soluble in donating solvents, such as pyridine, N,N-dimethylformamide, and methanol, but these solutions gradually turned brown.

Reagents. All the reagents were of a reagent grade. The solvents were purified by refluxing over sodium (ether), calcium chloride (dichloromethane, acetone), or magnesium (methanol), and then distilled. The acetonitrile was distilled twice from diphosphorus pentaoxide prior to use.

Measurements. The UV, VIS, and NIR spectra were obtained from Hitachi EPS-3 and 340 spectrophotometers. The IR spectra were recorded on a Hitachi EPI-215 grating spectrophotometer in the 700 to 4000 cm^{-1} regions and on a Hitachi EPI-L grating spectrophotometer in the 200 to 700 cm^{-1} regions. All the spectra were

measured in Nujol mulls or in a KBr disc. The magnetic susceptibilities were measured by the Gouy method at room temperature and by the Faraday method, using a Shimazu MB 11 apparatus for the temperature range from 77 to 300 K. The conductivities were determined on a Yanagimoto MY-7 conductivity outfit. The cyclic voltammetry was performed with a Yanagimoto P-8 polarograph connected with a Yanagimoto P-8-PT potentiostat. The working electrode was a platinum-inlay electrode, while the auxiliary electrode was a platinum wire. The reference electrode was a saturated calomel electrode which was inserted in an aqueous solution of 1 M (1 M = 1 mol dm^{-3}) KCl in a 100-cm^3 beaker connected with a conventional brown H-type cell by means of a

TABLE 1. ELEMENTAL ANALYSES AND MAGNETIC MOMENTS OF MANGANESE(III) COMPLEXES

Complex	Found (%)				Calcd (%)				μ_{eff}[a]
	C	H	N	Mn	C	H	N	Mn	BM
Mn(salen)Cl·H_2O	50.61	3.96	7.35	14.28	51.29	4.30	7.48	14.66	4.90
Mn(5-Brsalen)Cl	36.30	2.61	5.20	10.60	37.21	2.73	5.42	10.64	4.88
Mn(5-NO_2salen)Cl	41.00	2.96	11.74	11.60	41.18	3.46	12.00	12.24	5.01
Mn(5-Mesalen)Cl	56.68	4.76	7.28	14.26	56.19	4.72	7.28	14.28	5.02
Mn(salchxn)Cl	57.98	4.82	6.90	13.60	58.48	4.91	6.82	13.37	4.96
Mn(5-Brsalpln)Cl	38.64	2.76	5.59	10.37	38.63	2.67	5.30	10.39	4.88
Mn(5-Brsalpn)Cl·H_2O	37.01	2.91	5.08	9.51	37.36	2.95	5.12	10.05	5.04
Mn(*N*-Busai)$_2$Cl	58.80	6.32	6.21	12.53	59.67	6.37	6.33	12.40	5.03
Mn(*N*-Bu-5-NO_2sai)$_2$Cl	49.53	5.11	10.23	10.37	49.59	4.92	10.51	10.31	4.37
Mn(*N*-Bu-5,6-Benzosai)$_2$Cl	66.33	6.13	4.85	10.10	66.36	5.94	5.16	10.12	4.92
Mn(*N*-Bu-5-Brsai)$_2$Cl	43.77	4.52	4.80	9.17	43.97	4.36	4.66	9.15	5.01

a) Measured at room temperature.

TABLE 2. ELEMENTAL ANALYSES AND MAGNETIC MOMENTS OF MANGANESE(IV) COMPLEXES

Complex	Found (%)					Calcd (%)					μ_{eff}[a]
	C	H	N	X	Mn	C	H	N	X	Mn	BM
Mn(salen)Cl_2·$(CH_2Cl_2)_{0.5}$	45.17	3.55	6.49	24.86	12.80	45.60	3.48	6.45	24.47	12.68	3.91
Mn(5-Brsalen)Cl_2	34.82	2.28	5.00	41.99	9.77	34.82	2.56	5.08	41.80	9.95	3.94
Mn(5-NO_2salen)Cl_2	39.97	2.52	11.54	14.26	11.05	39.69	2.91	11.57	14.65	11.35	3.98
Mn(5-Mesalen)Cl_2·$(CH_2Cl_2)_{0.25}$	49.70	4.25	6.28	20.58	12.67	49.66	4.22	6.35	20.08	12.45	3.97
Mn(salchxn)Cl_2·$(CH_2Cl_2)_{0.6}$	49.96	4.21	5.66	22.84	10.90	49.76	4.30	5.69	22.82	11.05	4.04
Mn(5-Brsalpln)Cl_2·$(CH_2Cl_2)_{0.5}$	34.34	2.54	4.66	42.97	9.09	34.66	2.49	4.62	43.88	9.06	4.00
Mn(5-Brsalpn)Cl_2	35.77	2.52	4.82	41.63	9.96	36.21	2.59	4.97	40.91	9.74	4.02
Mn(*N*-Busal)$_2Cl_2$	54.79	5.76	5.70	15.47	12.03	55.24	5.90	5.86	14.87	11.49	4.10
Mn(*N*-Bu-5-NO_2sai)$_2Cl_2$	46.32	4.56	9.85	12.33	9.72	46.49	4.61	9.86	12.48	9.67	3.90
Mn(*N*-Bu-5,6-Benzosai)$_2Cl_2$	62.03	5.60	4.67	12.87	9.39	62.29	5.58	4.87	12.26	9.50	4.07
Mn(*N*-Bu-5-Brsai)$_2Cl_2$	40.95	4.00	4.19	35.22	8.54	41.54	4.12	4.40	36.30	8.64	4.09

a) Measured at room temperature.

4% agar-saturated KCl gel bridge. Tetrabutylammonium perchlorate, Bu_4NClO_4, was used as the supporting electrolyte. The dissolved oxygen was removed by passing nitrogen gas through a sample solution for 20 min.

Results and Discussion

Figure 2 shows the spectral changes on the addition of HCl to an acetone solution of Mn(salen)-Cl·H_2O in different molar ratios. The spectra change remarkably on the addition of HCl, and a new absorption band appears around 630 nm. Its intensity increases as the molar ratio of HCl to the complex increases to 4. The further addition of HCl leads to the decolorization of the solution, with the formation of white precipitates, which may consist of hydrogen chloride salts of the ligand. This was confirmed by a comparison of the IR spectra of the white precipitates and of the authentic compound obtained by the reaction between salenH_2 and HCl in ether.

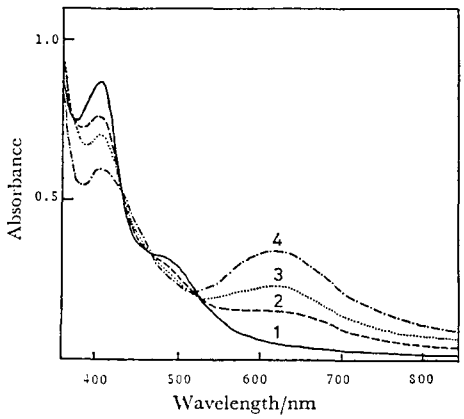

Fig. 2. Spectral changes on the addition of HCl to an acetone solution of 2×10^{-4} M Mn(salen)Cl·H_2O in different molar ratios.
(1): [HCl]/[complex]=0, (2): 1, (3): 2, (4): 4.

The deep green complexes isolated by the reactions between chloromanganese(III) Schiff base complexes and HCl are given in Table 2. Their analytical data are consistent with the empirical formula of $MnLCl_2$ or MnL'_2Cl_2, where L denotes a dianion of quadridentate Schiff base ligands, and L', a monoanion of bidentate Schiff base ligands. Some of them include dichloromethane as a crystalline solvent.

Magnetic Properties. The room-temperature magnetic moments for these complexes (given in Table 2) fall within the range of 3.9 to 4.1 BM, consistent with a calculated spin-only value expected for a complex with a d^3 high-spin configuration. Figure 3 shows the Curie-Weiss plot for $Mn(salen)Cl_2 \cdot (CH_2Cl_2)_{0.5}$ over the temperature range from 77 to 300 K. The magnetic susceptibilities obey the Curie-Weiss law, $\chi_A = C/(T + \theta)$. The same behavior was observed for the complexes of $Mn(5\text{-Mesalen})Cl_2 \cdot (CH_2Cl_2)_{0.25}$ and $Mn(N\text{-Bu-5-}NO_2\text{-sai})_2Cl_2$. Their Weiss constants are given in Table 3. These values were obtained from an extrapolation of the plot of the reciprocal of the molar susceptibilities, χ_A, against the absolute temperature. These small θ values indicate that there are very small magnetic interactions in these complexes. These results suggest that the oxidation state of the central manganese ion in the complexes is +IV.

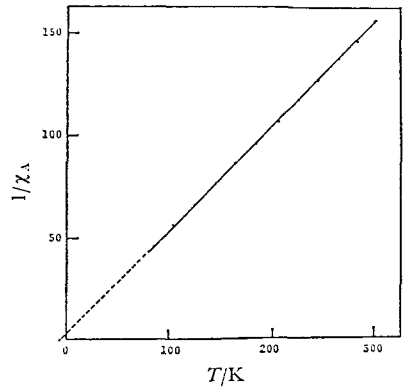

Fig. 3. Curie-Weiss plot for $Mn(salen)Cl_2 \cdot (CH_2Cl_2)_{0.5}$.

TABLE 3. WEISS CONSTANTS OF MANGANESE(IV) COMPLEXES

Complex	Weiss constant θ/K
$Mn(salen)Cl_2 \cdot (CH_2Cl_2)_{0.5}$	6
$Mn(5\text{-Mesalen})Cl_2 \cdot (CH_2Cl_2)_{0.25}$	3
$Mn(N\text{-Bu-5-}NO_2\text{sai})_2Cl_2$	9

Conductivities. The molar conductivities for several manganese(III) and manganese(IV) complexes are summarized in Table 4. These values indicate that they are essentially nonelectrolytes in acetonitrile. The slightly large value observed for the $Mn(N\text{-Busai})_2Cl_2$ complex may be caused by its lower solubility in acetonitrile. On the other hand, in methanol the molar

conductivity for $Mn(salen)Cl\cdot H_2O$ was found to be 71 S cm^2mol^{-1}, and that for $Mn(salen)Cl_2$-$(CH_2Cl_2)_{0.5}$, to be 191 S cm^2mol^{-1}. These values indicate that both complexes undergo considerable dissociation in methanol.

Table 4. Molar conductivities of manganese(III) and manganese(IV) complexes in acetonitrile

Complex	Λ[a] / S cm² mol⁻¹
$Mn^{III}(salen)Cl\cdot H_2O$	2.38
$Mn^{IV}(salen)Cl_2\cdot(CH_2Cl_2)_{0.5}$	3.48
Mn^{III}(*N*-Busai)$_2$Cl	8.35
Mn^{IV}(*N*-Busai)$_2Cl_2$	25.28[b]
Mn^{III}(*N*-Bu-5-NO_2sai)$_2$Cl	10.22
Mn^{IV}(*N*-Bu-5-NO_2sai)$_2Cl_2$	3.70

a) Measured at 25 °C. The concentration of the complexes was 10^{-3} M. b) The concentration of the complex was 5×10^{-4} M.

Electronic Spectra.

Figure 4 shows the electronic spectra of $Mn(salen)Cl\cdot H_2O$ and $Mn(salen)Cl_2\cdot(CH_2Cl_2)_{0.5}$ in dichloromethane. In the visible region, the spectrum of the manganese(III) complex shows three absorption bands, at 15600, 20800, and 23800 cm^{-1}. They have been previously assigned to the ligand-field transitions of $d_{xy}\rightarrow d_{x^2-y^2}$ and of $d_{yz},d_{xz}\rightarrow d_{x^2-y^2}$, and to the charge-transfer transition of $d\pi$(Mn) to π^* (azomethine), respectively.[12,13] On the other hand, the spectrum of the manganese(IV) complex shows two absorption bands, at 15400 and 23000 cm^{-1}. The lower-energy band is very intense compared with that of the manganese(III) complex. Therefore, it seems to be due to a charge-transfer transition.

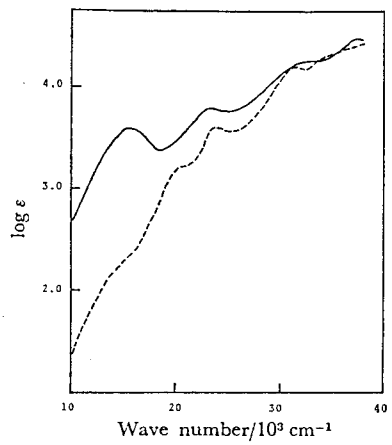

Fig. 4. Electronic spectra in dichloromethane. (——): $Mn^{IV}(salen)Cl_2\cdot(CH_2Cl_2)_{0.5}$, (– – –): Mn^{III}-$(salen)Cl\cdot H_2O$.

Moews has reported on the absorption spectrum of $K_2Mn^{IV}Cl_6$ in fluorocarbon grease mulls; it shows two absorption bands, at 15400 (very strong) and 27400 cm^{-1} (strong) in the visible region.[8d]

The lower-energy band has been assigned to a charge-transfer transition of chlorine to manganese. Later, Jeżowska-Trzbiatowska *et al.* claimed that the absorption spectrum of the same complex in 12 mol dm^{-3} HCl does not agree with that observed by Moews in the intensities on these bands.[14] However, as was pointed out by Moews, hexachloromanganate(IV) salts are rapidly converted to the corresponding aquapentachloromanganate(III) salts on standing in moist air. Therefore, it is uncertain as to whether or not $K_2Mn^{IV}Cl_6$ exists as the $Mn^{IV}Cl_6^{2-}$ ion in 12 mol dm^{-3} HCl.

The spectral data for the manganese(IV) complexes are summarized in Table 5. All the complexes show two intense bands around 16000 and 23000 cm^{-1} in the visible region. It can be seen that the absorption maxima of the lower-energy bands are affected by the Schiff base ligands. In the complexes of the salen type, the absorption maxima are shifted to higher energies in the order of the substituents of 5-Me < 5-Br < H < 5-NO_2. In the complexes of the N-butylsalicylideneamine type, similar shifts are observed in the order of the substituents of 5,6-Benzo < 5-Br < H < 5-NO_2. Furthermore, the absorption maxima of the former complexes are observed

Table 5. Spectroscopic data for manganese(IV) complexes

Complex	$\frac{\tilde{\nu}_{max}}{10^3\ cm^{-1}}$ ($\log \varepsilon$)[a]		$\frac{\nu(Mn\text{-}Cl)}{cm^{-1}}$
Mn(5-Mesalen)$Cl_2\cdot(CH_2Cl_2)_{0.25}$	14.9 (3.60)	22.8 (3.81)	323
Mn(5-Brsalen)Cl_2	15.3 (3.59)	23.1 (3.69)	337
Mn(salchxn)$Cl_2\cdot(CH_2Cl_2)_{0.6}$	15.6 (3.62)	23.7 (3.74)	350
Mn(salen)$Cl_2\cdot(CH_2Cl_2)_{0.5}$	15.4 (3.60)	23.0 (3.78)	341
Mn(5-NO_2salen)Cl_2	16.7 (3.40)	24.4 sh	356
Mn(5-Brsalpln)$Cl_2\cdot(CH_2Cl_2)_{0.5}$	15.3 (3.60)	24.1 (3.78)	339
Mn(5-Brsalpn)Cl_2	14.8 (3.63)	24.1 (3.83)	367
Mn(*N*-Busai)$_2Cl_2$	16.0 (3.52)	22.0 sh	346
Mn(*N*-Bu-5-NO_2sai)$_2Cl_2$	17.2 (3.80)	23.4 sh	359, 342
Mn(*N*-Bu-5-Brsai)$_2Cl_2$	15.5 (3.76)	22.7 sh	333
Mn(*N*-Bu-5,6-Benzosai)$_2Cl_2$	14.6 (3.71)	23.0 sh	334

a) Measured in dichloromethane.

at lower energies than those of the latter complexes. These results imply that the lower-energy bands may be assigned to a charge-transfer transition of Cl(pπ) to Mn(dπ). The absorption bands due to the ligand-field transitions expected for the manganese(IV) complexes may be obscured by these intense bands.

Infrared Spectra. In the region from 4000 to 500 cm^{-1} the infrared spectra of the manganese(IV) complexes are almost the same as those of the corresponding manganese(III) complexes, except around 1290 cm^{-1}, where the absorption band due to ν(C-O) should be observed. This indicates that there is no change in the coordination features of the Schiff base ligands in either manganese(III) or manganese(IV) complexes. In the ν(C-O) region, lower-energy shifts of about 10 cm^{-1} were observed on going from the manganese(III) complexes to the manganese(IV) complexes; they may be caused by the change of the oxidation state of the central manganese ion from +III to +IV. In the region from 200 to 500 cm^{-1}, the spectra of the manganese(IV) complexes show the strong absorption bands at about 340 cm^{-1}, unlike those of the corresponding manganese(III) complexes. Figure 5 a shows the spectra of $Mn^{IV}(salen)Cl_2\cdot(CH_2Cl_2)_{0.5}$ and $Mn^{III}(salen)Cl\cdot H_2O$.

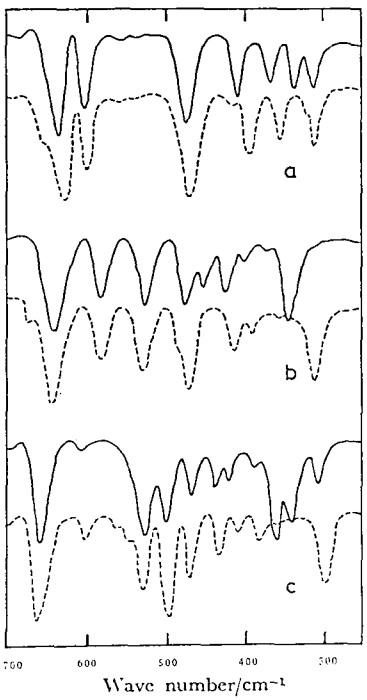

Fig. 5. Infrared spectra (in Nujol mulls). a) (——): $Mn^{IV}(salen)Cl_2\cdot(CH_2Cl_2)_{0.5}$; (– – –): $Mn^{III}(salen)Cl\cdot H_2O$, b) (——): $Mn^{IV}(N\text{-Busai})_2Cl_2$; (– – –): $Mn^{III}(N\text{-Busai})_2Cl$, c) (——): $Mn^{IV}(N\text{-Bu-5-NO}_2\text{-sai})_2Cl_2$; (– – –): $Mn^{III}(N\text{-Bu-5-NO}_2\text{sai})_2Cl$.

The band observed at 341 cm^{-1} for the manganese(IV) complex may be assigned to ν(Mn-Cl). Figure 5 b shows the spectra of Mn^{IV}(N-Busai)$_2Cl_2$ and Mn^{III}(N-Busai)$_2Cl$. The band observed at 348 cm^{-1} for the manganese(IV) complex may be assigned to ν(Mn-Cl). On the other hand, as is shown in Fig. 5 c, the spectrum of Mn^{IV}(N-Bu-5-NO_2sai)$_2Cl_2$ exhibits two strong bands, at 364 and 333 cm^{-1}, which may be assigned to ν(Mn-Cl). The frequencies of the characteristic bands assigned to ν(Mn-Cl) for the managnese(IV) complexes are summarized in Table 5. In the complexes of the salen type, one band assignable to ν(Mn-Cl) was observed, whereas in the Mn^{IV}(N-Bu-5-NO_2sai)$_2Cl_2$ complex, two bands were observed. For the octahedral complexes of the MA_4Cl_2 type (A denotes unidentate ligands such as ammonia), one band due to ν(M-Cl) should be observed in the case of a *trans*-configuration, whereas two strong bands should be observed in the case of a *cis*-configuration.[15] These results suggest that the manganese(IV) complexes of the salen type may have an octahedral *trans*-configuration, while in the manganese(IV) complexes of the bidentate Schiff bases, octahedral *trans*- and *cis*-configurations may be probable.

Electrochemical Properties. Figure 6 shows some typical current-potential curves of Mn^{III}(salen)$Cl\cdot H_2O$ and Mn^{IV}(salen)Cl_2-$(CH_2Cl_2)_{0.5}$ measured in acetonitrile. In the manganese(III) complex, one cathodic wave is observed at -0.38 V(*vs.*SCE); it can be assigned to the reduction of Mn(III) to Mn(II). On the other hand, in the manganese(IV) complex, two cathodic waves are observed, at +0.76 and -0.37 V(*vs.*SCE), with similar wave heights; they can be assigned to the reductions of Mn(IV) to Mn(III) and of Mn(III) to Mn(II) respectively. The separation of the peak potentials between the cathodic wave and the corresponding anodic wave for both redox

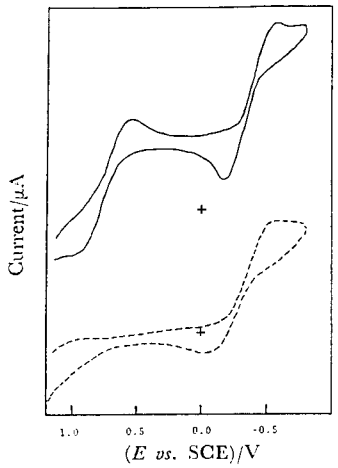

Fig. 6. Current potential curves in acetonitrile. (——): $Mn^{IV}(salen)Cl_2 \cdot (CH_2Cl_2)_{0.5}$; (– – –): $Mn^{III}(salen)Cl \cdot H_2O$.

Table 6. Reduction potentials for manganese(IV) complexes

Complex	$E_{p/2}$ vs. SCE[a] / V	
	$Mn^{IV} \rightarrow Mn^{III}$	$Mn^{III} \rightarrow Mn^{II}$
$Mn(salen)Cl_2 \cdot (CH_2Cl_2)_{0.5}$	0.76	−0.37 (−0.38)[b]
$Mn(5\text{-}Brsalen)Cl_2$	0.85	−0.16 (+0.01)
$Mn(5\text{-}NO_2salen)Cl_2$	0.90	−0.01 (+0.11)
$Mn(5\text{-}Mesalen)Cl_2 \cdot (CH_2Cl_2)_{0.25}$	0.85	−0.34 (−0.32)
$Mn(salchxn)Cl_2 \cdot (CH_2Cl_2)_{0.6}$	0.83	−0.29 (−0.32)
$Mn(5\text{-}Brsalpln)Cl_2 \cdot (CH_2Cl_2)_{0.5}$	1.00	−0.09 (−0.14)
$Mn(5\text{-}Brsalpn)Cl_2$	0.88	−0.05 (−0.02)
$Mn(N\text{-}Busai)_2Cl_2$	0.84	−0.11 (−0.08)
$Mn(N\text{-}Bu\text{-}5\text{-}Brsai)_2Cl_2$	0.94	+0.01 (−0.12)
$Mn(N\text{-}Bu\text{-}5\text{-}NO_2sai)_2Cl_2$	0.98	+0.08 (+0.24)

a) Measured in acetonitrile at 25 °C. b) Half-peak potentials observed for the corresponding manganese(III) complexes.

waves are larger than the 57 mV expected for a reversible one-electron redox wave, so these electrode reactions may be irreversible.

All the manganese(IV) complexes show two cathodic waves around +0.85 V and -0.20 V. The half-peak potentials for the reductions of the manganese(IV) complexes are summarized in Table 6, together with those of the corresponding manganese(III) complexes. As has been discussed in connection with the electronic spectra, the potentials for both reductions are also affected by the Schiff base ligands. The reduction potentials are shifted to more positive values upon the introduction of an electron-withdrawing substituent such as the $5\text{-}NO_2$ group in both types of the complexes. Furthermore, the reduction potentials for the complexes of the N-butylsalicylideneamine type are observed at more positive values than those for the complexes of the salen type. These shifts can be explained in terms of the electron density on the central manganese ion in the complexes.

Reactions. These manganese(IV) complexes have reduction potentials high enough to oxidize water. Thus, their reactions

with water have been attempted. Figure 7 shows the spectral changes on the addition of water to an acetonitrile solution of $Mn(salen)Cl_2 \cdot (CH_2Cl_2)_{0.5}$ in different molar ratios. The intensity of the characteristic absorption band at 624 nm decreased with an increase in the molar ratio of water to the complex. The final absorption spectrum is almost identical with that of the corresponding manganese(III) complex in the acetonitrile and water mixture, indicating that water reduced the manganese(IV) complex to the manganese(III) complex. The author has also succeeded in detecting free *"molecular oxygen"* liberated during the reactions of the manganese(IV) complexes with water by means of the spectrophotometry of an alkaline pyrogallol solution and a dissolved oxygen probe, as will be described in Chapter VI.

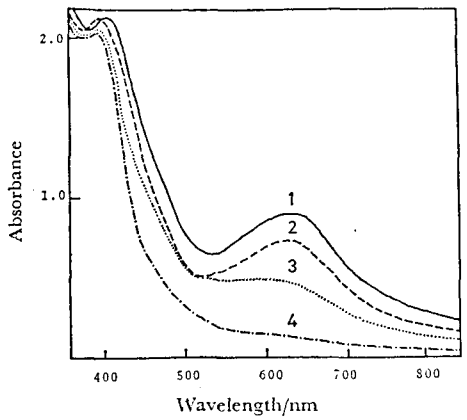

Fig. 7. Spectral changes on the addition of H_2O to an acetonitrile solution of 4×10^{-4} M $Mn(salen)Cl_2 \cdot (CH_2Cl_2)_{0.5}$ in different molar ratios. (1): $[H_2O]/[complex]=0$, (2): 10, (3): 20, (4): 40.

Some novel dichloromanganese(IV) Schiff base complexes have been prepared and characterized. The higher oxidation state of the manganese ion may be stabilized by charge neutralization with chloride ions. The mechanism for the reaction of the manganese(III) complexes with HCl has not been clarified in this study. However, some experimental evidence suggests that the manganese(IV) complexes may result from a disproportionation of the manganese(III) complexes: manganese(II) compounds are often formed as contaminants in the preparation of the manganese(IV) complexes, and their yields are always 50% or below.

Summary

Some chloromanganese(III) Schiff base complexes react with hydrogen chloride to give deep green complexes with the empirical formula of $MnLCl_2$ or MnL'_2Cl_2, where H_2L denotes quadridentate ligands such as N,N'-disalicylideneethylenediamine and its analogs, and where HL' denotes bidentate ligands such as N-butylsalicylideneamine and its analogs. These complexes are nonelectrolytes in acetonitrile. Their magnetic moments at room temperature fall within the range of 3.9 to 4.1 BM, and the magnetic susceptibilities obey the Curie-Weiss law with small θ values over the temperature range of 77 to 300 K, indicating that the oxidation state of the manganese ion in these complexes is +IV. The electronic spectra show an intense band around 16000 cm^{-1} which can be assigned to a charge-transfer transition. In the cyclic voltammograms, two cathodic waves are observed at half-peak potentials around +0.9 and -0.2 V(*vs.*SCE); they can be assigned to the reductions of Mn(IV) to Mn(III) and of Mn(III) to Mn(II) respectively. The probable configurations of the complexes are discussed on the basis of the infrared spectra.

References

1) G. D. Lawrence and D. T. Sawyer, *Coord. Chem. Rev.*, 27, 173 (1978)

2) I. Tabushi and S. Kojo, *Tetrahedron Lett.*, 1974, 1577; 1975, 305.

3) J. K. Howie and D. T. Sawyer, *J. Am. Chem. Soc.*, 98, 6698 (1976).

4) M. M. Morrison and D. T. Sawyer, *Inorg. Chem.*, 17, 333 (1978); 17, 338 (1978).

5) S. R. Cooper, C. C. Dismukes, M. P. Klein, and M. Calvin, *J. Am. Chem. Soc.*, 99, 6623 (1977); 100, 7248 (1978).

6) Y. Otsuji, K. Sawada, I. Morishita, Y. Taniguchi, and K. Mizuno, *Chem. Lett.*, 1977, 983.

7) W. Levason and C. A. McAuliffe, *Coord. Chem. Rev.*, 7, 353 (1972).

8) a) $[MnCl_2(diphos)_2](ClO_4)_2$: diphos=*o*-phenylenebisdimethylphosphine; L. F. Warren and M. A. Bennett, *Inorg. Chem.*, 15, 3126 (1976). b) $MnCl_4(bpy)$: bpy=bipyridine; H. A. Goodwin and R. N. Sylva, *Aust. J. Chem.*, 18, 1743 (1965); 20, 629 (1967). c) $[Mn(R_2dtc)_3]X$; R_2dtc=alkyldithiocarbamato monoanion and X=BF_4 or ClO_4; A. R. Hendrickson, R. L. Martin, and N. M. Rohde, *Inorg. Chem.*, 13, 1933 (1974). d) K_2MnCl_6; P. C. Moews Jr., *Inorg. Chem.*, 5, 5 (1966). e) O=Mn(3-MeOsalen)·2MeOH; in section I-1.

9) C. P. Prabhakaran and C. C. Patel, *J. Inorg. Nucl. Chem.*, 31, 3316 (1969).

10) B. C. Sharma and C. C. Patel, *Indian J. Chem.*, 8, 94 (1970).

11) A. V. Bergen, K. S. Murray, M. J. O'Connor, and B. O. West., *Aust. J. Chem.*, 22, 39 (1969).

12) L. J. Boucher, *J. Inorg. Nucl. Chem.*, 36, 531 (1974).

13) L. J. Boucher and D. R. Herrington, *Inorg. Chem.*, 13, 1105 (1974).

14) B. Jeżowska-Trzebiatowski, S. Wajda, M. Batuka, L. Natkaniec, and W. Wojciechowski, *Inorg. Chim. Acta*, 1, 205 (1967).

15) K. Nakamoto, "Infrared Spectra of Inorganic and Coordination Compounds," Wiley-Interscience, New York (1970), p. 215.

V - 2 Preparation and Characterization of Dichlorobis(N-alkylsalicylideneaminato)manganese(IV) Complexes

Introduction

In the preceding section V-1, the dichloromanganese(IV) complexes with the Schiff bases derived from substituted salicylaldehydes and diamines or butylamine have been described. These complexes are unstable toward moisture even in the solid state and decompose to the reduced manganese complexes. This may be caused because the coordinated chlorine atoms are displaced by water molecules. Thus, the author has aimed to obtain manganese(IV) complexes which are stable toward water.

In this section, the preparation and characterization of a series of dichloromanganese(IV) complexes with the bidentate Schiff bases derived from salicylaldehyde and primary monoamines (Fig. 1) will be described. Their reactivity toward water is found to decrease as the chain length of the alkyl groups increases.

Experimental

Preparation of Manganese(III) Complexes, Mn(N-Rsai)$_2$Cl. All the manganese(III) Schiff base complexes were obtained by a modification of the method described in section V-1.

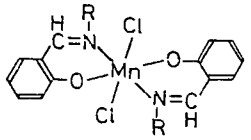

R	L	R	L
n-C_5H_7	*N*-Prsai	n-C_8H_{17}	*N*-Octsai
n-C_4H_9	*N*-Busai	n-$C_{12}H_{25}$	*N*-Dodsai
i-C_4H_9	*N*-*i*-Busai	n-$C_{18}H_{37}$	*N*-Octdsai
n-C_6H_{13}	*N*-Hxsai	$CH_2C_6H_5$	*N*-Bzsai
c-C_6H_{11}	*N*-*c*-Hxsai	$CH_2CH_2C_6H_5$	*N*-PEsai

Fig. 1. Manganese(IV) Schiff base complexes, Mn(*N*-Rsai)$_2$Cl$_2$.

Chlorobis(N-hexylsalicylideneaminato)manganese(III), Mn(N-Hxsai)$_2$Cl A tetrahydrofuran (THF) solution (50 cm^3) containing salicylaldehyde (2.44 g) and hexylamine (2.02 g) was refluxed for 1 h and then evaporated under reduced pressure. The resulting yellow oily

residue was dissolved in a mixture of dichloromethane (30 cm^3) and methanol (30 cm^3). Manganese(III) acetate dihydrate (2.68 g) and lithium chloride (0.63 g) were added to the solution. The mixture was refluxed for 1 h and then evaporated under reduced pressure to yield an olive-green solid. It was collected on a glass filter, washed with 2-propanol and ether, and dried *in vacuo*. It was recrystallized from dichloromethane. The yield was 3.2 g.

The other manganese(III) complexes were prepared in a similar manner. These complexes are soluble in dichloromethane, acetone, and acetonitrile. The analytical data are given in Table 1, together with the magnetic moments determined at room temperature.

Preparation of Manganese(IV) Complexes, Mn(N-Rsai)$_2$Cl$_2$. Dichlorobis(N-hexylsalicylideneaminato)manganese(IV), Mn(N-Hxsai)$_2$Cl$_2$: To a mixed solution of dichloromethane (20 cm^3) and 2-propanol (50 cm^3) of Mn^{III}(N-Hxsai)$_2$Cl (1.0 g) was added drop by drop a 2-propanol solution of HCl (1.5 molar-folds over the complex) with stirring at room temperature. The solution changed from greenish-brown to deep green with precipitation of deep green crystals. The mixture was cooled to 0 °C and allowed to stand for 3 h. The crystals precipitated were collected on a glass filter, washed with 2-propanol and ether, and then dried *in vacuo*. The yield was *ca.* 0.4 g. Further purification was not carried out.

The other manganese(IV) complexes (Fig. 1) were obtained in a similar manner. The analytical data are given in Table 2, together with the magnetic moments determined at room temperature. All the complexes are soluble in dichloromethane and the solutions show no noticeable change for an hour if kept isolated from contact with moisture. The complexes with R = Pr, Bu, *i*-Bu, Hx, *c*-Hx, Oct, Dod, Bz, and PE are soluble in acetone and acetonitrile; the complex

with R = Octd is slightly soluble in the above solvents. All the complexes are soluble in coordinating solvents such as dimethyl sulfoxide and pyridine, but the solutions change rapidly from deep green to yellow-brown. The complexes with R = Dod and Octd have been found to be unreactive toward water in the solid state.

Reagents. All reagents were of reagent grade. Solvents were purified by the method described in section V-1.

Measurements. All physical measurements were made by the methods described in section V-1.

TABLE 1. ELEMENTAL ANALYSES AND MAGNETIC MOMENTS OF MANGANESES(III) COMPLEXES

Complex	Found (%)				Calcd (%)				μ_{eff}[a]
	C	H	N	Mn	C	H	N	Mn	BM
Mn(*N*-Prsai)$_2$Cl	57.63	5.84	6.41	13.12	57.91	5.85	6.75	13.24	4.86
Mn(*N*-Busai)$_2$Cl	58.80	6.32	6.21	12.53	59.67	6.37	6.33	12.40	5.03
Mn(*N*-*i*-Busai)$_2$Cl	59.39	6.28	6.28	12.63	59.67	6.37	6.33	12.40	4.87
Mn(*N*-Hxsai)$_2$Cl	63.21	7.28	5.47	10.82	62.59	7.27	5.61	11.01	5.00
Mn(*N*-*c*-Hxsai)$_2$Cl·(H$_2$O)$_{0.5}$	61.50	6.59	5.61	11.28	61.96	6.60	5.55	10.90	4.89
Mn(*N*-Octsai)$_2$Cl	64.59	8.15	4.98	9·89	64.91	7.99	5.05	9.90	4.93
Mn(*N*-Dodsai)$_2$Cl	67.84	9.52	4.14	7.96	68.40	9.06	4.20	8.23	4.98
Mn(*N*-Octdsai)$_2$Cl	71.04	10.50	3.27	6.38	71.82	10.13	3.35	6.57	4.92
Mn(*N*-Bzsai)$_2$Cl	65.33	5.16	5.38	10.73	65.83	4.73	5.48	10.75	4.26
Mn(*N*-PEsai)$_2$Cl	66.88	5.21	5.20	10.20	66.86	5.24	5.20	10.19	4.85

a) Measured at room temperature.

TABLE 2. ELEMENTAL ANALYSES AND MAGNETIC MOMENTS OF MANGANESE(IV) COMPLEXES

Complex	Found (%)					Calcd (%)					μ_{eff}[a]
	C	H	N	Cl	Mn	C	H	N	Cl	Mn	BM
Mn(*N*-Prsai)$_2$Cl$_2$	53.15	5.34	6.17	15.76	12.50	53.35	5.37	6.22	15.75	12.20	3.96
Mn(*N*-Busai)$_2$Cl$_2$	55.12	5.95	5.80	15.35	11.32	55.24	5.90	5.86	14.82	11.49	4.06
Mn(*N*-*i*-Busai)$_2$Cl$_2$	55.18	5.89	5.83	14.50	11.70	55.24	5.90	5.86	14.82	11.49	3.84
Mn(*N*-Hxsai)$_2$Cl$_2$	58.33	6.93	5.21	13.50	10.15	58.43	6.79	5.24	13.27	10.28	4.09
Mn(*N*-*c*-Hxsai)$_2$Cl$_2$	59.28	6.36	5.14	12.48	10.05	58.88	6.08	5.28	13.37	10.36	4.07
Mn(*N*-Octsai)$_2$Cl$_2$	60.90	7.53	4.64	11.20	9.31	61.02	7.51	4.74	12.01	9.30	3.92
Mn(*N*-Dodsai)$_2$Cl$_2$	64.90	8.70	3.95	9.90	8.02	64.95	8.61	3.99	10.09	7.82	3.93
Mn(*N*-Octdsai)$_2$Cl$_2$	68.75	9.55	3.19	8.90	6.07	68.94	9.72	3.22	8.14	6.31	4.03
Mn(*N*-Bzsai)$_2$Cl$_2$·CH$_2$Cl$_2$	55.35	4.25	4.39	21.01	8.53	55.18	4.87	4.82	22.46	8.70	3.99
Mn(*N*-PEsai)$_2$Cl$_2$	62.85	4.87	4.82	12.13	9.19	62.73	4.91	4.88	12.34	9.56	3.95

a) Measured at room temperature.

Results and Discussion

The analytical data for the manganese(III) and manganese(IV) complexes are in agreement with the empirical formulas of MnL_2Cl and MnL_2Cl_2, respectively; here L denotes monoanion of N-alkylsalicylideneamines (Tables 1 and 2).

In general, most of the manganese(IV) compounds are not stable and are thus readily hydrolysed and reduced. The dichloromanganese-(IV) complexes such as $Mn^{IV}(salen)Cl_2$ are unstable in a moist air even in the solid state. Therefore, many difficulties arose in the syntheses of these complexes. In order to obtain water-resistant manganese(IV) complexes, a series of dichloromanganese(IV) Schiff base complexes (Fig. 1) has been prepared. This idea is based on the hope that the long-chain alkyl groups such as n-$C_{12}H_{25}$ and n-$C_{18}H_{37}$ may protect against the attack of water molecules on the central manganese atom of the complex.

Figure 2 shows the absorption spectral changes on the addition of water to an acetone solution of $Mn(N\text{-}c\text{-}Hxsai)_2Cl_2$. The intensity of the characteristic absorption band at 600 nm for the manganese(IV)

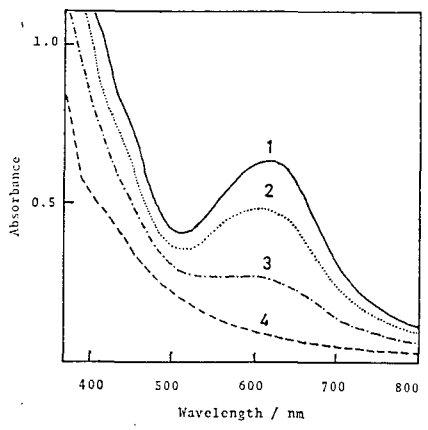

Fig. 2. Spectral changes on the addition of water (0.05 cm³) to an acetone solution of 1.6×10^{-4} M $Mn^{IV}(N\text{-}c\text{-}Hxsai)_2Cl_2$ (5 cm³).
1: No addition, 2: 7.5 min after addition of water, 3: 17.5 min, 4: 42.5 min. Cell length: 1 cm.

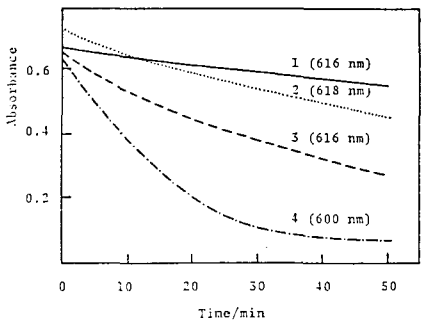

Fig. 3. Time courses of absorbances at absorption maxima of acetone solutions of Mn(IV) complexes (1.6×10^{-4} M, 5 cm³) caused by the addition of water (0.05 cm³).
1: $Mn(N\text{-}Dodsai)_2Cl_2$, 2: $Mn(N\text{-}Octsai)_2Cl_2$, 3: $Mn(N\text{-}Prsai)_2Cl_2$, 4: $Mn(N\text{-}c\text{-}Hxsai)_2Cl_2$. Cell length: 1 cm.

complex decreased with time. The final absorption spectrum is almost the same as that of $Mn^{III}(N\text{-}c\text{-}Hxsai)_2Cl$ in a mixture of acetone and water, indicating that water resulted in the reduction of the manganese(IV) complex. Figure 3 shows the time courses of the absorbances in the characteristic absorption bands for the complexes: $Mn(N\text{-}Prsai)_2Cl_2$, $Mn(N\text{-}c\text{-}Hxsai)_2Cl_2$, $Mn(N\text{-}Octsai)_2Cl_2$, and $Mn(N\text{-}Dodsai)_2Cl_2$, when water was added to these acetone solutions. It is apparent that their reactivity with water depends on the alkyl groups and decreases in the order of R = Dod < Oct < Pr < *c*-Hx. The most rapid change in absorbance observed for $Mn(N\text{-}c\text{-}Hxsai)_2Cl_2$ may be caused by the instability of the complex due to steric hindrance of the cyclohexyl group. In the case of $Mn(N\text{-}Octdsai)_2Cl_2$, such spectral changes could not be measured owing to its solubility restriction in acetone. However, this complex may be more water-resistant than the others investigated here, because that it showed no significant change on washing with water.

Magnetic Properties. The magnetic moments of the manganese-(III) complexes fall within the range of 4.85 to 5.03 BM, with the exception of $Mn(N\text{-}Bzsai)_2Cl$ (Table 1). This indicates that these complexes may have a d^4 high-spin electron configuration. The low value (4.26 BM) observed for the above complex may be caused by magnetic exchange interactions due to the formation of a binuclear complex in the solid state like Fe(salen)Cl.[1] Further investigation on the complex was not made in this study. On the other hand, the magnetic moments of the manganese(IV) complexes fall within the range of 3.84 to 4.08 BM; such moments are consistent with the spin-only value expected for a complex with a d^3 high-spin electron configuration.

Electronic Spectra. Figure 4 shows the electronic spectra

of the complexes $Mn^{III}(N\text{-Octsai})_2Cl$ and $Mn^{IV}(N\text{-Octsai})_2Cl_2$ in dichloromethane. In the manganese(III) complex, three absorption bands are observed in the visible region: at 15200, 21300 sh, and 26300 cm^{-1}. On the other hand, the electronic spectrum of the manganese(IV) complex shows an intense absorption band at 16000 cm^{-1} (log ε = 3.62). The frequencies of the absorption maxima for the manganese(III) and -(IV) complexes are summarized in Table 3. It is apparent from the Table that the alkyl groups of the Schiff base ligands have little effect on the frequencies for either manganese(III) or manganese(IV) complexes. These results suggest that the manganese(III) and manganese(IV) complex pairs may have similar configurations.

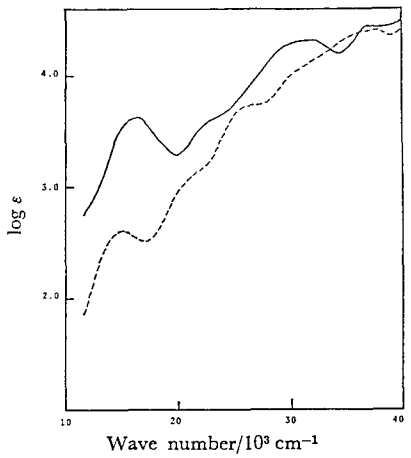

Fig. 4. Electronic spectra in dichloromethane.
——: $Mn^{IV}(N\text{-Octsai})_2Cl_2$, ----: $Mn^{III}(N\text{-Octsai})_2Cl$.

Recently, Boucher *et al.* have reported the absorption spectra of $Mn^{III}(X\text{-salen})Cl$[2] and $Mn^{III}(acacen)Cl$[3] in noncoordinating solvents; here X-salen and acacen denote dianions of

Table 3. Spectroscopic data for mangnese(III) and manganese(IV) complexes

R	$Mn^{III}(N\text{-Rsai})_2Cl$					$Mn^{IV}(N\text{-Rsai})_2Cl_2$				
	ν_{max} / 10^3 cm^{-1} (log ε)[a]				ν(Mn-Cl) / cm^{-1}	ν_{max} / 10^3 cm^{-1} (log ε)[a]				ν(Mn-Cl) / cm^{-1}
Pr	15.1	(2.59)	21.3 sh	26.3	(3.74)	299	16.1	(3.63)	23.7 sh	31.2	(4.33)	351
Bu	15.2	(2.62)	21.3 sh	26.5	(3.74)	315	16.1	(3.66)	23.6 sh	31.3	(4.36)	347
i-Bu	15.2	(2.64)	21.3 sh	26.5	(3.75)	327	15.9	(3.63)	23.5 sh	31.4	(4.33)	354
Hx	15.2	(2.48)	21.3 sh	26.7	(3.67)	314	16.1	(3.62)	23.5 sh	31.6	(4.40)	348
c-Hx	15.2	(2.54)	21.3 sh	25.9	(3.71)	317	16.6	(3.55)	23.5 sh	31.8	(4.31)	351
Oct	15.2	(2.60)	21.3 sh	26.3	(3.73)	317	16.0	(3.62)	23.6 sh	31.3	(4.32)	348
Dod	15.1	(2.62)	21.3 sh	26.5	(3.75)	321	16.1	(3.59)	23.6 sh	31.6	(4.44)	348
Octd	15.2	(2.61)	21.3 sh	26.5	(3.74)	322	16.2	(3.53)	23.6 sh	31.6	(4.35)	348
Bz	15.1	(2.64)	21.3 sh	26.3	(3.73)	318	16.2	(3.55)	22.7 sh	31.6	(4.30)	350
PE	15.1	(2.60)	21.3 sh	26.3	(3.75)	305	16.1	(3.53)	22.4 sh	31.4	(4.26)	347

a) Measured in dichloromethane.

N,N'-di(substituted salicylidene)ethylenediamine and N,N'-bis(2-acetyl-1-methylethylidene)ethylenediamine, respectively. The X-ray structural analysis of the latter complex has revealed that its coordination polyhedron approximates an idealized C_{4v} symmetry.[3] They have assigned the three absorption bands observed for Mn(acacen)Cl in chloroform as follows; the band at 16400 cm^{-1} (log ε = 2.31) to $d_{xy} \rightarrow d_{x^2-y^2}$, the band at 22400 cm^{-1} (3.23) to $d_{xy} \rightarrow \pi^*$(azomethine) involving $d_{yz}, d_{zx} \rightarrow d_{x^2-y^2}$ as a lower energy shoulder, and the band at 26200 cm^{-1} (3.81) to $d_{yz}, d_{zx} \rightarrow \pi^*$ (azomethine). The absorption spectra of the present manganese(III) complexes are similar to that of the above complex, suggesting that these manganese(III) complexes may have a five-coordinate structure ($\approx C_{4v}$) in dichloromethane. Therefore, the absorption bands near 15200 cm^{-1} can be safely assigned to the ligand field transition due to $d_{xy} \rightarrow d_{x^2-y^2}$.

On the other hand, the intense absorption bands near 16000 cm^{-1} observed for the manganese(IV) complexes can be assigned to the charge-transfer transition due to Cl to Mn on the basis of the intensities, as described in section V-1. The ligand field transitions which are expected for a complex with a d^3 high-spin configuration may be obscured by the intense charge-transfer band. Therefore, the absorption bands near 23600 cm^{-1} cannot be easily assigned.

Infrared Spectra. The IR spectra of the manganese(IV) complexes are almost the same as those of the corresponding manganese(III) complexes in the 4000 to 500 cm^{-1} region, indicating that the Schiff base ligands coordinate with manganese ions by the same fashion in both complexes. However, in the 500 to 250 cm^{-1} region, the IR spectra of the manganese(III) and manganese(IV)

complexes differ markedly, especially in the region sensitive to the ν(Mn-Cl). The absorption bands observed at 310 cm^{-1} for $Mn(N\text{-}Prsai)_2Cl$[4], at 290 cm^{-1} for $Mn(acac)_2Cl$,[5] and at 279 cm^{-1} for Mn(acacen)Cl[3] have been assigned to the ν(Mn-Cl); here acac denotes the monoanion of acetylacetone. In the present manganese(III) complexes, strong bands were observed around 310 cm^{-1}; these may be assigned to the ν(Mn-Cl). The band positions are listed in Table 3. On the other hand, the IR spectra of the manganese(IV) complexes showed strong bands around 350 cm^{-1}. The absorption band observed at 358 cm^{-1} for $K_2Mn^{IV}Cl_6$ has been assigned to the ν(Mn-Cl).[6] It is expected that the band due to the ν(Mn-Cl) may be shifted to higher frequencies on going from Mn(III) to Mn(IV), since the manganese(III) complexes have a five-coordinate structure, while the manganese(IV) complexes have a six-coordinate structure. The absorption bands observed around 350 cm^{-1} for the manganese(IV) complexes are assigned to the ν(Mn-Cl). The band positions are listed in Table 3. In the preceding section, it has been pointed out that the dichloromanganese(IV) complexes with the bidentate Schiff base ligands may have a *cis*- or *trans*-octahedral configuration; with the complexes in which two chlorine atoms coordinate with manganese ion in a *cis*-form two absorption bands due to the ν(Mn-Cl) would be observed, while there is only one band in a *trans*-form. In the present manganese(IV) complexes, one strong band assignable to the ν(Mn-Cl) was observed, suggesting that two chlorine atoms may coordinate with manganese ion in a *trans*-form.

The coordination features of the bidentate Schiff base ligands cannot be determined from the available data. However, the structures of the nickel(II) complexes with the N-alkylsalicylidene-

amines have been investigated and explained as follows. The complexes with *n*-alkyl groups have a *trans*-planar configuration. If the alkyl chain is branched at the β-carbon, as in the Ni(N-*i*-Busai)$_2$, the steric situation is very similar to the *n*-alkyl case and no tetrahedral form is observed.[7] In this study, attepmts to isolate Mn^{IV}(N-Rsai)$_2Cl_2$ (R = *i*-C_3H_7 and *s*-C_4H_9) were unsuccessful, perhaps because of the instability due to the steric hindrance of these groups. These results suggest that the present manganese(IV) complexes are in a *trans*, six-coordinate configuration, as shown in Fig. 1, but the Schiff base ligands may deviate from planarity to varying degrees.

Electrochemical Properties. The current-potential curve of the complex Mn^{IV}(N-*i*-Busai)$_2Cl_2$ is shown in Fig. 5. Two-step cathodic waves with a similar wave height were observed at the half-peak potentials of +0.81 and -0.18 V(*vs.*SCE); these can be assigned to the reductions of Mn(IV) to Mn(III) and Mn(III) to Mn(II), respectively. The reduction potentials for the manganese-(IV) complexes are given in Table 4, together with those for the

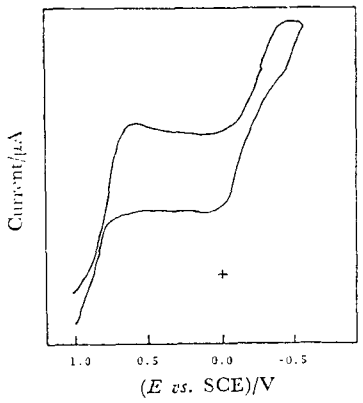

Fig. 5. Current-potential curve of Mn^{IV}(*N*-*i*-Busai)$_2Cl_2$ measured in acetonitrile at 25 °C. Scan rate was 0.06 V s^{-1}.

Table 4. Reduction potentials for manganese(IV) complexes

Complex	$E_{p/2}$ *vs.* SCE[a] / V	
	$Mn^{IV}\rightarrow Mn^{III}$	$Mn^{III}\rightarrow Mn^{II}$
Mn(*N*-Prsai)$_2Cl_2$	0.84	−0.12 (−0.18)[b]
Mn(*N*-Busai)$_2Cl_2$	0.84	−0.17 (−0.13)
Mn(*N*-*i*-Busai)$_2Cl_2$	0.81	−0.18 (−0.15)
Mn(*N*-Hxsai)$_2Cl_2$	0.82	−0.12 (−0.15)
Mn(*N*-*c*-Hxsai)$_2Cl_2$	0.75	−0.21 (−0.15)
Mn(*N*-Octsai)$_2Cl_2$	0.83	−0.12 (−0.16)
Mn(*N*-Dodsai)$_2Cl_2$[c]	0.79	−0.17 (−0.15)
Mn(*N*-Octdsai)$_2Cl_2$[c]	0.75	−0.11 (−0.16)
Mn(*N*-Bzsai)$_2Cl_2\cdot CH_2Cl_2$	0.87	−0.05 (−0.12)
Mn(*N*-PEsai)$_2Cl_2$	0.84	−0.11 (−0.13)

a) Measured in acetonitrile containing 0.1 M Bu_4NClO_4 at 25 °C. b) Half-peak potentials for the corresponding manganese(III) complexes. c) Measured in acetonitrile-dichloromethane (2/1 volume ratio).

manganese(III) complexes. The potentials for both reductions are not much affected by the alkyl groups of the Schiff base ligands. These results are consistent with the spectroscopic data.

Summary

The chlorobis(N-alkylsalicylideneaminato)manganese(III) complexes, $Mn^{III}(N\text{-}Rsai)_2Cl$, react with hydrogen chloride to give the corresponding dichloromanganese(IV) complexes, $Mn^{IV}(N\text{-}Rsai)_2Cl_2$, as deep green crystals; R can be *n*-C_3H_7, *n*-C_4H_9, *i*-C_4H_9, *n*-C_6H_{13}, *c*-C_6H_{11}, *n*-C_8H_{17}, *n*-$C_{12}H_{25}$, *n*-$C_{18}H_{37}$, $CH_2C_6H_5$, or $CH_2CH_2C_6H_5$. These complexes were characterized by the magnetic susceptibilities, electronic spectra, infrared spectra, and cyclic voltammograms. The complexes (R = *n*-$C_{12}H_{25}$ and *n*-$C_{18}H_{37}$) are found to be stable toward water in the solid state. A *trans*, six-coordinate configuration is proposed for the manganese(IV) complexes on the basis of the infrared spectra.

References

1) M. Gerloch and F. E. Mabbs, *J. Chem. Soc., A*, 1967, 1900.
2) a) L. J. Boucher and M. O. Farrell, *J. Inorg. Nucl. Chem.*, 35, 3731 (1973); b) L. J. Boucher, *ibid.*, 36, 531 (1974).
3) L. J. Boucher and V. W. Day, *Inorg. Chem.*, 16, 1360 (1977).
4) A. van den Bergen, K. S. Murray, M. J. O'Connor, and B. O. West, *Aust. J. Chem.*, 22, 39 (1969).
5) K. Isobe and S. Kawaguchi, *Bull. Chem. Soc. Jpn.*, 48, 250 (1975).
6) D. M. Adams and D. M. Morris, *J. Chem. Soc., A*, 1968, 694.
7) R. H. Holm, G. W. Everett. Jr., and A. Chakravorty, *Prog. Inorg. Chem.*, 7, 83 (1966).

V - 3 Preparation and Characterization of Dichlorobis(N-alkyl-substituted salicylideneaminato)manganese(IV) Complexes

Introduction

In the previous sections, V-1 and V-2, the preparation and characterization of a series of dichloromanganese(IV) Schiff base complexes have been described. These manganese(IV) complexes are not stable toward water even in the solid state and decompose gradually to their reduced manganese(III) complexes. In the complexes of the bidentate Schiff bases, $Mn(N\text{-}Rsai)_2Cl_2$, the complexes with R = n-$C_{12}H_{25}$ and n-$C_{18}H_{37}$ are found to be more stable toward water than those with n-C_3H_7 and n-C_4H_9.

In this section, the preparation and characterization of new dichloromanganese(IV) Schiff base complexes shown in Fig. 1 will be described.

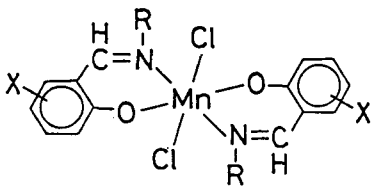

$Mn(N\text{-}R\text{-}X\ sai)_2Cl_2$

R	X
n-C_8H_{17} (Oct)	5-Br
n-$C_{12}H_{25}$ (Dod)	5,6-Benzo
n-$C_{18}H_{37}$ (Octd)	5-NO_2
$CH_2C_6H_5$ (Bz)	

Fig. 1. Mn(IV) complexes.

Experimental

Preparation of Manganese(III) Schiff Base Complexes, $Mn(N\text{-}R\text{-}X\text{-}sai)_2Cl$. Chlorobis(N-dodecyl-5-bromosalicylideneaminato)manganese-(III), $Mn(N\text{-}Dod\text{-}5\text{-}Brsai)_2Cl$: N-Dodecyl-5-bromosalicylideneamine (N-Dod-5-BrsaiH) was prepared by the condensation of 5-bromo-salicylaldehyde and equimolar dodecylamine in tetrahydrofuran (THF). This was recrystallized from ether. The other bidentate Schiff bases were prepared in a similar manner. Their melting points and analytical data are listed in Table 1.

To an ethanol solution (100 cm^3) of N-Dod-5-BrsaiH (7.37 g, 0.02 mol) were added manganese(III) acetate dihydrate (2.68 g, 0.01 mol) and lithium chloride (0.84 g, 0.02 mol). The mixture was warmed at 60 ^oC for 1 h with stirring and then evaporated to remove the solvent under reduced pressure. The resulting brown solid was collected on a glass filter, washed with a small amount of ethanol, and dried *in vacuo*. It was extracted with dichloromethane (150 cm^3), and the solution was evaporated to give a brown solid. It was recrystallized from acetonitrile.

The other manganese(III) complexes were prepared in a similar manner. The solvents employed for recrystallization were acetonitrile for Mn(N-Oct-5-Brsai)$_2$Cl, Mn(N-Oct-5,6-Benzosai)$_2$Cl, Mn(N-Dod-5,6-Benzosai)$_2$Cl, Mn(N-Oct-5-NO_2sai)$_2$Cl, and Mn(N-Dod-5-NO_2sai)$_2$Cl, acetone for Mn(N-Octd-5-Brsai)$_2$Cl and Mn(Octd-5,6-Benzosai)$_2$Cl, dichloromethane for Mn(N-Bz-5-Brsai)$_2$Cl and Mn(N-Octd-5-NO_2sai)$_2$Cl, methanol for Mn(N-Bz-5-Brsai)$_2$Cl, and N,N-dimethylformamide for Mn(N-Bz-5-NO_2sai)$_2$OH. These complexes are soluble in dichloromethane, methanol, and acetonitrile, slightly soluble in ether, and insoluble in water. The analytical data are given in Table 2.

Preparation of Manganese(IV) Schiff Base Complexes, Mn(N-R-X-sai)$_2$Cl$_2$. Dichlorobis(N-dodecyl-5-bromosalicylideneaminato) manganese(IV), Mn(N-Dod-5-Brsai)$_2$Cl$_2$: To a 2-propanol (70 cm^3) containing Mn(N-Dod-5-Brsai)$_2$Cl (1.0 g) was added a 2-propanol solution of hydrogen chloride (1.5 molar folds over the complex) at room temperature. The mixture was stirred for 1 h to give a deep green precipitate. It was collected on a glass filter, washed with 2-propanol, and dried *in vacuo*. It was recrystallized from benzene to give deep green crystals. The yield was *ca.* 0.2g.

This complex is soluble in dichloromethane, benzene, and acetone to give deep green color. These solutions show no measurable change in color allowing to stand for 1 h in an aerial atmosphere. This complex also is soluble in pyridine and methanol but these solutions change in color from green to brown gradually.

The other dichloromanganese(IV) Schiff base complexes were prepared in a similar manner. The analytical data for the manganese(IV) complexes are given in Table 3.

Measurements. The melting points were determined by means of a Yanagimoto MP-1 melting point apparatus and uncorrected. The other physical measurements were carried out by the method described in section V-1.

Materials. All reagents were of reagent grade. The solvents were purified by a usual manner.

Table 1. Melting points and analytical data of Schiff base ligands

Ligand	M.P. °C	Found (Calcd) (%) C	H	N
N-Dod-5-BrsaiH	24 - 25	61.51(61.95)	8.30(8.21)	3.83(3.80)
N-Octd-5-BrsaiH	50.5 - 51	65.98(66.36)	9.39(9.36)	3.07(3.10)
N-Dod-5,6-BenzosaiH	64.5	81.07(81.61)	9.80(9.53)	4.20(4.14)
N-Octd-5,6-BenzosaiH	82 - 82.5	82.25(82.41)	10.84(10.49)	3.37(3.31)
N-Dod-5-NO_2saiH	93 - 93.5	67.97(68.23)	9.05(9.04)	8.31(8.38)
N-Octd-5-NO_2saiH	99.5 - 100	71.69(71.73)	10.18(10.11)	6.78(6.69)

Table 2. Analytical data for manganese(III) Schiff base complexes

$Mn(N\text{-}R\text{-}Xsai)_2Cl$		Found (Calcd) (%)			
R	X	C	H	N	Mn
Oct	5-Br	50.88(50.54)	6.08(5.94)	3.96(3.93)	7.62(7.71)
Dod	5-Br	55.33(55.32)	7.12(7.09)	3.32(3.40)	6.74(6.66)
Octd	5-Br	60.06(60.45)	8.30(8.32)	2.84(2.82)	5.59(5.53)
Bz	5-Br	50.30(50.29)	3.40(3.32)	4.07(4.19)	8.32(8.22)
Oct	5,6-Benzo	69.52(69.66)	7.44(7.38)	4.19(4.28)	8.46(8.38)
Dod	5,6-Benzo	72.31(72.00)	8.56(8.41)	3.71(3.65)	7.13(7.16)
Octd	5,6-Benzo	74.19(74.45)	9.40(9.48)	2.96(2.99)	6.02(5.87)
Bz	5,6-Benzo	70.61(70.77)	4.69(4.62)	4.54(4.58)	9.02(8.99)
Oct	$5\text{-}NO_2$	55.50(55.86)	8.60(8.69)	6.63(6.56)	8.45(8.52)
Dod	$5\text{-}NO_2$	59.79(60.27)	7.77(7.72)	7.38(7.40)	7.11(7.25)
Octd	$5\text{-}NO_2$	64.80(64.88)	9.07(8.93)	5.95(6.05)	5.92(5.94)
Bz	$5\text{-}NO_2$ [a)]	57.96(57.64)	4.06(3.97)	9.54(9.60)	9.38(9.42)

a) Values for $Mn(N\text{-}Bz\text{-}5\text{-}NO_2sai)_2OH$

Table 3. Analytical data for manganese(IV) Schiff base complexes

$Mn(N\text{-}R\text{-}Xsai)_2Cl_2$		Found (Calcd) (%)				
R	X	C	H	N	Cl	Mn
Oct	5-Br	48.28(48.15)	5.82(5.66)	3.74(3.74)	30.55(30.84)[a)]	7.33(7.34)
Dod	5-Br	53.12(53.04)	6.90(6.79)	3.28(3.26)	26.56(26.81)[a)]	6.52(6.38)
Octd	5-Br	57.92(58.37)	8.18(8.03)	2.81(2.72)	22.91(22.53)[a)]	5.31(5.34)
Bz	5-Br	47.96(47.76)	3.26(3.15)	3.95(3.98)	32.62(32.77)[a)]	7.80(7.80)
Oct	5,6-Benzo	66.39(66.08)	7.11(7.01)	4.42(4.06)	10.75(10.27)	8.11(7.95)
Dod	5,6-Benzo	68.58(68.82)	8.09(8.03)	3.50(3.49)	8.67(8.83)	7.05(6.84)
Octd	5,6-Benzo	71.44(71.73)	9.21(9.13)	2.91(2.88)	7.52(7.30)	5.70(5.66)
Bz	5,6-Benzo	66.69(66.89)	4.41(4.37)	4.45(4.33)	11.10(10.97)	8.54(8.50)
Oct	$5\text{-}NO_2$	52.74(52.95)	6.23(6.22)	8.39(8.24)	10.00(10.42)	8.10(8.07)
Dod	$5\text{-}NO_2$	57.74(57.57)	7.53(7.37)	7.05(7.07)	9.05(8.94)	6.93(6.93)
Octd	$5\text{-}NO_2$	62.24(62.49)	8.78(8.50)	5.92(5.83)	8.34(7.34)	5.69(5.72)
Bz	$5\text{-}NO_2$ [b)]	50,19(50.42)	3.53(3.42)	8.22(8.25)	16.33(15.67)	8.56(8.09)

a) Cl + Br. b) Inclusion of $(CH_2Cl_2)_{0.5}$ as a crystalline solvent.

Results and Discussion

Preparation. The dichlorobis(N-butyl-substituted salicylideneaminato)manganese(IV) complexes, $Mn(N\text{-}Bu\text{-}Xsai)_2Cl_2$ (X = 5-Br, 5,6-Benzo, and 5-NO_2), which have previously been obtained, are decomposed gradually to the reduced manganese(III) complexes by moisture allowing to stand in an aerial condition even in the solid state. Thus, in order to obtain pure manganese(IV) complexes much care should be taken to remove trace amounts of water in the solvents used. As described in section V-2, the central manganese ion of the dichloromanganese(IV) complexes with bidentate Schiff bases can be protected from attack of water molecules by incorporating long-chain alkyl groups such as *n*-$C_{12}H_{25}$ and *n*-$C_{18}H_{37}$. These findings led the author to prepare a series of dichloromanganese(IV) Schiff base complexes having long-chain alkyl groups. All the manganese(III) complexes have a composition of $Mn(N\text{-}R\text{-}Xsai)_2Cl$, with the exception of $Mn(N\text{-}Bz\text{-}5\text{-}NO_2sai)_2OH$ (Table 2). All the manganese(IV) complexes have a composition of $Mn(N\text{-}R\text{-}Xsai)_2Cl_2$ (Table 3). The properties of the manganese(III) and manganese(IV) complexes are summarized in Tables 4 and 5, respectively.

Melting Points. The manganese(III) complexes having the long-chain alkyl groups showed low melting points without decomposition. As seen in Table 4, the longer the alkyl groups the lower melting points are obtained in the order of Bz > Oct > Dod > Octd. As for the substituents on the aromatic ring the melting points are lowered in the order of 5-NO_2 > H > 5-Br > 5,6-Benzo groups. The melting points for $Mn(N\text{-}Rsai)_2Cl$ which were prepared in the preceding study are 154 - 155, 129 - 130, 119.5 - 120, and 205 - 206 ^{o}C for R = Oct, Dod, Octd, and Bz, respectively. On the other hand, the melting points of the manganese(IV) complexes are lower

than those of the corresponding manganese(III) complexes, and they decompose at near melting points, showing color changes from green to brown (Table 5). As for the alkyl groups the melting points are lowered in the same order as that for the manganese(III) complexes, and as for the substituents on the aromatic ring they are lowered in the order of 5-NO_2 > 5-Br > H > 5,6-Benzo groups, with the exception of $Mn(N\text{-}Bzsai)_2Cl_2$. The melting points of $Mn(N\text{-}R\text{-}sai)_2Cl_2$ which were prepared in the preceding study are 106 - 107, 97.5 - 98.5, 94 - 95, and 112 - 113 °C for R = Oct, Dod, Octd, and Bz, respectively.

Magnetic Moments. The magnetic moments of the manganese(III) complexes fall within the range of 4.82 - 4.95 BM, with the

Table 4. Properties of manganese(III) Schiff base complexes

$Mn(N\text{-}R\text{-}Xsai)_2Cl$ R	X	M.P. °C	μ_{eff} [a] BM	ν_{max} [b] 10^3 cm^{-1} (log ε)	ν(Mn-Cl) [c] cm^{-1}	$E_{p/2}$ vs. SCE [d] V Mn(III)→Mn(II)
Oct	5-Br	141-145	4.95	14.97 (2.72)	306	0.08
Dod	5-Br	122-123	4.92	14.93 (2.75)	305	0.08
Octd	5-Br	104-105	4.83	14.97 (2.75)	306	0.07
Bz	5-Br	229-230 [e]	4.91	14.86 (2.77)	330	0.08
Oct	5,6-Benzo	136-137	4.91	15.11 (2.70)	306	-0.09
Dod	5,6-Benzo	109-110	4.83	15.15 (2.72)	305	-0.08
Octd	5,6-Benzo	94-95	4.82	15.13 (2.71)	305	-0.06
Bz	5,6-Benzo	208-209 [e]	3.25	15.08 (2.70)	313	-0.07
Oct	5-NO_2	197-198	3.89	15.92 (2.84)	293	0.28
Dod	5-NO_2	181-182	3.79	15.67 (2.70)	294	0.25
Octd	5-NO_2	179-180	3.53	15.72 (2.72)	293	0.30
Bz	5-NO_2	220-222 [e]	4.20	15.82 (2.65)	293	0.28

a) Measured at room temperature. b) Measured in dichloromethane. c) Measured in Nujol mulls. d) Measured in acetonitrile containing 0.1 M Bu_4NClO_4 at 25 °C, e) With decomposition.

exception of $Mn(N\text{-}Bz\text{-}5,6\text{-}Benzosai)_2Cl$ and all the 5-nitro derivatives (Table 4). These values are consistent with the spin-only value expected for a complex having a d^4 high-spin electron configuration. The lower values observed for the above complexes may be caused by antiferromagnetic interaction between manganese atoms due to a binuclear structure in which they are bridged by two phenolic oxygen atoms. No further investigation on magnetic properties for these complexes has been made.

The magnetic moments of the manganese(IV) complexes fall within the range of 3.87 - 4.10 BM (Table 5). These values are consistent with the spin-only value expected for a complex having

Table 5. Properties of manganese(IV) Schiff base complexes

$Mn(N\text{-}R\text{-}Xsai)_2Cl_2$ R	X	M.P.[a] °C	μ_{eff}[b] BM	ν_{max}[c] 10^3 cm^{-1} (log ε)	ν(Mn-Cl)[d] cm^{-1}	$E_{p/2}$ *vs.* SCE[e] V Mn(IV)→Mn(III)	Mn(III)→Mn(II)
Oct	5-Br	123-124	4.07	15.72 (3.72)	329	0.87	-0.12
Dod	5-Br	115-116	4.02	15.72 (3.73)	326	0.85	-0.10[f]
Octd	5-Br	111-112	4.07	15.67 (3.66)	337	0.85	-0.10[f]
Bz	5-Br	184-185	3.87	15.77 (3.55)	337	0.90	-0.03
Oct	5,6-Benzo	94-95	4.02	14.84 (3.68)	336	0.40	-0.13
Dod	5,6-Benzo	86-87	4.04	14.75 (3.77)	327	0.39	-0.13[f]
Octd	5,6-Benzo	83-84	3.91	14.75 (3.75)	326	0.40	-0.07[f]
Bz	5,6-Benzo	148-149	3.90	14.83 (3.77)	326	0.41	-0.07
Oct	5-NO_2	190-193	3.93	16.98 (3.72)	358	0.93	0.06
Dod	5-NO_2	185-190	4.06	17.01 (3.77)	354	0.92	0.06
Octd	5-NO_2	180-184	4.10	16.85 (3.74)	358	0.93	0.12[f]
Bz	5-NO_2	280	3.94	17.12 (3.74)	355	1.00	0.21

a) With decomposition. b) Measured at room temperature. c) Measured in dichloromethane. d) Measured in Nujol mulls. e) Measured in acetonitrile containing 0.1 M Bu_4NClO_4 at 25 °C. f) Measured in acetonitrile-dichloromethane (1/1 volume ratio).

a d^3 high-spin electron configuration.

Electronic Spectra. The electronic spectra of the manganese(III) complexes measured in dichloromethane show the absorption bands (log ε = 2.7) around 15000 cm^{-1}. These complexes may have a five-coordinate configuration around the central manganese ion in such a noncoordinating solvent.[1] Therefore, these bands can be assigned to a ligand field transition due to $d_{xy} \rightarrow d_{x^2-y^2}$. The absorption maxima are affected by the aromatic ring substituents and are shifted to higher energies in the order of 5-NO_2 > H > 5,6-Benzo > 5-Br groups (Table 4). The alkyl groups attached to the nitrogen atoms have little effect on the absorption maxima. On the other hand, the electronic spectra of the manganese(IV) complexes measured in dichloromethane show the more intense absorption bands (log ε = 3.7) in the range of 14700 - 17100 cm^{-1} than those for the manganese(III) complexes. These bands can be assigned to a charge-transfer transition due to Cl($p\pi$) → Mn($d\pi$) from their intensities as discussed in the previous sections, V-1 and V-2. These absorption maxima are also affected by the aromatic ring substituents and are shifted to higher energies in the order of 5-NO_2 > H > 5-Br > 5,6-Benzo groups (Table 5). The alkyl groups have little effect on the absorption maxima as well as the manganese(III) complexes.

Infrared Spectra. The IR spectra of the manganese(IV) complexes show almost the same pattern as those of the manganese(III) complexes in the region from 500 to 4000 cm^{-1}, but both spectra are significantly different in the region from 200 to 500 cm^{-1}. In this region the absorption bands due to Mn-Cl stretching vibrations should be observed.[2] Both manganese(III) and manganese(IV) complexes showed one absorption band assignable to ν(Mn-Cl)

(Tables 4 and 5). The frequencies for the manganese(IV) complexes are observed in higher energies than those for the corresponding manganese(III) complexes. This may be caused by the change in the oxidation state of the central manganese ion from Mn(III) to Mn(IV). The results that one absorption band due to ν(Mn-Cl) is observed for the manganese(IV) complexes imply that two chlorine atoms coordinate to the manganese atom as a *trans*-configuration. Thus, a *trans*-octahedral configuration is proposed for the manganese(IV) Schiff base complexes investigated here as shown in Fig. 1.

Electrochemical Properties. The cyclic voltammograms of the manganese(III) and manganese(IV) complexes were measured in acetonitrile. Some of the manganese(IV) complexes were measured in a mixture of acetonitrile and dichloromethane (1/1 volume ratio) owing to their poor solubility in acetonitrile. The current-potential curves for the manganese(III) complexes showed the one cathodic wave around 0.0 V (*vs.*SCE) in the +1.2 to -0.8 V range. This can be assigned to the one-electron reduction from Mn(III) to Mn(II).[3] On the other hand, the current-potential curves for the manganese(IV) complexes showed the two-step cathodic waves around +0.9 and 0.0 V with similar wave heights. These waves can be assigned to the one-electron reductions from Mn(IV) to Mn(III) and from Mn(III) to Mn(II), respectively. The separations of the peak potentials between the cathodic wave and the corresponding anodic wave for both redox waves are larger than the 57 mV expected for a reversible one-electron redox wave, so these electrode reactions may be irreversible. Thus, the half-peak potentials ($E_{p/2}$) of the cathodic waves for the manganese(III) and manganese(IV) complexes are summarized in Tables 4 and 5, respectively. The reduction potentials for the manganese(III) complexes are affected by the

aromatic ring substituents and are shifted to more positive potentials in the order of 5-NO_2 > 5-Br > 5,6-Benzo groups. And they are little affected by the alkyl groups. On the other hand, the reduction potentials for the manganese(IV) complexes are significantly affected by the aromatic ring substituents and are shifted to more positive potentials in the order of 5-NO_2 > 5-Br > 5,6-Benzo groups. These potential shifts can be explained by the electron-withdrawing ability of the substituent groups. And also the alkyl groups have little effect on the reduction potentials. These results are not inconsistent with those obtained in the electronic and IR spectra.

Summary

A series of dichlorobis(N-alkyl-substituted salicylideneaminato)manganese(IV) complexes, Mn(N-R-xsai)$_2$Cl$_2$, was prepared by the reaction of Mn(N-R-Xsai)$_2$Cl complexes with hydrogen chloride, where R can be *n*-C_8H_{17} (Oct), *n*-$C_{12}H_{25}$ (Dod), *n*-$C_{18}H_{37}$(Octd), and $CH_2C_6H_5$ (Bz) and X can be 5-bromo, 5-nitro, and 5,6-benzo groups. These complexes were characterized by the magnetic susceptibilities, IR and electronic spectra, and cyclic voltammograms.

References.

1) L. J. Boucher and V. W. Day, *Inorg. Chem.*, 16, 1360 (1977).
2) K. Nakamoto, "Infrared Spectra of Inorganic and Coordination Compounds," p. 214. Wiley-Interscience, New York (1970).
3) W. M. Coleman, R. R. Goehring, L. T. Taylor, J. G. Mason, and R. K. Boggess, *J. Am. Chem Soc.*, 101, 2311 (1979).

Chapter VI

Reactions of Dichloromanganese(IV) Schiff Base Complexes with Water as a Model for Water Oxidation in Photosystem II

Introduction

Manganese ions with higher oxidation states such as +III and/or +IV have been believed to be involved in water oxidation process of photosystem II in green plants.[1 - 4] Several attempts and assumption for this process have been published.[5 - 8] However, it has not yet been reported that molecular oxygen is liberated by direct reactions of synthetic manganese complexes with water as a model for the primary event in photosystem II.

In this Chapter, the preparation and characterization of dichloromanganese(IV) Schiff base complexes shown in Fig. 1 and their reactions with water will be described.

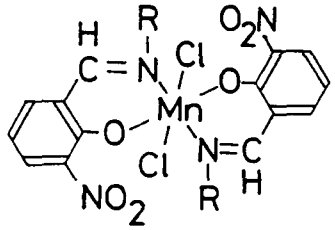

R = *n*-C_3H_7 (Pr), *n*-C_4H_9 (Bu), *n*-C_6H_{13} (Hx), *n*-C_8H_{17} (Oct), *n*-$C_{12}H_{25}$ (Dod), $CH_2C_6H_5$ (Bz).

Fig. 1. Manganese(IV) Schiff base complexes, $Mn(N\text{-}R\text{-}3\text{-}NO_2sai)_2Cl_2$.

Experimental

Preparation of Chloromanganese(III) Schiff Base Complexes. Chlorobis(N-octyl-3-nitrosalicylideneaminato)manganese(III), Mn(N-Oct-3-NO_2sai)$_2$Cl: All the manganese(III) Schiff base complexes were prepared by the following modification of the method described in Chapter III-1. 3-Nitrosalicylaldehyde (3-NO_2salH) was prepared by the method described in the literature.[9] The Schiff base ligands were prepared by the condensation of 3-NO_2salH with alkylamines,

RNH_2 (R = n-C_3H_7, n-C_4H_9, n-C_6H_{13}, n-C_8H_{17}, n-$C_{12}H_{25}$, and $CH_2C_6H_5$) in tetrahydrofuran (THF). They were recrystallized from appropriate organic solvents such as ethanol and ether.

To a mixed solution of dichloromethane (50 cm^3) and methanol (50 cm^3) containing N-octyl-3-nitrosalicylideneamine (N-Oct-3-NO_2-saiH, 5.57 g, 10 mmol) were added $Mn(CH_3COO)_3 \cdot 2H_2O$ (1.34 g, 5 mmol) and LiCl (0.32 g, 7.5 mmol). The mixture was refluxed for 30 min with stirring and then evaporated to dryness under reduced pressures. The resulting brown solid was recrystallized from dichloromethane to give the title complex as brown crystals.

Other manganese(III) Schiff base complexes were prepared in a similar manner. The analytical data are given in Table 1. These complexes include dichloromethane as a crystalline solvent.

Preparation of Dichloromanganese(IV) Schiff Base Complexes. Dichlorobis(N-octyl-3-nitrosalicylideneaminato)manganese(IV), Mn(N-Oct-3-NO_2sai)$_2Cl_2$: To a 2-propanol(50 cm^3) containing Mn(N-Oct-3-NO_2sai)$_2$Cl (0.5 g) was added dropwise a 2-propanol solution of hydrogen chloride (1.5 molar folds over the complex) with stirring at room temperature. The deep green crystals which precipitated were filtered, washed with 2-propanol, and dried *in vacuo*. The yield was *ca.* 0.2 g.

Other dichloromanganese(IV) complexes were obtained in a similar manner. The analytical data are given in Table 2.

Determination of Molecular Oxygen Liberated. In this study, two methods were employed for detection and determination of molecular oxygen which was liberated during the reactions between manganese(IV) complexes and water. The method A was based on colorization of an alkaline pyrogallol solution [pyrogallol (0.2 g) in an aqueous KOH solution (9 mol dm^{-3}, 4 cm^3)] by the reaction with gaseous O_2.

The colorization was monitered by measuring the absorbance at 420 nm with a spectrophotometer. An apparatus for spectrophotometric determination is shown in Fig. 2. The quantities of O_2 liberated were calculated from the calibration curve which was obtained by using air under the same conditions. The method B was based on a dissolved oxygen electrode. An EIL Model 8012-1 dissolved oxygen probe connected with a Yanaco pH-7 pH meter was used. This was calibrated with an air-saturated water and an aqueous solution of Na_2SO_3 (5%). The buffer solutions were prepared by acetate and phosphate buffer systems.

Measurements. All physical measurements were carried out by the methods described in Chapter V.

Materials. All the reagents were of reagent grade. Solvents were purified by a usual manner.

Table 1. Analytical data for the manganese(III) complexes, $Mn(N\text{-}R\text{-}3\text{-}NO_2sai)_2Cl$

Complex[a]	Found (%)				Calcd (%)			
R	C	H	N	Mn	C	H	N	Mn
Pr	44.95	4.30	9.65	10.35	44.95	4.24	10.24	10.04
Bu	47.25	5.00	9.57	9.67	47.01	4.73	9.75	9.56
Hx[b]	47.57	5.43	8.47	8.59	48.12	5.38	8.31	8.15
Oct[b]	50.32	6.59	7.78	7.94	51.01	6.08	7.67	7.52
Dod	58.54	7.57	7.09	6.88	57.82	7.44	7.01	6.87
Bz	53.47	3.95	8.41	8.63	53.24	3.61	8.71	8.55

Inclusion of dichloromethane as a crystalline solvent: a) $(CH_2Cl_2)_{0.5}$ and b) (CH_2Cl_2) per a complex.

Table 2. Analytical data for the manganese(IV) complexes, $Mn(N\text{-}R\text{-}3\text{-}NO_2sai)_2Cl_2$

Complex	Found (%)					Calcd (%)				
R	C	H	N	Cl	Mn	C	H	N	Cl	Mn
Pr	44.99	4.49	10.19	13.69	10.34	44.46	4.11	10.37	13.13	10.17
Bu	46.70	4.76	9.84	13.17	9.79	46.49	4.62	9.86	12.84	9.67
Hx	49.87	5.37	8.74	11.65	8.94	50.00	5.50	8.97	11.35	8.80
Oct	52.24	6.34	8.45	10.81	8.13	52.93	6.23	8.23	10.42	8.07
Dod	57.67	7.52	7.01	8.77	6.89	57.56	7.39	7.07	8.94	6.93
Bz	52.24	3.81	8.77	11.59	8.61	52.84	3.49	8.81	11.14	8.63

Results and Discussion

Characterization of the Manganese(III) and Manganese(IV) Complexes. The analytical data for the manganese(III) complexes are in agreement with an empirical formula of $Mn(N\text{-}R\text{-}3\text{-}NO_2sai)_2Cl\cdot(CH_2Cl_2)_n$ (n = 0.5 or 1) (Table 1). Dichloromethane was included as crystalline solvents. The analytical data for the manganese(IV) complexes are in agreement with an empirical formula of $Mn(N\text{-}R\text{-}3\text{-}NO_2sai)_2Cl_2$ (Table 2). The magnetic moments of the manganese(III) complexes are within the range of 4.85 to 4.95 BM, with the exception of $Mn(N\text{-}Bz\text{-}3\text{-}NO_2sai)_2Cl$ (Table 3). These values indicate that the manganese(III) complexes may adopt a d^4 high-spin electron configuration. The low value (4.24 BM) of the above complex may be caused by antiferromagnetic interaction due to a dimeric structure where manganese ions are bridged by the phenolic oxygen atoms. On the other hand, the magnetic moments of the manganese(IV) complexes are within the range of 3.88 to 4.02 BM (Table 4). These values are consistent with the spin-only value expected for a complex

having a d^3 high-spin electron configuration.

The electronic spectra of the manganese(III) complexes show an absorption band around 16000 cm^{-1} with moderate intensities in the visible region (Table 3). This can be assigned to the ligand field transition. The band positions are little affected by the alkyl groups. On the other hand, the electronic spectra of the manganese(IV) complexes show an intense absorption band (log ε = 3.7) around 17000 cm^{-1} in the visible region (Table 4). This can be assigned to a charge-transfer transition from Cl($p\pi$) to Mn($d\pi$) as described in Chapter V-1. The band positions are little affected by the alkyl groups as well as the manganese(III) case.

The cyclic voltammograms of the manganese(III) complexes measured in acetonitrile show a cathodic wave around 0.2 V (*vs.* SCE) (Table 3). This can be assigned to the one-electron reduction from Mn(III) to Mn(II). The cyclic voltammograms of the manganese(IV) complexes show two-step cathodic waves around 1.0 and 0.2 V (Table 4). These waves can be assigned to the reductions from Mn(IV) to Mn(III) and from Mn(III) to Mn(II), respectively. The most positive reduction potential is observed for $Mn(N\text{-}Pr\text{-}3\text{-}NO_2sai)_2Cl_2$ among the manganese(IV) complexes, although the reduction potentials for both manganese(III) and manganese(IV) complexes are little affected by the alkyl groups.

The infrared spectra of the manganese(IV) complexes exhibit one absorption band assignable to Mn-Cl stretching vibration around 340 cm^{-1}. This suggests that these manganese(IV) complexes have an octahedral *trans*-configuration where two chlorine atoms coordinate to the central manganese atom by a *trans*-form. The same behavior has been found for the dichlorobis(N-alkyl-salicylidene-aminato)manganese(IV) complexes, $Mn(N\text{-}Rsai)_2Cl_2$ (*cf.* V-2).

Table 3. Magnetic moments, absorption maxima, and reduciton potentials of the manganese(III) complexes, $Mn(N\text{-}R\text{-}3\text{-}NO_2sai)_2Cl$

Complex R	μ_{eff} [a] / BM	ν_{max} [b] / 10^3 cm^{-1} (log ε)	$E_{p/2}$ *vs.* SCE [c] / V Mn(III)→ Mn(II)
Pr	4.93	16.13 (2.43)	0.25
Bu	4.98	16.03 (2.57)	0.28
Hx	4.94	16.23 (2.62)	0.21
Oct	4.85	16.10 (2.43)	0.14
Dod	4.95	16.18 (2.53)	0.02
Bz	4.24	16.18 (2.42)	0.27

a) Measured at room temperature. b) Measured in acetonitrile. c) Measured in acetonitrile containing 0.1 mol dm^{-3} Bu_4NClO_4 at 25 °C.

Table 4. Magnetic moments, absorption maxima, and reduction potentials of the manganese(IV) complexes, $Mn(N\text{-}R\text{-}3\text{-}NO_2sai)_2Cl_2$

Complex R	μ_{eff} [a] / BM	ν_{max} [b] / 10^3 cm^{-1} (log ε)	$E_{p/2}$ *vs.* SCE [c] / V Mn(IV)→ Mn(III)→ Mn(II)	
Pr	3.96	17.01 (3.46)	1.04	0.28
Bu	3.99	17.06 (3.42)	0.99	0.25
Hx	4.02	17.30 (3.43)	0.98	0.18
Oct	3.88	17.04 (3.73)	0.98	0.11
Dod	3.97	17.18 (3.47)	0.96	0.15
Bz	4.01	16.95 (3.41)	0.98	0.22

a) Measured at room temperature. b) Measured in acetonitrile. c) Measured in acetonitrile containing 0.1 mol dm^{-3} Bu_4NClO_4 at 25 °C.

Reaction of the Manganese(IV) Complexes with Water. As mentioned above, the reduction potentials of the first cathodic wave of the manganese(IV) complexes match with the redox potential for the couple of O_2/H_2O (E_o' = 0.81 V *vs.* NHE) at neutral pH. Therefore, these manganese(IV) complexes can oxidize water to liberate molecular oxygen (O_2). In this study, the detection and determination of O_2 have been examined which may be liberated by the reactions of the manganese(IV) complexes with water. Figure 2 shows an apparatus for the spectrophotometric determination of small quantities of gaseous O_2 by use of an alkaline pyrogallol solution. The concentration of O_2 liberated in the system can be measured indirectly by absorption spectrophotometry of the oxidation product of pyrogallol.[10] In this study, a diffusion system was chosen because a flow system may suffer a disadvantage in effenciency of O_2 absorption by pyrogallol solution. Figure 3 shows a time course of absorbance of the pyrogallol solution at 420 nm during the reaction of

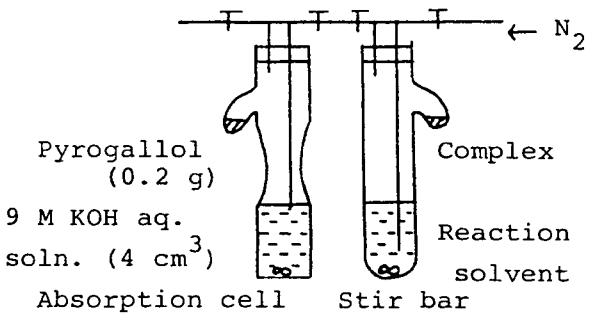

Fig. 2. Apparatus for spectrophotmetric measurements.

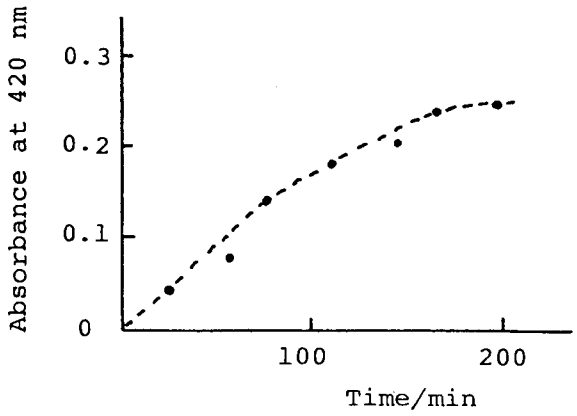

Fig. 3. Changes in absorbance of pyrogallol solution during the reaction of $Mn(N\text{-}Pr\text{-}3\text{-}NO_2sai)_2Cl_2$ (0.2 g) with water in a mixed solvent of acetonitrile (5 cm^3) and water (5 cm^3).

$Mn(N\text{-}Pr\text{-}3\text{-}NO_2sai)_2Cl_2$ with water in a mixed solvent of acetonitrile and water. As time elapsed, the solution of the complex turned green to dark yellow and an increase in absorbance of the pyrogallol solution was clearly observed. From the increase of absorbance observed after 200 min, the quantity of O_2 liberated out of the reaction system was estimated to be 0.068 mole of O_2 per one mole of complex on the basis of the calibration curve. However, dissolved oxygen in the solution of the complex could not be measured in this method. Thus, measurements of dissolved oxygen were made by using a dissolved oxygen probe. Large decreases in pH of the solutions were found to occur in the reactions of the dichloro-manganese(IV) complexes with water so buffer solutions were employed for the reaction solvent.

Figures 4 A and 4 B show the pH effects on the quantities of

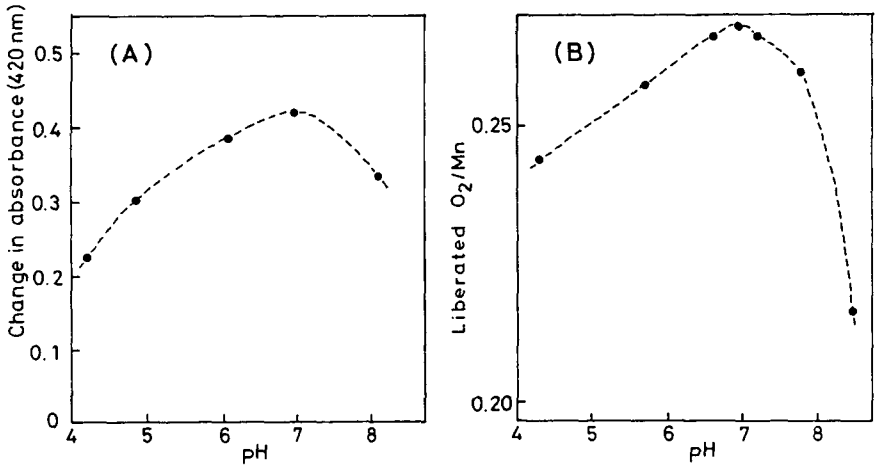

Fig. 4. The pH effects on quantities of molecular oxygen liberated during the reaction of $Mn(N\text{-}Pr\text{-}3\text{-}NO_2sai)_2Cl_2$ with water.
(A): Determined spectrophotometrically with an alkaline pyrogallol solution; complex, 0.2 g; solvent, a mixed solution of acetonitrile (5 cm^3) and buffer solution (5 cm^3).
(B): Determined with an oxygen electrode; complex, 0.02 g; solvent, a mixed solution of 2-propanol (5 cm^3) and buffer solution (20 cm^3).

O_2 liberated in the reactions of $Mn(N\text{-}Pr\text{-}3\text{-}NO_2sai)_2Cl_2$ with water, which were measured by the methods A and B, respectively. In both cases, the maximal liberation of O_2 is observed at neutral pH region. This is of interest in connection with the natural chloroplast.

Table 5 summarizes the quantities of O_2 liberated in the reactions of the dichloromanganese(IV) Schiff base complexes with water. All the manganese(IV) complexes investigated here are found to react with water to liberate O_2. Among them, the maximal value is observed for $Mn(N\text{-}Pr\text{-}3\text{-}NO_2sai)_2Cl_2$, which has the most positive reduction potential +1.04 V.

In the reactions of the manganese(IV) complexes with water, the following facts were observed: (1) pH of the reaction mixtures decreases largely, (2) free chloride ions are determined almost quantitatively, and (3) manganese(II) complexes are isolated from the reaction mixtures. These observations suggest that the present reaction of the manganese(IV) complexes with water takes place as

Table 5. Quantities of molecular oxygen liberated during the reactions of the manganese(IV) complexes (20 mg) with water in a mixed solvent of water (20 cm^3) and 2-propanol (5 cm^3) which was adjusted to pH = 7 by a phosphate buffer

Complex	O_2 liberated [a] / Mn
$Mn(N\text{-}Pr\text{-}3\text{-}NO_2sai)_2Cl_2$	0.27
$Mn(N\text{-}Bu\text{-}3\text{-}NO_2sai)_2Cl_2$	0.25
$Mn(N\text{-}Hx\text{-}3\text{-}NO_2sai)_2Cl_2$	0.14
$Mn(N\text{-}Oct\text{-}3\text{-}NO_2sai)_2Cl_2$	0.20
$Mn(N\text{-}Dod\text{-}3\text{-}NO_2sai)_2Cl_2$	0.12
$Mn(N\text{-}Bz\text{-}3\text{-}NO_2sai)_2Cl_2$	0.17

a) Determined with an oxygen electrode at 15 ± 0.1 °C.

follows,

$$2Mn^{IV}(L)_2Cl_2 + 2H_2O \longrightarrow 2Mn^{II}(L)_2 + O_2 + 4H^+ + 4Cl^-$$

where L denotes monoanion of the bidentate Schiff base ligands.

Summary

The dichloromanganese(IV) Schiff base complexes, $Mn(N\text{-}R\text{-}3\text{-}NO_2\text{-}sai)_2Cl_2$ (R = Pr, Bu, Hx, Oct, Dod, and Bz) have been prepared and characteriazed by the magnetic susceptibilities, electronic and infrared spectra, and cyclic voltammograms. All the manganese(IV) complexes are found to react with water to liberate molecular oxygen. This is confirmed by means of a spectrophotometry with an alkaline pyrogallol solution and by using a dissolved oxygen electrode. The maximal liberation of O_2 is observed at neutral pH region. The following reaction scheme is proposed,

$$2Mn^{IV}(L)_2Cl_2 + 2H_2O \longrightarrow 2Mn^{II}(L)_2 + O_2 + 4H^+ + 4Cl^-.$$

References

1) K. Sauer, *Acc. Chem. Res.*, 13, 249 (1980).

2) G. M. Cheniae, *Ann. Rev. Plant Physiol.*, 21, 467 (1970).

3) G. D. Lawrence and D. T. Sawyer, *Coord. Chem. Rev.*, 27, 173 (1978).

4) Govindjee, T. Wydrzynski, and S. R. Marksin, "Bioenergetics of Membranes," ed by L. Packer *et al.*, Elsevier/North Holland, Amsterdam (1977), p. 305.

5) G. Renger, *FEBS Lett.*, 81, 223 (1977).

6) D. T. Sawyer, M. E. Bodini, L. A. Willis, T. L. Riechel, and K. D. Magers, *Adv. Chem. Ser.*, 162, 330 (1977).

7) I. Tabushi and S. Kojo, *Tetrahedron Lett.*, 1974, 1577; *ibid.*, 1975, 305.

References (Contd)

8) P. A. Loach and M. Calvin, *Biochem.*, 2, 361 (1963); *Biochim. Biophys. Acta*, 79, 379 (1964).

9) C. C. Hach, L. M. Liggett, and H. Diehl, *Chem. Abstr.*, 42, 1240 (1948).

10) I. A. Duncan, A. Harriman, and G. Porter, *Anal. Chem.*, 51, 2206 (1979).

Chapter VII

Oxidative Dehydrogenation of Bis(salicylideneaminato)copper(II) Complex in Pyridine and Formation of 2-Cyanophenolato Complex

Introduction

It is well known that copper(II) salts catalyze significantly the oxidation of organic substances by molecular oxygen.[1] Brackman *et al.*[2] have reported that the ammoxidation of alcohols and aldehydes catalyzed by copper(II) salts gives the corresponding nitriles in good yields, and have proposed that the imino function (RCH=NH) which formed by condensation of aldehyde with ammonia was oxidized to nitrile *via* an intermediate of an imino radical (RCH=N·), involving a Cu(II)/Cu(I) redox system. Misono *et al.*[3] have investigated the kinetics of the formation of benzonitrile from benzaldehyde and ammonia catalyzed by some copper compounds, and have proposed that benzilideneamine is an important intermediate. They have reported that 2-cyanophenol was formed by thermal decomposition of bis(salicylideneaminato)copper(II), $[Cu(salam)_2]$.[4]

The oxidative dehydrogenation of amino and alkylamino groups coordinated to metal ions has been reported.[5] Diamond *et al.*[6] have found that pentaammine(benzylamine)ruthenium(II) ion reacts with molecular oxygen to give pentaammine(benzonitrile)ruthenium ion. Keene *et al.*[7] have reported that the complexes, $[Ru(bpy)_2(NH_2CH_2R)_2]^{+2}$ (NH_2CH_2R = allylamine, benzylamine, and butylamine) were oxidized chemically and electrochemically to give the corresponding bis(nitrile) complexes, $[Ru(bpy)_2(NC\text{-}R)_2]^{+2}$ and proposed that the reactions proceed by initial oxidation of Ru(II) to Ru(III), followed by a series of stepwise dehydrogenation reactions which occur *via* the imine intermediate. Recently, the oxidative dehydrogenation of the coordinated secondary amine

moieties to the copper atom has been reported for Cu(II)-4,4'-(ethane-1,2-diyldiimino)bis(pent-3-en-2-one) complex[8] and bi-Cu(I)-macrocyclic complex.[9]

In this Chapter it will be described that [Cu(salam)$_2$] reacts with molecular oxygen to give quantitatively the 2-cyanophenolato complex. This reaction should afford good information on the mechanism of the ammoxidation catalyzed by copper compounds.

Experimental

Preparation of Copper(II) Complexes with Salicylideneamine and Its Analogs. All the complexes with the Schiff bases used in this study were obtained by the method described in the literature. They are abbreviated as follows: Bis(salicylideneaminato)copper(II): [Cu(salam)$_2$][10a]; bis(substituted salicylideneaminato)copper(II): [Cu(X-salam)$_2$][10b], where X can be 5-Me, 3-Me, 3-MeO, 4-Cl, 5-Br, 5,6-Benzo, and 5-NO_2; bis[1-(*o*-hydroxyphenyl)ethylideneaminato]-copper(II): [Cu(hpam)$_2$][10c]; bis(N-methylsalicylideneaminato)-copper(II): [Cu(N-Mesalam)$_2$][10c].

Isolation of Oxidized Products. *Oxidized Product of [Cu(salam)$_2$]:* A pyridine solution (300 cm^3) of [Cu(salam)$_2$] (1.0 g) was kept at 70 °C, with dried air bubbled through it. The green solution turned brown gradually. The reaction was followed by monitering the visible absorption spectra of small portions of the solution at regular intervals. The spectral changes were no longer observed after *ca.* 7 h; the resulting solution was evaporated under reduced pressure. The brown solid was collected on a glass filter, washed with hexane, and dried *in vacuo*. The yield was quantitative. The product is soluble in pyridine (py), N,N-dimethylformamide (DMF), and dimethyl sulfoxide (DMSO), slightly soluble in dichloromethane,

methanol, and benzene, but insoluble in water. This was reprecipitated from pyridine and ether.

The oxidized product of [Cu(salam)$_2$] could be obtained from the reaction between its pyridine solution and an aqueous solution of hydrogen peroxide (30%) at room temperature. This was identified to be the same product as the above. The reaction of [Cu(salam)$_2$] with molecular oxygen in dioxane was found to give the pale brown product. This is soluble in pyridine, but insoluble in noncoordinating solvents; its formula is [Cu(2-CNphO)(OH)], where 2-CNphOH denotes 2-cyanophenol. All the reaction conditions are summarized in Table 1, together with the empirical formulas of the products. The analytical data for these products are given in Table 2, along with their magnetic moments determined at room temperature and the frequencies due to ν(CN).

Isolation of 2-Cyanophenol from the Oxidized Product of [Cu(salam)$_2$]. The oxidized product (0.1 g) of [Cu(salam)$_2$] was dissolved in pyridine (10 cm^3). A solution (100 cm^3) of 1 M (1 M = 1 mol dm^{-3}) hydrochloric acid was added to it. Hydrogen sulfide gas was passed through the solution for 10 min, followed by passing nitrogen gas for 20 min. A black precipitate was filtered and washed with ether (50 cm^3). The filtrate was extracted with ether (50 cm^3). The ethereal washings and extract were combined and dried over anhydrous sodium sulfate, and then evaporated under reduced pressure to yield a pale yellow solid. It was recrystallized from hexane to give white crystals. The yield was 0.04 g. This was identified to be 2-cyanophenol from the elemental analysis, infrared spectrum, and melting point (96.5 $^{\circ}$C).

Preparation of 2-Cyanophenolato Complexes. Bis(2-cyanophenolato)bis(pyridine)copper(II), [Cu(2-CNphO)$_2$(py)$_2$]: This

complex was obtained by a modification of the method described in the literature.[11] To an aqueous solution (20 cm^3) containing $CuSO_4 \cdot 5H_2O$ (0.75 g, 3 mmol) and pyridine (0.48 g, 6 mmol) was added dropwise an aqueous solution (15 cm^3) of 2-cyanophenol (0.72 g, 6 mmol) and sodium hydroxide (0.24 g, 6 mmol) with stirring. An olive-green solid which precipitated was collected on a glass filter, washed with water and then with small volumes of ethanol and ether, and dried *in vacuo*. This was recrystallized from dichloromethane to give greenish brown crystals.

2,2'-Bipyridinebis(2-cyanophenolato)copper(II), $[Cu(2\text{-}CNphO)_2(bpy)]$: This complex was obtained in a similar way to that used for the above complex, using 2,2'-bipyridine in place of pyridine.

The analytical data for the 2-cyanophenolato complexes are given in Table 2, together with their magnetic moments determined at room temperature and the frequencies due to ν(CN).

Materials. All reagents were of reagent grade. The solvents were purified in the usual manner.

Measurements. The UV, VIS, and NIR spectra were recorded on a Hitachi 340 recording spectrophotometer. The diffused reflectance spectra were obtained by using the above instrument along with a Hitachi R-10 A integrating sphere unit and a NIR integrating sphere unit. The infrared spectra and magnetic susceptibilities were obtained by the method described in Chapter III-1.

TABLE 1. OXIDATION CONDITIONS FOR COPPER(II) COMPLEXES AND THEIR PRODUCTS

Complex[a]	Solvent[b]	Temp °C	Time h	Atmosphere	Reaction produdt		
					Yield/%	Formula	Color
$[Cu(salam)_2]$	Pyridine	70	7	Air	95	$[Cu(2\text{-}CNphO)_2(py)_2]$	Greenish brown
$[Cu(salam)_2]$	Pyridine[c]	30	0.5	Air	90	$[Cu(2\text{-}CNphO)_2(py)_2]$	Greenish brown
$[Cu(salam)_2]$	Dioxane	70	7	Air	60	$[Cu(2\text{-}CNphO)(OH)]$	Pale brown
$[Cu(hpam)_2]$	Pyridine	80	10	Air	90	$[Cu(2\text{-}CNphO)_2(py)_2]$	Greenish brown
$[Cu(N\text{-}Mesalam)_2]$	Pyridine	110	100	O_2		No reaction	

a) Complex: 3 mmol. b) Solvent: 300 cm^3. c) Addition of aqueous H_2O_2 solution (30%, 6 mmol).

Results and Discussion

A pyridine solution of $[Cu(salam)_2]$ has been found to change the color from green to greenish brown on being allowed to stand for a few days at room temperature under air. The author is interested in the cause of such a color change.

Absorption Spectral Changes. Figure 1 shows the absorption spectral changes of a pyridine solution of $[Cu(salam)_2]$ at 70 °C under air. The absorption bands at 366 and 598 nm observed for the original spectrum can be assigned to charge-transfer and ligand field transitions, respectively. The absorption spectrum changes remarkably with time, showing the isosbestic points at 351 and 408 nm; the absorption band at 366 nm decreases in intensity and a new absorption band appears at 333 nm (Fig. 1 A), and the absorption band at 598 nm is shifted to lower energies with increasing the intensity around 500 nm (Fig. 1 B). These spectral changes indicate that a marked change occurs in the coordinated ligand and the environment around the central copper atom.

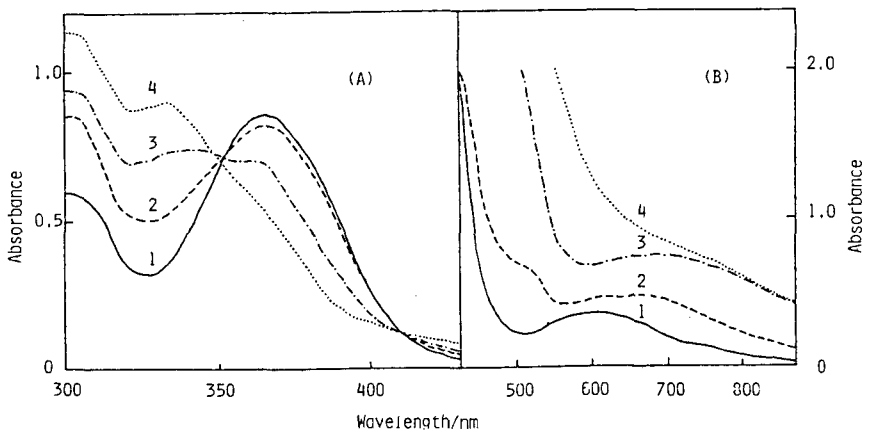

Fig. 1. Absorption spectral changes of pyridine solutions of 8×10^{-5} M (A) and 8×10^{-3} M (B) $[Cu(salam)_2]$ at 70 °C under air, cell length 1cm.
(A): 1) Reaction time = 0; 2), 265; 3), 325; 4), 385 min.
(B): 1) Reaction time = 0; 2), 26; 3), 80; 4), 385 min.

Characterization of the Reaction Product. The analytical data for the reaction product of $[Cu(salam)_2]$ in pyridine are in agreement with an empirical formula of $[Cu(2\text{-}CNphO)_2(py)_2]$. The magnetic moment is 2.05 BM. The electronic spectrum measured in pyridine shows an intense absorption band around 23000 cm^{-1} and a broad absorption band around 14000 cm^{-1} (Fig. 2). These bands can be assigned to a charge-transfer transition between the phenolic oxygen atom and copper atom and the ligand field transition from higher energies.[12] Figure 3 shows the infrared spectra of

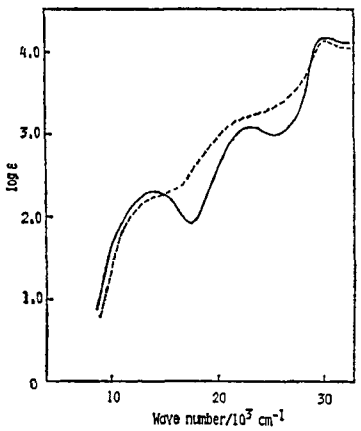

Fig. 2. Electronic spectra in pyridine
---: Oxidized product of $[Cu(salam)_2]$,
——: authentic complex, $[Cu(2\text{-}CNphO)_2(py)_2]$.

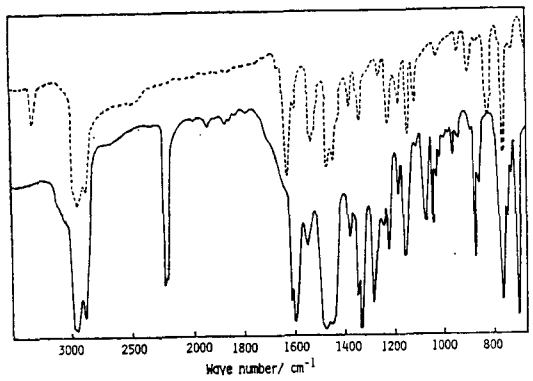

Fig. 3. Infrared spectra of $[Cu(salam)_2]$ (---) and its oxidized product (——) in Nujol mulls.

TABLE 2. ANALYTICAL DATA, MAGNETIC MOMENTS, AND ν(CN) FREQUENCIES FOR 2-CYANOPHENOLATO COPPER COMPLEXES

Complex	Found (%)			Calcd (%)			μ_{eff}[b]	ν(CN)[c]
	C	H	N	C	H	N	BM	cm^{-1}
$[Cu(2\text{-}CNphO)_2(py)_2]$[a]	62.75	3.65	12.50	62.94	3.96	12.23	2.05	2220, 2205
$[Cu(2\text{-}CNphO)_2(py)_2]$	62.91	3.93	12.07	62.94	3.96	12.23	1.91	2220, 2205
$[Cu(2\text{-}CNphO)_2(bpy)]$	63.03	3.43	11.90	63.22	3.54	12.29	1.91	2220, 2208
[Cu(2-CNPhO)(OH)]	42.46	2.32	7.16	42.31	2.53	7.05	1.46	2238

a) Oxidized product. b) Measured at room temperature. c) Measured in Nujol mulls.
ν(CN): 2237 cm^{-1} for 2-CNphOH; 2205 cm^{-1} for 2-CNphONa.

[Cu(salam)$_2$] and its reaction product. In the latter compound, the absorption bands at 3280 and 1625 cm^{-1} are due to ν(N-H) and ν(C=N), respectively, which were observed for [Cu(salam)$_2$], disappear and new absorption bands are observed at 2220 and 2205 cm^{-1} and at 1221, 1072, and 691 cm^{-1}. The bands at 2220 and 2205 cm^{-1} can be assigned to the stretching vibrations of nitrile group from their frequencies. The latter three bands can be assigned to the characteristic bands of the coordinated pyridine. These results indicate that the imino groups coordinated to the copper atom are oxidized to the nitrile groups by the oxidative dehydrogenation.

The authentic complex which was prepared by the reaction of $CuSO_4$, 2-cyanophenol, and pyridine has the same composition, formulated as [Cu(2-CNphO)$_2$(py)$_2$], and shows the same infrared spectrum as that for the oxidized product (Table 2). In the electronic spectra, the absorption maxima for the oxidized product are in agreement with those for the authentic complex (Table 3). However, the intensities around 19000 cm^{-1} are slightly higher in the oxidized product than those in the authentic complex (Fig. 2). This may be caused by the difference in orientation of the coordinated 2-cyanophenolato ligands between these complexes as shown below. A molecular model for them suggests that a free rotation

Table 3. Electronic spectral data for 2-cyanophenolato copper complexes

Complex	Solvent	$\frac{\nu_{max}}{10^3\ cm^{-1}}$ (log ε)				
[Cu(2-CNphO)$_2$(py)$_2$]	Pyridine		14.0(2.23)	23.2(3.10)	30.3(4.15)	
	DMF	12.4 sh	14.4(1.86)	23.4(2.80)	30.3(3.38)	33.4(4.00)
	Solid	12.7 sh	16.2	23.1	31.1	33.1
[Cu(2-CNphO)$_2$(py)$_2$]$^{a)}$	Pyridine		14.4(2.20)	22.5(3.20)	30.5(4.11)	
	Solid	13.0 sh	15.8 sh	23.1	31.1	33.1
[Cu(2-CNphO)$_2$(bpy)]	Solid		15.9	23.1	30.0	34.1

a) Oxidized product. sh: Shoulder.

of the 2-CNphO at the Cu-O bond is restricted by the coordinated pyridine molecules. Therefore, on the basis of steric repulsion, the form (A) is a possible configuration for the authentic complex.

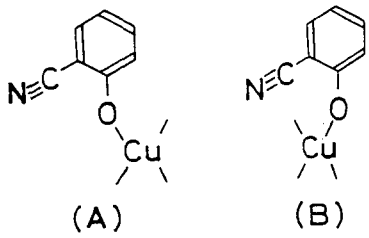

(A) (B)

On the contrary, the form (B) may be maintained in the oxidized product, because the original $[Cu(salam)_2]$ has a *trans*-planar configuration. In this form, a planar configuration around the central copper atom may distort to a tetrahedral configuration by steric requirement. This is one reason why high intensities are observed in the oxidized product.

The magnetic moment of the authentic complex is a slightly lower value (1.91 BM) than that of the oxidized product. This may be caused by a slight differnece between configurations of the authentic and the oxidized complexes, as mentioned above.

It should be noted that the doublet bands due to ν(CN) are observed for the 2-cyanophenolato complexes and both peaks are of equal intensity. Moreover, the C-O stretching vibrations of the coordinated 2-cyanophenol are observed around 1320 cm^{-1} as doublet bands. These results suggest that 2-cyanophenolato ligands coordinate to the copper atom in two different fashions. It has been reported that nitrile groups can coordinate to metal ions through either nitrogen atom or π-bond of nitrile.[13] In the former case, the ν(CN) frequencies shift to higher energies than that of the free ligand, whereas in the latter case, they shift to lower energies. In the present copper complexes, the ν(CN) frequencies are within a range of 2237 cm^{-1} for 2-CNphOH to 2205 cm^{-1} for 2-CNphONa (Table 2) This indicates that coordination of nitrile groups is not involved

in these copper complexes. Therefore, a binuclear structure shown in Fig. 4 is proposed for $[Cu(2\text{-}CNphO)_2(py)_2]$ in which the copper atoms are bridged by the phenolic oxygen atoms. This structure could be easily broken up in pyridine solution. The infrared spectra taken on pyridine solutions of the oxidized and authentic complexes showed only one band due to ν(CN) at 2212 cm^{-1}.

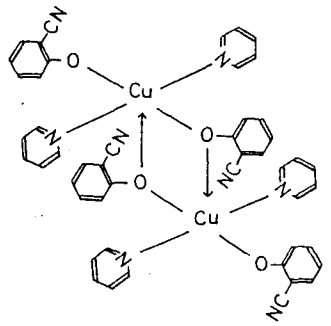

Fig. 4. Proposed structure for $[Cu(2\text{-}CNphO)_2(py)_2]$.

Such a binuclear structure has been revealed by X-ray analysis of [Cu(salen)], where salen denotes dianion of N,N'-disalicylidene-ethylenediamine, and its magnetic data (1.84 to 2.0 BM) are not inconsistent with the present results.[14] The facts that the original complex, $[Cu(salem)_2]$, has a *trans*-configuration[15] and that the two bands due to ν(CN) are of equal intensity suggest that a *trans*-form is probable for the oxidized complex, although either a *trans*- or *cis*-configuration is possible for $[Cu(2\text{-}CNphO)_2(py)_2]$. On the other hand, the complex, $[Cu(2\text{-}CNphO)_2(bpy)]$, may have a *cis*-configuration and the infrared spectrum shows two absorption bands due to ν(CN). Thus, this complex also may have a binuclear structure in the solid state.

Mechanism for Oxidative Dehydrogenation. In order to clarify the mechanism for the oxidative dehydrogenation of $[Cu(salam)_2]$ the following effects on the oxidation were investigated.

Solvent Effects: The $[Cu(salam)_2]$ complex was allowed to react with molecular oxygen in various solvents such as pyridine, dioxane, ethanol, and benzene under these conditions: The concentration of the complex was 8×10^{-5} M, at 70 °C, and under air. Absorption

spectral changes were observed in the former three solvents, but no spectral change was observed in benzene. The time required for the oxidation increased in the order pyridine (4.5 h) < dioxane (5 h) < ethanol (20 h). The oxidized product could be obtained from the dioxane solution of $[Cu(salam)_2]$ and was identified to be [Cu(2-CNphO)(OH)], as mentioned in Experimental.

Effects of Added Bases: The oxidative dehydrogenation of $[Cu(salam)_2]$ in dioxane has been found to be accelerated by the addition of organic aromatic bases such as 1,10-phenanthroline(phen), 2,2'-bipyridine (bpy), and pyridine as shown in Fig. 5. The apparent reaction rates increased in the order phen > bpy > py, and increased with an increase in concentration of the added base.

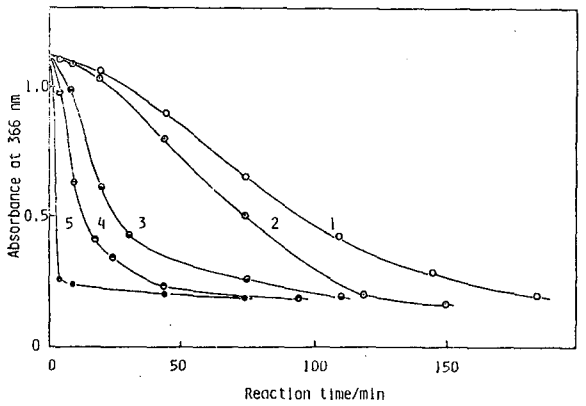

Fig. 5. Effects of added bases to dioxane solutions of $[Cu(salam)_2]$ (10^{-4} M) on oxidation at 70 °C under air, cell length 1 cm. Added bases: 1), none; 2), py (10^{-3} M); 3), bpy (10^{-3} M); 4), bpy (10^{-2} M), 5), 1,10-phenathroline (10^{-3} M).

Concentration of Complex: The reaction of $[Cu(salam)_2]$ in pyridine was made by varying the concentration from 8×10^{-5} M to 1.6×10^{-3} M. All the reactions showed some induction periods. Thus, the maximal rate constants (k_{obsd}) were calculated graphically from the constant slopes after the induction periods obtained in the plots of $\ln(a - x)$ *vs.* reaction time, where a and x are the concentrations at time equal to t_0 and t, respectively, with assumption of the following equation:

$$[Cu(salam)_2] + O_2 \xrightarrow[py]{k_{obsd}} [Cu(2\text{-}CNphO)_2(py)_2] + 2H_2O. \quad (1)$$

A plot of $\log(k_{obsd})$ *vs.* log a shows a linear relation with a slope nearly equal to unity, as shown in Fig. 6. This indicates that the oxidative dehydrogenation of $[Cu(salam)_2]$ depends on the first order of the complex concentration. The induction periods are found to be decreased with an increase in the complex concentration.

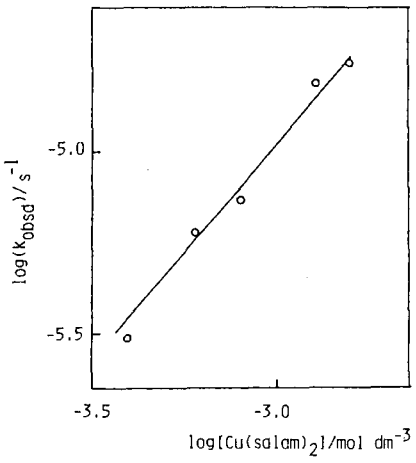

Fig. 6. A plot of $\log(k_{obsd})$ *vs.* $\log[Cu(salam)_2]$.

Effects of Substituents on Aromatic Ring: Figure 7 shows the plots of the decreases in the complex concentration against reaction time. The complex concentration was calculated according to the following equation:

$$x = a(A_0 - A_t)/(A_0 - A_\infty) \quad (2)$$

where A_0, A_t, and A_∞ represent the absorbances at time equal to t_0, t, and at the final state, respectively. Clearly, the induction periods and the maximal rate constants are affected by the substituents on the

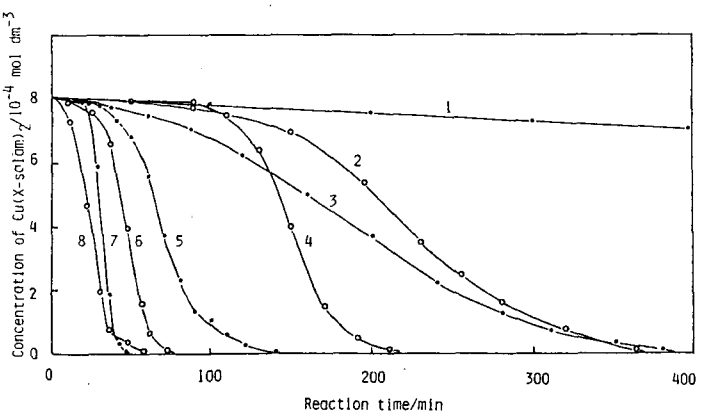

Fig. 7. Effects of substituents of the aromatic ring on oxidation of $[Cu(X\text{-}salam)_2]$ (8×10^{-4} M) in pyridine at 70 °C under air.
1): X = 5-NO_2, 2): 4-Cl, 3): 5,6-Benzo, 4): 5-Br, 5): 3-MeO, 6): H, 7): 5-Me, 8): 3-Me.

aromatic ring; the electron-donating groups accelerate the reaction, whereas the electron-withdrawing groups retard it. The maximal rate constants increased in the order 5-Me > 3-Me > H > 3-MeO > 5-Br > 4-Cl > 5,6-Benzo > 5-NO_2, as listed in Table 4. It should be noted that [Cu(5-NO_2salam)$_2$] did not show any spectral change under the same conditions.

Table 4. Effects of the substituents of aromatic ring on the maximal rate constants and the induction periods for the oxidative dehydrogenation of [Cu(X-salam)$_2$] in pyridine at 70 °C under air

Substituent X	Maximal rate constant k_{obsd} / 10^{-4} s^{-1}	Induction period Time / min
5-Me	27.8	25
3-Me	15.2	8
H	13.5	40
3-MeO	8.8	50
5-Br	8.7	110
4-Cl	2.8	180
5,6-Benzo	2.1	95
5-NO_2	—	—

Concentration of complexes was 8×10^{-4} M.

Effects of Substituents on Nitrogen and Carbon Atoms of Imino Groups: Several copper(II) complexes, [Cu(hpam)$_2$], [Cu(N-Mesalam)$_2$], [Cu(salen)], and [Cu(N-OHsalam)$_2$], were made to react in pyridine at 70 °C under air, where N-OHsalamH denotes salicylaldehyde oxime. Among them, the carbon atom-substituted complex, [Cu(hpam)$_2$], gave the oxidized product, [Cu(2-CNphO)$_2$(py)$_2$], while the other nitrogen atom-substituted complexes did not show any oxidation under the above conditions. These results indicate that the oxidative dehydrogenation of [Cu(salam)$_2$] may be initiated by a splitting of the N-H bond of the coordinated imino groups.

Effects of Addition of Hydrogen Peroxide: Figure 8 shows the plots for the oxidation of [Cu(salam)$_2$] *vs.* reaction time when various concentrations of hydrogen peroxide were added to the pyridine solutions of the complex at 70 °C under air. With the addition of an equimolar amount of hydrogen peroxide to the complex, a nearly half-mole of the complex was oxidized within 5 min, and the oxidation was completed within 100 min after showing a short induction period (curve 1). With the addition of one-tenth amount

of hydrogen peroxide, the initial induction period disappeared, but the reaction rate retarded with time, and a fast oxidation again occurred after 50 min (curve 2). On the other hand, with the addition of one-hundredth of hydrogen peroxide, the reaction pattern (curve 3) was similar to the case of no addition (curve 4).

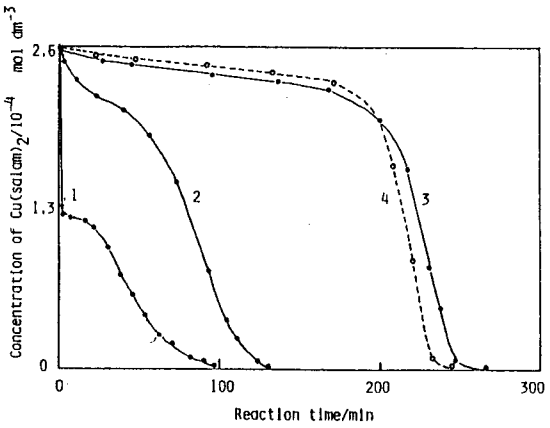

Fig. 8. Effects of added hydrogen peroxide on oxidation of $[Cu(salam)_2]$ (2.6×10^{-4} M) in pyridine at 70 °C under air.
1): $[H_2O_2] = 2.6\times10^{-4}$ M, 2): 2.6×10^{-5} M, 3): 2.6×10^{-6} M, 4): no addition.

The available results suggest that the oxidative dehydrogenation of the coordinated imino groups in pyridine may occur according to the following scheme:

$$Cu(II)(R\text{-}CH{=}NH)_2 \rightleftharpoons Cu(I)(R\text{-}CH{=}\dot{N}H^{+})(R\text{-}CH{=}NH) \quad (3)$$

$$Cu(I)(R\text{-}CH{=}\dot{N}H^{+})(R\text{-}CH{=}NH) + O_2 \longrightarrow Cu(II)(R\text{-}CH{=}\dot{N})(R\text{-}CH{=}NH) + HO_2\cdot \quad (4)$$

$$Cu(II)(R\text{-}CH{=}\dot{N})(R\text{-}CH{=}NH) + HO_2\cdot \longrightarrow Cu(II)(R\text{-}CN)(R\text{-}CH{=}NH) + H_2O_2 \quad (5)$$

$$Cu(II)(R\text{-}CN)(R\text{-}CH{=}NH) + H_2O_2 \xrightarrow{py} Cu(II)(R\text{-}CN)_2(py)_2 + 2H_2O. \quad (6)$$

The initiation reaction is considered to be a thermal one-electron transfer from the imino nitrogen atom to the copper atom, as shown in Eq. 3. The induction periods observed in the oxidation investigated here may be due to the back reaction in Eq. 3, which is the oxidation of copper(I) to copper(II) by the imino radical. In the presence of molecular oxygen, the reactions shown in Eqs. 4 and 5 may occur in competetion with the above back reaction.

The effects of the added aromatic bases (Fig. 5) can be related to Eq. 3. That is, these bases can function as an acceptor of proton(H^+) liberated and as a promoter of electron transfer from the imino group to the copper atom by coordination. Thus, the increasing order of the apparent reaction rates (phen > bpy > py) is not correlated with the order of the pK_a values (py > phen > bpy).

The substituent effects that the electron-donating groups on the aromatic ring accelerate the reaction rates and shorten the induction periods can be explained by taking account of Eqs.3 and 4; the electron-donating groups may facilitate the electron transfers from the imino group to the copper atom (Eq. 3) and from the copper atom to molecular oxygen (Eq. 4). Such a behavior has been found in the autoxidation of the substituted phenylhydroxylamines.[16] And also the autoxidation of phenylhydroxylamine has been found to be accelerated by copper(II) ion.[17]

As described above, the oxidative dehydrogenation investigated here proceeded rapidly after showing induction periods. This indicates that the radical chain autoxidation may be involved in this system. The chain reaction may propagate by the direct attack of molecular oxygen to the imino radical and by the catalytic decomposition of hydrogen peroxide with the copper complex. A tentative scheme for the radical chain autoxidation is proposed, as follows:

$$Cu(II)(R\text{-}CH{=}\dot{N})(R\text{-}CH{=}NH) + O_2 \longrightarrow Cu(II)(R\text{-}CN)(R\text{-}CH{=}NH) + HO_2\cdot \quad (7)$$

$$Cu(II)(R\text{-}CN)(R\text{-}CH{=}NH) + HO_2\cdot \longrightarrow Cu(II)(R\text{-}CN)(R\text{-}CH{=}\dot{N}) + H_2O_2 \quad (8)$$

$$Cu(II)(R\text{-}CN)(R\text{-}CH{=}\dot{N}) + O_2 \longrightarrow Cu(II)(R\text{-}CN)_2 + HO_2\cdot \quad (9)$$

Decomposition of hydrogen peroxide

$$Cu(II)(R\text{-}CH{=}NH)_2 + H_2O_2 \longrightarrow Cu(I)(R\text{-}CH{=}NH)_2 + HO_2\cdot + H^+ \quad (10)$$

$$Cu(I)(R\text{-}CH{=}NH)_2 + H_2O_2 \longrightarrow Cu(II)(R\text{-}CH{=}NH)_2 + HO\cdot + HO^- \quad (11)$$

$$Cu(I)(R\text{-}CH{=}\dot{N}H^+)(R\text{-}CH{=}NH) + H_2O_2 \longrightarrow Cu(II)(R\text{-}CH{=}\dot{N})(R\text{-}CH{=}NH) + HO\cdot + H_2O \quad (12)$$

followed by abstraction of hydrogen atom with $HO_2\cdot$ and $HO\cdot$. The above reaction scheme is supported by the results that the reactions of $[Cu(salam)_2]$ with O_2^- [18] and H_2O_2 in pyridine occurred readily at room temperature.

In the catalytic decomposition of hydrogen peroxide, Sigel *et al.* have found that coordinatedly saturated copper(II) complexes (four-coordinate complexes) are essentially inactive.[19] And Kochi has pointed out that in the reaction of hydrogen peroxide catalyzed by iron ion the reaction represented in Eq. 13 is more facile than that represented in Eq. 14, because hydrogen peroxide is a strong oxidizing agent but only a mild reducing agent.[20]

$$Fe^{II} + H_2O_2 \longrightarrow Fe^{III} + HO\cdot + HO^- \quad (13)$$

$$Fe^{III} + H_2O_2 \longrightarrow Fe^{II} + HO_2\cdot + H^+ \quad (14)$$

Therefore, in the present oxidation, the reaction represented in Eq. 12 is considered to be more important than those represented in Eqs. 10 and 11.

As shown in Fig. 8, the initial induction period was made to disappear by the addition of an equimolar amount of hydrogen peroxide to the complex, but a short induction period was observed again after producing about a half oxidation of the complex.

Furthermore, the catalytic amount of hydrogen peroxide ($[H_2O_2]$: [complex] = 1 : 100) had no effect on the reaction. These results indicate that the radical chain sequence induced by decomposition of hydrogen peroxide may be not so long. These facts suggest that the rate-determining step in the present oxidative dehydrogenation of $[Cu(salam)_2]$ is the splitting of the N-H bond of the coordinated imino group, along with the reduction of copper(II) to copper(I), as shown in Eq. 3.

The author has also found that $[Ni(salam)_2]$ and $[Co^{II}(salam)_2]$ were oxidized by molecular oxygen in pyridine to give their 2-cyanophenolato complexes. In the nickel complex, the severe conditions were required to obtain the fully oxidized product: for 120 h at 115 ^{o}C under O_2 1 atm. This suggests that the oxidative dehydrogenation of $[Ni(salam)_2]$ may be initiated by the electron transfer from the coordinated imino group to molecular oxygen without change in the oxidation state of the nickel ion. On the other hand, the oxidized product of $[Co^{II}(salam)_2]$ was obtained in the conditions similar to the case of $[Cu(salam)_2]$. In the cobalt complex, the initial reaction is considered to be the oxidation of Co(II) to Co(III) by molecular oxygen, followed by the stepwise dehydrogenation of the coordinated imino groups through a redox couple of Co(II)/Co(III) as in the copper case.

Summary

The copper(II) complex of salicylideneamine reacts with molecular oxygen in pyridine to give the 2-cyanophenolato complex, $[Cu(2\text{-}CNphO)_2(py)_2]$, in good yield. This complex was characterized by the infrared and electronic spectra and by its magnetic susceptibilities, and was compared with the authentic complex. The

mechanism for the oxidation of the coordinated imino groups is proposed.

References

1) a) B. A. Marshall and W. A. Waters, *J. Chem. Soc.*, 1960, 2392; b) K. Wuthrich and S. Fallab, *Helv. Chim. Acta*, 47, 1440 (1964), 47, 1609 (1964).

2) W. Brackman and P. J. Smit, *Recl. Trav. Chim. PaysBas*, 82, 757 (1963).

3) A. Misono, T. Osa, and S. Koda, *Bull. Chem. Soc. Jpn.*, 40, 912 (1967).

4) A. Misono and S. Koda, *Bull. Chem. Soc. Jpn.*, 41, 2795 (1968).

5) C. J. Hipp and D. H. Busch, *"Coordination Chemistry"* ACS Monograph 174, ed by A. E. Martell, Am. Chem. Soc., Washington, D. C. (1978), Vol. 2, p. 435.

6) S. E. Diamond, G. M. Tom, and H. Taube, *J. Am. Chem. Soc.*, 97, 2661 (1975).

7) F. R. Keene, D. J. Salmon, and T. Meyer, *J. Am. Chem. Soc.*, 98, 1884 (1976).

8) S. Dilli and A.M. Maitra, *J. Chem. Soc., Chem. Commun.*, 1979,133.

9) M. G. Burnett, V. McKee, and S. M. Nelson, *J. Chem. Soc., Chem. Commun.*,1980, 829.

10) a) G. N. Tyson, Jr., and S. C. Adams, *J. Am. Chem. Soc.*, 62, 1228 (1940); b) Prepared according to a); c) P. Pfeiffer and H. Glaser, *J. Prakt. Chem.*, 153, 265 (1939).

11) J. F. Harrod, *Can. J. Chem.*, 47, 637 (1969).

12) E. W. Ainscough, A. G. Bingham, A. M. Brodie, J. M. Husbands, and J. E. Plowman, *J. Chem. Soc., Dalton Trans.*, 1981, 1701.

13) B. N. Storhoff, *Coord. Chem. Rev.*, 23, 1 (1977).

14) M. D. Hobday and T. D. Smith, *Coord. Chem. Rev.*, 9, 311 (1972 - 1973).

15) H. S. Maslen and T. N. Waters, *Coord. Chem. Rev.*, 17, 137 (1975).

16) Y. Ogata, Y. Sawaki, and T. Morimoto, *J. Am. Chem. Soc.*, 86, 3854 (1964).

17) Y. Ogata and T. Morimoto, *J. Org. Chem.*, 30, 597 (1965).

18) The reaction of $[Cu(salam)_2]$ with KO_2 was made in pyridine at room temperature in the presence of 18-crown-6. The oxidized product was obtained within an hour and identified to be $[Cu(2\text{-}CNphO)_2(py)_2]$.

19) H. Sigel and U. Müller, *Helv. Chim. Acta*, 49, 671 (1966).

20) J. K. Kochi "Free Radicals," ed by J. K. Kochi, Wiley-Interscience, New York (1973), Vol. 1, p. 628.

SUMMARY

The first-row transition metal complexes (chiefly manganese complexes) with the Schiff base ligands have been synthesized and their reactions with O_2, O_2^-, and H_2O have been investigated in order to clarify the functions of metalloenzymes involved in the biological oxygen cycle.

The conclusions obtained in the studies will be summarized as follows.

1) By the reactions of the manganese(II) Schiff base complexes with O_2, the following three types of oxygenated and oxidized manganese complexes are isolated and characterized; μ-peroxo complexes [Mn-O-O-Mn], catena-μ-oxo complexes $+$ Mn-O$+_n$, and oxo complexes [Mn=O]. The formation of these complexes is found to depend on the solvents used, the oxygen partial pressure, and the substituents on the aromatic ring.
   The iron(II) Schiff base complexes supported on polystyrene are found to combine with O_2 reversibly in solution.
2) A probable structure of $[Mn(acac)_2]_2DMF$ is drawn to be a dimer bridged by two acetylacetonato ligands.
3) In the reactions of O_2^- with a series of mononuclear manganese(III) complexes, two different reaction pathways, of which one involves the formation of the oxygenated complexes and the other the reduction from the manganese(III) complex to manganese(II) complex, are found to occur. The reactivity of the complexes toward O_2^- can be correlated with polarographic half-wave potentials corresponding to the reduction from Mn(III) to Mn(II) complexes. With the binuclear manganese(III) complexes, both the reduction and oxygenation are found to occur. On the other hand, the oxygenation occurs in the polynuclear complexes.

4) In the reactions of O_2^- with a series of mononuclear, binuclear, and polynuclear iron(III) complexes, three different reaction pathways are found to occur; (a) the formation of μ-oxo dimers, (b) the formation of the oxygenated complexes, probably adducts with dioxygen, and (c) the reduction from the iron(III) complex to the iron(II) complex. The reactivity of the complexes can be correlated with their steric configurations.

5) The novel dichloromanganese(IV) Schiff base complexes have been synthesized and fully characterized. These complexes exhibit an intense absorption band around 16000 cm^{-1}, which can be assigned to a charge-transfer transition from Cl(pπ) to Mn(dπ). They show a redox potential high enough to oxidize water around +0.9 V (*vs.* SCE). An octahedral *trans*-configuration is proposed for these complexes on the basis of the IR spectra.

6) The dichloromanganese(IV) Schiff base complexes react with water to generate free O_2, indicating that they can function as a model to the active sites of manganese-containing enzymes in chloroplasts.

7) Bis(salicylideneaminato)copper(II) reacts with O_2 to produce the 2-cyanophenolato copper(II) complex quantitatively. The reaction mechanism involving a radical chain autoxidation is proposed.

Acknowledgment

The author is sincerely grateful to Professor Toshiyuki Shono, Osaka University, for his continuing guidance and encouragement throughout this work.

The author is particularly indebted to Emeritus Professor Koichiro Shinra, Osaka University, and to Professor Isao Masuda, Fukuoka University, for their continuing advices and encouragements during this work.

The author is also particularly indebted to Professor Jiro Shiokawa and Professor Toshio Tanaka, Osaka University, for their helps in the preparation of this thesis and the many useful suggestions for its improvement.

Grateful acknowledgment is also given to Associate Professor Minoru Tanaka, Dr. Keiichi Kimura, and Miss Yuko Yamashoji for their helpful suggestions.

The author further wishes to thank for helpful discussions and experimental assistances from his colleagues: Messrs. Isao Fujimoto, Toru Okuyama, Masahiro Nishiyoshi, Teruyoshi Makino, Ryohei Adachi, Tatsuo Yarino, Mikio Torii, Hiroshi Iida, Yusuke Miyazaki, Yasuo Hayashi, Isao Ueki, Makoto Kaneda, Akira Sugitani, Hiroshi Kono, Masanobu Fukuda, Mitsuru Nishino, Yoshihisa Hirata, Manabu Fujiwara, and Masanobu Yuasa. Furthermore, the author wishes to thank all the members of the Shono Laboratory and all his friends for their occasional discussions and friendships.

Finally, the author would like to thank his mother Tomie Matsushita and his wife Megumi for their understanding and encouragements.